

DOE/NASA/0263-1
NASA CR-174659
SwRI-6948

NASA-CR-174659
19840020891

Development of Carbon Slurry Fuels for Transportation (Hybrid Fuels-Phase II)

T. W. Ryan, III, and L. G. Dodge
Southwest Research Institute

May 1984

LIBRARY COPY

MAY 13 1984

LANGLEY RESEARCH CENTER
LIBRARY, NASA
HAMPTON, VIRGINIA

Prepared for
NATIONAL AERONAUTICS AND SPACE ADMINISTRATION
Lewis Research Center
Under Contract DEN 3-263

for

U.S. DEPARTMENT OF ENERGY
Conservation and Renewable Energy
Office of Vehicle and Engine R&D



NF00424

DISCLAIMER

This report was prepared as an account of work sponsored by an agency of the United States Government. Neither the United States Government nor any agency thereof, nor any of their employees, makes any warranty, express or implied, or assumes any legal liability or responsibility for the accuracy, completeness, or usefulness of any information, apparatus, product, or process disclosed, or represents that its use would not infringe privately owned rights. Reference herein to any specific commercial product, process, or service by trade name, trademark, manufacturer, or otherwise, does not necessarily constitute or imply its endorsement, recommendation, or favoring by the United States Government or any agency thereof. The views and opinions of authors expressed herein do not necessarily state or reflect those of the United States Government or any agency thereof.

Printed in the United States of America

Available from

National Technical Information Service
U.S. Department of Commerce
5285 Port Royal Road
Springfield, VA 22161

NTIS price codes¹

Printed copy: A09

Microfiche copy: A01

¹Codes are used for pricing all publications. The code is determined by the number of pages in the publication. Information pertaining to the pricing codes can be found in the current issues of the following publications, which are generally available in most libraries: *Energy Research Abstracts (ERA)*; *Government Reports Announcements and Index (GRA and I)*; *Scientific and Technical Abstract Reports (STAR)*; and publication, NTIS-PR-360 available from NTIS at the above address.

17

1 1 RN/NASA-CR-174659
DISPLAY 17/2/1

84N28960** ISSUE 19 PAGE 2992 CATEGORY 26 RPT#: NASA-CR-174659
DOE/NASA/0263-1 NAS 1.26:174659 SWRI-6948 CNT#: DEN3-263
DE-A101-81CS-50006 84/05/00 174 PAGES UNCLASSIFIED DOCUMENT

UTTL: Development of carbon slurry fuels for transportation (hybrid fuels, phase 2)

AUTH: A/RYAN, T. W., III; B/DODGE, L. G.

CORP: Southwest Research Inst., San Antonio, Tex. AVAIL. NTIS SAP: HC A08/MF A01

MAJS: /*COMBUSTION EFFICIENCY/*DIESEL ENGINES/*ENGINE DESIGN/*FUEL COMBUSTION/*
FUEL TESTS/*PROPULSION SYSTEM CONFIGURATIONS

MINS: / CHEMICAL ANALYSIS/ ENERGY TECHNOLOGY/ FUEL INJECTION/ PARTICLE SIZE
DISTRIBUTION/ SLURRY PROPELLANTS

ABA: M.A.C.

ABS: Slurry fuels of various forms of solids in diesel fuel are developed and evaluated for their relative potential as fuel for diesel engines.

Thirteen test fuels with different solids concentrations are formulated using eight different materials. A variety of properties are examined including ash content, sulfur content, particle size distribution.

DOE/NASA/0263-1
NASA CR-174659
SwRI-6948

Development of Carbon Slurry Fuels for Transportation (Hybrid Fuels-Phase II)

T. W. Ryan, III, and L. G. Dodge
Southwest Research Institute
San Antonio, Texas 78284

May 1984

Prepared for
National Aeronautics and Space Administration
Lewis Research Center
Cleveland, Ohio 44135
Under Contract DEN 3-263

for
U.S. DEPARTMENT OF ENERGY
Conservation and Renewable Energy
Office of Vehicle and Engine R&D
Washington, D.C. 20585
Under Interagency Agreement DE-AI01-81CS50006

This Page Intentionally Left Blank

TABLE OF CONTENTS

I.	INTRODUCTION	1
II.	OBJECTIVE	6
III.	COMPONENT SELECTION	7
IV.	FUEL FORMULATION AND CHARACTERIZATION	19
V.	INJECTION AND ATOMIZATION STUDIES	25
	5.1 Injection Bombs	25
	5.2 High-Speed Movies	25
	5.3 High-Resolution Photography	32
VI.	ENGINE EXPERIMENTS	46
	6.1 Test Equipment and Procedures	46
	6.2 Experimental Results	49
VII.	DISCUSSION	59
	7.1 Component Selection	59
	7.2 Fuel Formulation	59
	7.3 Injection and Atomization	60
	7.4 Engine Experiments	61
	7.5 Preliminary Specification	63
VIII.	SUMMARY	67
	8.1 Fuel Formulation	67
	8.2 Injection and Atomization	67
	8.3 Engine Experiments	68
IX.	REFERENCES	69
	ACKNOWLEDGEMENTS	71
	APPENDIX A - PROCESS SYNOPSES AND SUPPLEMENTAL REFERENCES	A-1
	APPENDIX B - SPRAY PENETRATION VERSUS TIME DATA	B-1
	APPENDIX C - ENGINE PERFORMANCE AND EXHAUST EMISSIONS DATA	C-1
	APPENDIX D - HEAT RELEASE RATE DIAGRAMS	D-1
	APPENDIX E - HIGH CONCENTRATION CARBON BLACK SLURRY TEST RESULTS	E-1

This Page Intentionally Left Blank

I. INTRODUCTION

A very large portion of the domestic energy resources of the United States occur in nature as solid materials, such as coal and various biomass and waste materials. Development of modern transportation systems, however, have been dependent on supplies of liquid fuels tailored to meet the specific needs of a variety of heat engine systems. This dependence on liquid fuels has, of course, resulted from the convenience of plentiful supplies of petroleum. Because petroleum is a mixture of hydrocarbon liquids it can be easily recovered from nature, transported, and converted to liquid fuels.

The shortages of petroleum which have occurred over the past 10 years have strengthened, at least within the technical community, the realization that the world petroleum reserves are very limited. As a result of this realization, a great deal of work has been devoted to the development of fuels from other natural resources including those mentioned previously plus oil shale and tar sands. A vast majority of this work has involved the development of liquid fuels which are very similar to those produced from petroleum. In some cases, such as the oil shale and the tar sands, the liquefaction is a natural step in the processing of the raw material. In other cases, the processing to liquid fuels may not be the most efficient way to utilize the raw materials. It appears that the most efficient use of coal would involve direct utilization in some form of in situ combustion process to produce thermal energy. The opposite extreme appears to be the synthesis of hydrocarbon liquids which resemble gasoline and/or distillate fuels. Obviously, the direct application of coal to self-contained transportation systems requires, as a minimum, the removal of the coal from the earth. Additional processing could involve washing, grinding, ash removal, and sulfur removal. The types and the degree of processing depend on the application and the time frame of interest. For instance, dry-powder coal has and can be used as a fuel for such Rankine cycle applications as railroad and waterway transportation systems. A similar application to highway transportation is difficult to envision because of the volume requirements of the fuel handling and heat transfer equipment used in the Rankine systems.

Direct utilization of dry-powder coal in internal combustion engines has historically been of interest to engine designers and researchers. The earliest recorded attempt at the design of a solid fuel engine was in 1780.^{(1)*} Dr. Rudolf

*Numbers in parentheses designate entries in the reference list.

Diesel was most probably the first researcher to actually attempt the operation of an internal combustion engine on coal powder. Pavolikowski⁽²⁾ and Morrison⁽³⁾ both published articles describing their work with the German "Rupa" engine; a slow speed engine designed to operate on coal dust. Soehngen⁽⁴⁾ presented an excellent review of the German work done on the development of a coal dust diesel engine. The conclusions drawn from the review indicate that high-speed coal dust engines are possible. A similar review of the literature by Rich and Walker⁽¹⁾ resulted in the development of a low-compression ratio coal dust diesel engine which used a pilot injection of diesel fuel and fumigation of the coal into the intake air. The test results were less than satisfactory due to coal delivery problems and what appeared to be the relatively large size of the coal particles (large percentages in excess of 200 mesh).

In 1978, the U.S. Department of Energy initiated a program at Southwest Research Institute to investigate the potentials of minimally processed and hybrid fuels for highway transportation.⁽⁵⁾ As a part of that work, a variety of solid materials were considered, first, for direct application, and then as components in slurries. Early in the project it was realized that the direct utilization of any solid in highway transportation systems (high-speed diesel engines) would require major hardware development efforts in three areas:

1. Fuel preparation and on-board handling systems;
2. Fuel metering and injection systems; and
3. Pistons/combustion chambers/rings designed to segregate the dispersed dry powder from lube oil wetted surfaces.

In conjunction with the hardware-related efforts, more basic studies were required in order to define the powder fuel requirements in terms of particle size, composition, contaminant concentrations, moisture content and energy content. Based upon these considerations, it was felt that the utilization of dry-powder fuels in highway transportation diesel engines represented a very long-term approach to the utilization of solid fuels. On the other hand, the use of slurry fuels appeared to be a logical intermediate step in the utilization solid form energy sources, intermediate between dry powder and liquefaction. Marshall and Walters,⁽⁶⁾ Tataiah and Wood,⁽⁷⁾ Marshall, et al.⁽⁸⁾, and Ryan, et al.,^(5,9) have reported results of engine experiments with a variety of slurries.

A 15-percent slurry of solvent-refined coal in JP-4 was produced and tested in a prechamber engine by Marshall and Walters.⁽⁶⁾ The combustion and engine efficiency data were not presented, but it appears that satisfactory performance was obtained using the slurry fuel. Although it was not indicated in the paper, the refined coal was apparently SRC-I. The particle size was not reported. The authors indicated that some difficulties were encountered with fouling and sticking of the injection system. Possible causes for these problems were excessive particle size and/or melting and refusion of the SRC-I solids in the tight clearances in the system (fusion temperature of SRC-I is 177°C (350°F)).

Tataiah and Wood⁽⁷⁾ recently tested 10-, 20-, and 30-percent coal slurries in a four-stroke, direct injection diesel engine. The suspended coal particles were reported to be 100 percent below 10 microns. Heat release calculations, based on the pressure diagrams, indicated that the coal was either not undergoing complete combustion or that the heat transfer to the coolant was increased due to radiation from the solid particles. These data were obtained at 800 rpm in the test engine. At the test conditions, there is a maximum (based on 90° of revolution for combustion) of 18 msec available for combustion. From well stirred reactor data, Essenhigh⁽¹⁰⁾ indicated that the maximum coal particle size which will burn out in 18 msec is approximately 10 microns. It should be realized that the actual time available for useful combustion is much less than that based on 90° of revolution. It is possible that the incomplete combustion observed by Tataiah and Wood⁽⁸⁾ was due to particle sizes too large to burn out in the time available. Marshall, et al.⁽⁸⁾ reported the results of experiments with 20 to 40 weight-percent slurries of raw coal in No. 2 diesel fuel (DF-2). The authors reported high wear rates, incomplete combustion, and degraded performance. The coals used in the experiment were apparently untreated and probably had relatively high ash and sulfur contents; ash contents were not reported. In addition, it appears that a large mass fraction of the particles had large diameters (greater than 7 microns). The large particles may not have had sufficient time to burn out during the combustion process. Incomplete combustion in conjunction with high ash content could have resulted in the high wear rates observed during the experiments.

Ryan, et al.⁽⁵⁾ reported results of experiments in which a variety of slurries were tested in a single cylinder, four-stroke, direct-injection engine. The results of the experiments indicated that slurries could be made to work efficiently in high speed diesel engines (greater than 1000 rpm) if the slurries are formulated using the proper material and the proper size distribution. This work was extended by Ryan, et al.⁽⁹⁾ in

a series of experiments in which a variety of carbon blacks were used to determine the range of properties (particle size, surface area, and porosity) and engine/fuel system modifications required for satisfactory performance of slurry fuels.

The past experience with the preparation and testing of number of different slurries^(5,9) indicated that there are basically five areas of concern in formulating slurry fuels for diesel engines. They are:

1. Grinding and/or dispersion characteristics of the solid component;
2. Flow and stability characteristics of the slurry;
3. Injection and atomization characteristics of the slurry;
4. Injection system and engine durability characteristics with the slurry; and
5. Engine combustion characteristics of the solid component and the slurry.

All of the above mentioned areas are affected by certain basic properties of the solid component. Hardness of the solid determines the type (grinding, homogenation, dispersion, etc.) and the degree of processing required to produce the desired particle-size distribution in the slurry. The particle-size distribution, in turn, affects the rheological, the stability, and the injection and atomization characteristics of the resulting slurry. These characteristics are also affected by the surface area of the particles which, in turn, is related to the porosity as well as the size distribution of the particles. Injection system and engine durability are also affected by particle hardness and particle-size distribution as well as by contaminants such as ash and sulfur. The engine combustion characteristics are affected to some degree by all of the properties mentioned above. In addition, the combustion process is affected by the density, heat of combustion, and the composition of the solid component.

A necessary step in the advancement of new fuel concepts is the development of a preliminary specification of the fuel for a specific application. Ideally a fuel specification limits or controls all of the properties which affect the performance of the fuel in the specific type of engine. Such an ideal specification for slurry fuels would include specific limitations on the properties of the solids, such as hardness, surface area, particle-size distribution, and contaminant concentration of the solid component of the fuel. Processing techniques such as those used in the preparation of carbon black could theoretically be used to produce the ideal solid component. Such an approach may not be practical since one of the attractions of the slurry concept is the potential for minimizing the processing requirements of energy resources such as

coal. Therefore, it appears that a realistic approach would involve the specification of certain general slurry properties such as the mean particle size, apparent viscosity, stability, and ash and sulfur contents. The simplistic approach is especially important if one considers that all of the more basic properties (particle-size distribution, particle surface area, etc.) interact with each other and with the various processes (injection, atomization, and combustion), such that a specification based on these properties may be impossible to apply to practical solid fuel components. There is, however, an obvious need for a preliminary specification encompassing the current knowledge and experience with slurry fuels. It is felt that such a specification would serve as the basis and provide a guide for future development of slurry-fuel technology.

II. OBJECTIVE

Based upon the above considerations, the overall objectives of this work were:

1. To develop a number of different slurries using solid components representative of the various sources; and
2. To define a preliminary specification of slurry fuels for conventional diesel engines.

The work required to meet the overall objectives is most conveniently considered in terms of four major work areas or tasks. They are:

1. Selection of representative solid components;
2. Formulation and characterization of slurry test fuels;
3. Characterization of the injection and atomization properties of the fuels; and
4. Characterization of the engine performance and combustion characteristics of the test fuels.

The experimental apparatus, procedures and results are discussed separately in the following sections. The results are discussed in terms of the overall objectives in the Summary section.

III. COMPONENT SELECTION

A literature review resulted in the development of a list of 31 different potential components. The list, compiled in Table 1, includes materials derived from biomass and biomass waste, petroleum by-product, and a large number of materials produced from coal. The selection criteria included availability, economics, and the properties of the materials, mainly the ash and sulfur contents.

Eight materials were selected from the list for formulation of test fuels. The final selection of test materials for this work was based primarily on the properties with some consideration for the source (biomass, by-product, or coal). Table 2 is a list of the eight materials by name, an indication of the source, and the various references in which the various processes are described in detail. Appendix A contains synopses describing the various processes and a supplemental reference list relevant to the carbonaceous materials. As can be seen, the sources include natural gas, by-products from petroleum processing, biomass, coal, and a number of processed coals. All of the components were obtained in either pebble form or as dry powders.

As indicated previously, complete descriptions of the processes used in producing the various solid materials listed in Table 2 are presented in Appendix A. In order to provide a "better feel" for the various materials each is described very briefly in terms of the source, the processing, and the visual appearance.

Mogul L is a carbon black produced from petroleum residual oil and natural gas using the furnace process. It is considered to be a high quality black, used mainly as pigment in printer ink. The visual appearance is a very fine powder, flat black in color, indicating a very porous surface. The Mogul L was selected as the baseline solid material to act as a reference and to provide continuity with the previous work.^(5,9)

Petroleum coke is a by-product of modern petroleum refining technology resulting from cracking of the residual oil. It is removed from the coker in large pieces which are relatively easy to grind or fracture to coarse powder which is flat black in color.

The k-Fuel used in this study was produced from wood by controlled pyrolysis. The process can be adapted to any solid carbonaceous material. The dark brown

TABLE 1 SUMMARY CHART
Slurry Fuel Material Screening

No.	Type of Benefication	Raw Material	Status	Brief Description of Process	Advantages & Disadvantages	Estimate of Process Energy	Characteristics of Final Product	Ref. (c)
1	Solvent Refined Coal (SRC-1)	Coal	Pilot Plant	Raw coal pulverized to minus 1/8" x 0"; slurried with with solvent, heated (450°F and 2000 psig) and combined with H ₂ . Heat increased to 750°F and pumped to dissolver. At 840-870°F, coal is hydrogenated & polymerized causing dissolution of coal. After removal of solvent and undissolved solids, residue (SRC-1) is recovered.	Converts high sulfur, high-ash coals to low sulfur and low ash coals	Not available	Ash, 0.2 wt% Sulfur, 0.7 wt% (organic) Density, 1.2 g/ml HV, 16,000 Btu/lb. Carbon, 88 wt% Hydrogen, 5.9 wt% Nitrogen, 2.2 wt% Fusion Pt. 3500° F	1, 12
2	Hydrothermal (Battelle)	Coal	Miniplant 0.25-0.33 ton/day	Crushed and mixed with a leaching fluid (10% NaOH and 2% Ca(OH) ₂ in H ₂ O) to form slurry. Transferred to pressure vessels, held for 30 minutes at 350-2500 psi and 437-662° F. The chemicals are filtered off, regenerated and recycled. Coal is washed and dried.	Remove all in-organic sulfur & half organic sulfur. Coal is impregnated with alkali which probably would be harmful if run as fuel in a diesel engine.	\$55.90/Ton(a)	Inorganic sulfur reduced 80-90%. Organic sulfur reduced 10-30%.	2, 3, 18 42 61
3	High Gradient Magnetic Separation	Coal	Pilot plant (now closed down)	Coal is diamagnetic, pyrite is paramagnetic. Fluidized bed is subjected to a high-gradient magnetic field which enables the paramagnetic pyrites to be separated from the remaining coal.	Produce relatively low-sulfur, low ash product.	Estimated cost about \$0.50 in a 500 ton/hr plant.	Remove up to 90% pyrite sulfur	15, 16, 17, 25,61
4	Koppelman Process	Wood waste; peat; lignite; brown coal; subbituminous coal; seaweed; etc.	Pilot Plant	Advanced form of pyrolysis. Feedstock is restructured in the reactor, under controlled high temperature and pressure. Process temperatures depends on type of feedstock used and product desired. Removed during the chemical restructuring are the products of chemical decomposition. High carbon fuel remains. Yield depends on moisture and oxygen content of feedstock.	Attains high thermal efficiency; uses aqueous slurry feed; can process wide range of particle sizes; reduces sulfur content.	Competitive w/conventional energy sources.	Typical from brown coal: Ash, 8.24 wt% S, 0.85 wt% HHV, 13,250 Btu/lb.	5,6, 7,8, 9, 10, 11

(a) Product cost includes a cost of coal (1977 dollars)

(b) Processing costs (1979 dollars) - costs associated with process and does not include initial coal cost.

(c) Reference numbers refer to supplemental reference list in Appendix A

No.	Type of Benefication	Raw Material	Status	Brief Description of Process	Advantages & Disadvantages	Estimate of Process Energy	Characteristics of Final Product	Ref.
5	Solvent Refined Coal Two-stage Liquefaction	Coal	Demonstration plant being built, operational late 1984. Pilot plant currently operational.	Similar to SRC process described in No. 1 except it has LC-Finer or referred to as two-stage liquefaction (TSL).	TSL solids has a lower sulfur & lower ash than the typical SRC-I.	Estimated to cost \$3.25/MM	Sulfur, 0.15-0.3% Ash, 0.2% HHV, 16,250 Btu/lb.	i
6	Chemical leaching (Meyer's Process)	Coal containing pyritic sulfur	Process Dev. unit (8 tons a day) was being built for EPA in 1975. Now dormant.	Process steps are crushing, chemical treating, sulfur removal & solution regeneration. Aqueous ferric sulfate is used to oxidize selectively the pyritic sulfur. The iron sulfate product dissolves in solution & free sulfur is removed by solvent extraction or vaporization. The oxidizing agent is regenerated with air or oxygen and recycled. Iron sulfates are removed by liming and/or crystallization.	Physical form remains unchanged. Wide applicability for converting U.S. coal reserves to a sulfur level consistent with present & proposed gov't. sulfur oxide emission standards.	\$43.40/Ton ^(a)	Removes 90-95% pyritic sulfur	22, 23, 38, 45, 61
7	Eureka Process	Canadian Oil Sands; vacuum resid.	Pilot plant using Canadian oil sands; 20,000 B/D commercial in Japan since using vacuum resid.	The feed (usually vacuum tower bottoms) goes to a preheater prior to it entering bottom of fractionator and is mixed with recycle oil from the above. The mixture is fed to a charge heater and then to the reactor system. Superheated steam is injected into the reactor to strip cracked product and to supply 20% of heat required for the reaction. The pitch is drawn off and pumped to flaker where it is solidified and flaked.	Homogeneity of pitch permits handling in molten state. Less coke is formed (compared to delayed coker) as products are removed as soon as formed. Reaction temp. is relatively low.	Not available	Using vacuum resids. of Middle East crudes: Sulfur, 6% Ash, 0.2-0.3%	14

(a) Product cost includes cost of coal (1977 dollars)

No.	Type of Beneficiation	Raw Material	Status	Brief Description of Process	Advantages & Disadvantages	Estimate of Process Energy	Characteristics of Final Product	Ref.
8	Gravimelt	Coal	10-200 lb range	Molten sodium hydroxide & potassium hydroxide are used to remove organic sulfur from coal. Coal and above mixture are heated. Salts react with sulfur-bearing compounds to form sulfides; these are removed.	Very low ash and sulfur.	\$2.80/MM Btu; \$20/Ton (b)	Ash, 0.20-0.40 Sulfur, 0.25-0.64	51, 52, 53, 61
9	Dry table	Coal	In development stage	The dry table is designed so that size & bulk density separations take place. Incoming feed causes the overturning of the bed and a flow away from the feed, resulting in a helical motion. Particles migrate according to size, shape and density.	Simplicity	Not available pyrite sulfur and ash content	Reduction in the	4
10	Otisca Media Process	Coal	125TPH plant constructed and tested. 5-10TPH pilot plant operational.	The process exploits the gravimetric differences between coal and its impurities in a static bath of organic, low viscosity liquid.	Can handle "friable" or soft coals. High energy content yields.	Low process heat requirements; low maintenance cost; \$0.30/million Btu including capital recovery	Sulfur reduced 60% Ash reduced 90%	57
11	Otisca T-Process	Coal	200 lb/hr pilot plant underway. Expected start up mid 1982	Grinding to 15 microns; agglomeration.	Recovers almost 100% of the energy content of the feed.	Extremely efficient.	Ash, 1% or less	58
12	Microwave Process	Coal	Laboratory	¾" size coal particles are subjected to microwaves. This converts pyrite to FeS, which have strong magnetic properties. Crushing the coal further (30-100 mesh) and further microwave treatment combined with NaOH treatment can remove 80-90% of sulfur from coal.	Potential of meeting environmental requirements for burning coal.	undetermined	Inorganic sulfur reduced 85%. Organic sulfur reduced 60%.	54 61
13	Chemical Comminution	Coal	Laboratory	Treatment with liquid ammonia causes coal to fracture in highly selective manner. Breaks occur in those internal boundaries that had previously been weakened by infiltration of pyrite, ash, and other minerals.		\$37.00/Ton (a)	Sink float products had 55% reduction in ash, and 73% reduction in organic sulfur. Capable of removing up to 80% inorganic sulfur.	19, 20, 61

(a) Product cost includes cost of coal (1977 dollars)

(b) Processing costs (1979 dollars) - cost associated with process and does not include initial coal cost.

No.	Type of Beneficiation	Raw Material	Status	Brief Description of Process	Advantages & Disadvantages	Estimate of Process Energy	Characteristics of Final Product	Ref.
14	Flash Desulfurization	Coal	Work on process stopped. Bench scale.	Oxidative pretreatment to eliminate coking and assist in subsequent hydrotreatment (750°F and 1 ft/sec). Tests in batch reactor were at 1400-1500°F and near-atmospheric hydrogen pressure.	Still high in ash	Not available	Approx. 25-30% coal sulfur is removed during pretreatment. Final product - as much as 98.6% sulfur removed.	32
15	Low-Temperature Chlorinolysis	Coal	Process in early stages of development	Scission of carbon-sulfur and sulfur-sulfur bonds take place and the organic sulfur is converted to sulfonate sulfur and sulfate sulfur using chlorine.	Still high in ash	At 12,500 tons of coal/day \$9-10/Ton of coal	Sulfur reduction of 51%. Reduced concentration of toxic trace elements such as Pb ₅ , Va, P, Li, Be, As, etc.	(33)
16	Electronic	Coal	Bench scale	The coal is finely ground and is introduced into an ionization chamber by means of a carrier gas. The particles are charged, kept separated, and sent to an electrostatic separator. The pyrite and ash are thus removed.		Reported to be 25-50% that of FDG See Ref. 70.	Total sulfur removal 33-68%	61,68 69,70
17	Microbial	Coal	Laboratory	Microorganisms oxidize organic sulfur to soluble sulfates.		Not available	95% of dibenzothiophenes can be converted to soluble material	61
18	Microbial	Coal	Laboratory	Microorganisms oxidize pyrites.		\$5-14/Ton ^(b)	Can remove up to 90% of inorganic sulfur	61,66 59,
19	Magnex	Coal	Development Stage	Ground coal is contacted with vapors of iron carbonyl. The pyrites in the coal react with the carbonyl to form magnetic iron sulfide that can be separated magnetically.	Does not remove organic sulfur	\$40.70/Ton ^(a)	Removes 80% inorganic sulfur	56

(a) Product cost includes cost of coal (1977 dollars)

(b) Processing costs (1979 dollars) - costs associated with process and does not include initial coal cost.

<u>No.</u>	<u>Type of Beneficiation</u>	<u>Raw Material</u>	<u>Status</u>	<u>Brief Description of Process</u>	<u>Advantages & Disadvantages</u>	<u>Estimate of Process Energy</u>	<u>Characteristics of Final Product</u>	<u>Ref.</u>
20	Coking	Coal	In use	Conventional process for making metallurgical coke and used by U.S. Steel.	Well-known technology	Commercial Feasible	Volatile matter reduced to 6.9% Ash, 5.5% Sulfur, 0.63%	
21	Combination Heavy media, vibrating table flotation cells	Coal	In use	A heavy medium is used to separate the coarse coal out. A vibrating table is used to make the size separation and flotation cells are used for the "fines".		Not available	Analysis not available	39
22	Anthracite	Premium anthracite coal	In use	"Rice coal" (5/16" x 3/16").	Low ash, Low sulfur, High fixed carbon	Mining and cleaning expense	Volatile matter, 4.0% Sulfur, 0.6% Ash, 8.5%	
23	Linear Acceleration	Coal	Lab stage	The coal is pulverized by hot high-velocity gas (5,000 ft/s). Ash is removed by centrifugal force. A chemical process involving fluorine can follow.	Many unknowns	Estimated at \$1.48 million Btu	Sulfur, 0.50-0.5%	61
24	Liquid SO ₂	Coal	Under development	Liquid SO ₂ is contacted with coal under pressure and at a temperature of 300°F. The SO ₂ attacks the co-valently bound organic sulfur compounds and permits them to be extracted.		Not available	Removal of 50-60% sulfur	61
25	Froth Flotation	Coal	Under development	Process exploits the differences in the surface properties of the coal and the refuse particles. Coal is sized down to 1/32" or smaller and placed in a large mixing tank (flotation cell). Contents of tank are mixed with special agents added to promote bubbling and the attachment of coal particles to these bubbles. The bubbles (with coal particles) rise to the surface and coal is removed. The pyrite and ash are left behind in suspension.		Not available	Reduced ash and inorganic sulfur content	21 26

<u>No.</u>	<u>Type of Beneficiation</u>	<u>Raw Material</u>	<u>Status</u>	<u>Brief Description of Proces</u>	<u>Advantages & Disadvantages</u>	<u>Estimate of Process Energy</u>	<u>Characteristics of Final Product</u>	<u>Ref.</u>
26	Oxidiation	Coal	Bench	Coal is dried and pulverized followed by treatment with hot NO ₂ gas. The sulfur compounds are oxidized with some of the sulfur being removed as SO ₂ , and and some as sulfates.		\$47.50/Ton ^(a)	Inorganic sulfur reduced 95-100%. Organic sulfur reduced 30-70%.	61
27	Oxygen Leaching	Coal	Postponed	The coal is ground and then leached in an acidic solution or in ammonia.		\$46.90/Ton ^(a)	Removal of 90-100% of the inorganic sulfur	
28	Oil Agglomeration	Coal	Japanese-10 Ton/hr Research in U.S., Canada, and India	Removes fine particles from suspension by selective wetting and agglomeration with oil.	Highly selective and capable of cleaning -200 mesh material	N.A.	Reduces Ash: 40% to 4% for Coal (80% > 75 μ m) 58% to 18% for Coal (42% > 75 μ m) 20% to 30% for Coal (70% > 75 μ m) 16% to 8% for Coal (100% > 75 μ m)	2
29	Coal-pyrite flotation process - U.S. Bureau of Mines	Coal	Laboratory and pilot-plant	Two-stage froth flotation process removes pyrite sulfur from fine-sized coals. First stage standard coal flotation step to remove high-ash refuse and coarser pyrite as tailings. First stage is treated in second bank of flotation cells in presence of a coal depressant and xanthate flotation collector to selectively float remaining pyrite.	Looks promising for removal of sulfur from coals containing finely disseminated or unliberated pyrite that cannot be removed adequately by other flotation methods	Not available	90% of pyrite removed	28 29, 30
30	Oxydesulfurization	Coal	Laboratory scale	Coal/water slurry and compressed air is heated to 300°F. The sulfur is removed as soluble compounds.		\$51.60/Ton ^(a)	Inorganic sulfur reduced 80-90%. Organic sulfur reduced 20-50%.	24 61

(a) product cost includes cost of coal (1977 dollars)

<u>No.</u>	<u>Type of Beneficiation</u>	<u>Raw Material</u>	<u>Status</u>	<u>Brief Description of Process</u>	<u>Advantages & Disadvantages</u>	<u>Estimate of Process Energy</u>	<u>Characteristics of Final Product</u>	<u>Ref.</u>
31	Convertol Process	Coal	Commercial in Germany	The coal is slurried in water to 40-45% solids. Oil is injected into the slurry under vigorous agitation. Coal particles agglomerate; are washed, dewatered, flocculated, and centrifuged.	Large oil consumption.	Economically feasible when coal product is for metallurgical coke production.	Ash content greatly reduced	41
32	Using a heavy organic liquid (gravity separation)	Coal	Laboratory	Separation using heavy organic liquid -(perchloro-ethylene)		N.A.	Low ash Low sulfur	31

**Table 2. Components Selected for
Slurry Fuel Formulation**

<u>Name</u>	<u>Source</u>	<u>Ref.</u>
Mogul L Carbon Black	Residual Oil/ Natural Gas	11
Petroleum Coke	Residual Oil	-
k-Fuel	Wood	12-18
Clean Coal (Bituminous)	Coal	-
Fairless Coke	Coal	19
Otisca-T	Coal	20
SRC-I	Coal	21
Eureka	Residual Oil	22

material used in this study came as small non-uniform pieces which were extremely easy to reduce to coarse powder.

The clean bituminous coal was a non-uniform coarse powder. The coal was supplied as representative of a low-sulfur, low-ash coal typically supplied to a steel mill for coke production.

Fairless coke, typical of most low sulfur metallurgical cokes, was produced by conventional means at the U.S. Steel Fairless Works. It was supplied as a coarse flat-black powder.

The Otisca-T process has been designed as a means to remove ash from coal. In the process, coal is ground to approximately 15 microns by conventional means. Ash removal is accomplished by washing the coal in two immiscible liquids which selectively collect the ash or coal due to differences in the surface properties of the ash and coal. The resulting material is a very fine powder with a flat black appearance.

The SRC-I is the residue remaining after the solvent refining of coal. The SRC process is designed to remove sulfur and ash by solvent extraction. The SRC-I solid is recovered as large chunks of glossy brown material which fracture easily.

The Eureka process was designed to recover hydrocarbon liquids from vacuum tower bottoms, oil sands and possible coal tar pitch. The solid material recovered in this process is glossy black in appearance and is generally supplied as uniform size pebbles which are easily fractured to powder.

The key properties of the various solid components are listed in Table 3. Also included in Table 3 is an indication of the form, dry powder or pebble, of the various materials as received for use in this work. As experience was gained with the various materials, it became obvious that other properties are important. These observations will be discussed further in later sections of the paper.

Examination of the data in Table 3 reveals fairly broad ranges in the composition of the various materials. Carbon content varied from 70.9 to 92.3 percent, hydrogen from 0.6 to 6.7 percent, oxygen from 2.6 to 19.4 percent, nitrogen from 0.4 to 3.6 percent, sulfur from 0 to 3.5 and ash from 0 to 7.6 percent. The gravimetric heats of

Table 3. Physical Properties and Composition of the Solid Components

<u>Material</u>	<u>Form</u>	<u>%C</u>	<u>%H</u>	<u>%O</u>	<u>%N</u>	<u>%S</u>	<u>% Ash</u>	<u>Gross HC mJ/kg</u>
Mogul L	Powder	92.3	0.6	5.2	0.4	1.0	0.4	31.2
Petroleum Coke	Powder	86.7	3.8	3.3	1.8	3.5	0.0	34.7
k-Fuel	Pebble	70.9	4.6	19.4	0.8	0.0	3.8	26.7
Clean Coal	Pebble	85.1	4.9	4.8	2.7	0.7	0.0	35.9
Fairless Coke	Powder	82.3	0.8	5.3	3.6	0.5	7.6	29.5
Otisca-T	Powder	79.9	5.9	9.7	.3	0.6	0.9	34.4
SRC-I	Pebble	85.4	6.7	3.5	2.9	0.6	0.0	38.1
Eureka	Pebble	84.8	5.8	2.6	2.7	0.1	0.2	36.9

combustion varied from 27 to 38 mJ/kg. With some exceptions, the sulfur and ash contents were low. Petroleum coke had high sulfur and low ash content while the k-Fuel had low sulfur and high ash content. The Fairless coke had low sulfur content, but the highest ash content of the test materials. The ash and sulfur contents were not considered as a limiting factors because the primary concern in this study was engine combustion and performance. In addition, it was realized that current diesel fuel specifications for sulfur and ash contents are most probably applicable to slurries due to limitations of current conventional equipment. Since it was not possible to control the history and thus the exposure of the various materials to the atmosphere, all probably contained water. This is reflected in the oxygen contents, and somewhat in the hydrogen contents, of the various materials.

IV. FUEL FORMULATION AND CHARACTERIZATION

Fuel formulation was performed in two phases. In the first phase, two concentrations each (10 and 20 percent by mass) of Mogul L, SRC-I, k-Fuel and Otisca-T were formulated in the baseline specification DF-2. After the first group of fuels were tested, the clean coal, the Eureka material, Fairless coke and petroleum coke were all used in the second phase to produce 30-percent slurries in the baseline fuel. The purpose for splitting the fuel formulation task was to use information gained during the testing of the first group of fuels to modify and thus improve the formulation of the second group of fuels. Preliminary work was also performed on the development and testing of a high-concentration carbon black slurry. Since this work was of a preliminary nature, the fuel description and the engine test results are presented in Appendix E.

The actual procedures used in preparing the test fuels varied somewhat from fuel to fuel depending upon the form and the properties of the particular material. Certain general procedures were, however, followed for all of the fuels. The fuels were always prepared well in advance of testing. This insured that the materials were thoroughly wetted by the carrier liquid (baseline DF-2). All fuels were homogenized for one hour prior to testing to insure homogeneity of the sample and to break-up agglomerations formed during storage. All of the fuels, except the Mogul L slurries, were prepared in a rolling ball mill, where particle size reduction was accomplished. The baseline particle size of the Mogul L carbon black was small enough that direct formulation was possible.

The rolling ball mill used to prepare the test fuels consisted of a 56 liter, cylindrical, stainless steel vessel which could be mounted on a variable speed drum roller. The ball charge consisted of 90 kg of 3 mm and approximately 9 kg of 12 mm diameter carbon steel balls. The capacity of the mill was approximately 18 liters of balls, 18 liters of slurry, and 18 liters of void space. The design speed of rotation was 45 rpm. In general, standard practice was followed in the design and operation of the mill. It was found, however, that the performance was improved by installation of four 3.8 cm wide baffles parallel to the axis of rotation in order to prevent slippage of the charge and thus improved the tumbling action.

As indicated previously, some of the solids were in the form of pebbles. The first step in the blending process was to dry-grind the pebbles to approximately 40

microns before mixing with the diesel fuel. The coarse blends were placed in the ball mill and rolled until there were no particles larger than 10 microns, as indicated by microscopic analysis of the slurries. This criterion was subsequently made more stringent by attempting to limit the Sauter mean diameter (SMD) to 0.5 microns. This limit was generally approached if microscopic analysis indicated that there were no particles larger than 5 microns. Table 4 is a listing of the grinding times and the SMD of the slurries produced from the various solid materials.

The properties of the various slurries were, in many cases, very similar. Table 5 is a listing of some of the more commonly measured fuel properties for all of the slurries produced and tested in this project. The carbon and hydrogen contents are all very similar, with reduced hydrogen contents as compared to the base fuel. The heating values vary somewhat due to the relatively large variations in the heating values of the solid materials. The volumetric heating values were included to show that, on a volumetric basis, the slurries have higher energy contents than the base fuel. This is an important consideration because the fuel delivery capacity of typical diesel injection systems are limited by volume constraints. Assuming that the slurries would burn in the same fashion as the base fuel, higher engine output could be obtained with the slurries because more energy can be introduced with each injection. Overfueling in this situation would be somewhat compensated for by the reduced oxygen requirement resulting from the lower hydrogen content of the slurries. Another consideration with the high volumetric energy content is the potential for increased range in those vehicles which have volume constraints on fuel storage capacity.

The iron concentration data in Table 5 provides an indication of the contamination introduced by attrition of the ball charge in the ball mill. Some of the solids had high iron concentrations before processing. In such cases, the iron was not necessarily introduced in the ball mill; for instance, the iron in the k-Fuel slurries could be accounted for in the unprocessed solids. The two coke slurries, on the other hand, had very high iron contents due to the long grinding times which are, in turn, an indication of the relative hardness of the various solids.

The pentane insolubles were determined using ASTM D893. The objective of performing this test was to verify the solid concentrations of the various slurries. In most cases, the desired and measured concentrations were very similar; the exceptions were the two SRC-I slurries. Application of extraction procedures using diesel fuel

**Table 4. Grinding Time and SMD Data
for the Eight Test Materials**

<u>Test Material</u>	<u>Grinding Time (hours)</u>	<u>SMD (microns)</u>
Mogul L	0	0.5
SRC-I	12	0.7
Otisca-T	38	1.0
k-Fuel	20	1.4
Clean Coal	32	0.5
Eureka	34	0.5
Fairless Coke	208	0.3
Petroleum Coke	110	0.3

Table 5. Selected Slurry Fuel Properties

<u>Fuel</u>	<u>% C (wt%)</u>	<u>% H (wt%)</u>	<u>Fe ppm</u>	<u>Pentane Insols (wt%)</u>	<u>Gross Heat of Combustion mJ/kg</u>	<u>mJ/liter</u>
Baseline DF-2	86.7	13.0	0	-	44.8	38.1
10% Mogul L	86.8	11.5	0	10.1	44.3	39.7
20% Mogul L	87.4	10.4	0	20.2	43.2	41.0
30% Mogul L	87.9	9.5	0	28.8	41.3	39.2
10% SRC-I	86.6	12.1	0	7.1	44.6	40.0
20% SRC-I	86.7	11.6	66	14.5	43.6	41.4
10% k-Fuel	85.4	12.2	925	8.1	43.9	39.4
20% k-Fuel	83.3	11.1	1940	19.9	42.0	39.9
10% Otisca-T	86.2	12.1	141	9.4	44.5	39.9
20% Otisca-T	85.9	11.5	177	19.9	43.4	41.2
30% Petroleum Coke	85.9	10.1	2100	29.7	41.8	42.2
30% Fairless Coke	86.5	10.0	9652	27.6	41.6	42.0
30% Clean Coal	86.6	10.7	767	29.7	42.2	42.6
30% Eureka	86.4	10.9	78	26.2	43.1	43.6

and various solvents revealed that the large discrepancies in the SRC-I slurries were due to extraction of soluble material from the SRC-I by the diesel fuel.

Determination of the flow properties of the various slurries was made difficult by the fact that all of the slurries exhibited non-Newtonian fluid behavior, necessitating the use of a viscometer that provides a known and constant shear rate, such as a rotational "Couette" viscometer. Preliminary analysis indicated that the slurries are thixotropic, demonstrating shear stress dependence on time and shear rate. The shear-rate dependence is shown clearly in Figure 1, which is a log-log plot of relative apparent viscosity (wrt baseline fuel) versus shear rate for the 30-percent slurries. The lower concentration slurries demonstrated similar behavior, but to a lesser extent. As can be seen in the figure, the apparent viscosities vary from slurry to slurry and as functions of shear-rate. More detailed analysis of the 30-percent Mogul L slurry (carbon black) indicated that the rheological characteristics of the slurries are very complex. For example, at low shear rate (below 50 sec^{-1}), the Mogul L slurry demonstrated flow characteristics typical of slip. The importance of slip was established by the fact that the apparent viscosity decreased with gap size in the viscometer at low (less than 50 sec^{-1}) shear rates.⁽²³⁾ At moderate shear rates (50 to 1000 sec^{-1}), all of the slurries exhibited shear thinning as shown in Figure 1. At the high shear rates (greater than 1000 sec^{-1}), it appears that the apparent viscosity increases with time and shear rate.

One of the most interesting aspects is the appearance of structure forming tendencies and the strong particle-to-particle interactions demonstrated by these slurries. The phenomena are demonstrated by the fact that viscosity ratios of the slurries are typically an order of magnitude larger than the theoretical value for the same concentrations of solid spheres.⁽²⁴⁾

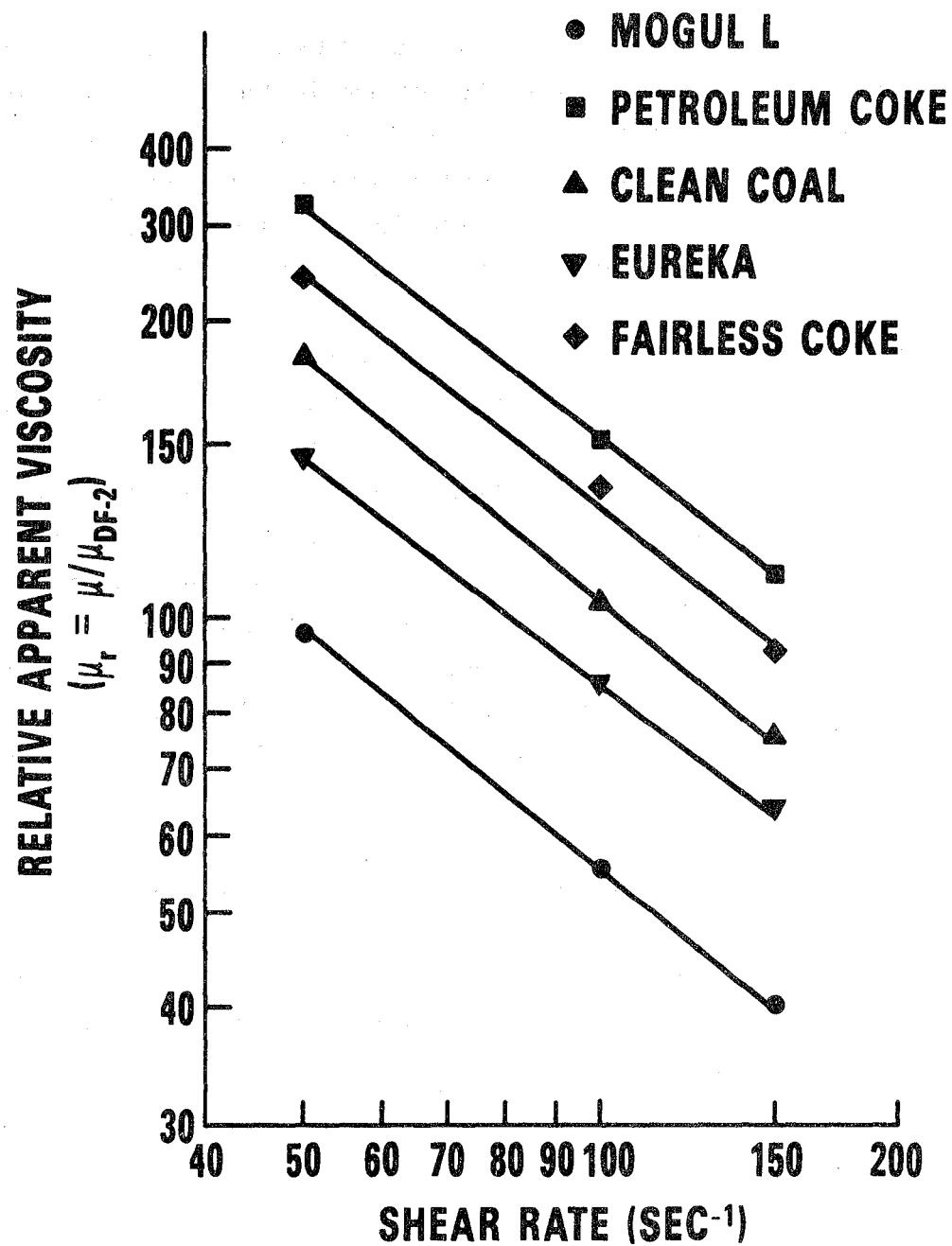


FIGURE 1. RELATIVE APPARENT VISCOSITY VERSUS SHEAR RATE FOR THE 30-PERCENT SLURRIES

V. INJECTION AND ATOMIZATION STUDIES

5.1 INJECTION BOMBS - The injection and atomization studies were performed using a device described in earlier publications.^(9,25) Basically, the apparatus consists of a high-pressure, high-temperature cylindrical bomb equipped with quartz windows which allow direct visual observation through the bomb. Figure 2 is a cross-sectional schematic of the bomb showing the location and orientation of the two different types of injection nozzles which were used in this study. As will be described in another section, two different engine configurations were used during the engine tests; a direct-injection configuration (DI) and a pre-chamber configuration (IDI). A four-hole injection nozzle was used in the DI engine tests while an inward-opening throttling pintle nozzle was used in the IDI engine tests.

The bomb was designed to allow direct observation of the characteristics of diesel-type fuel injection sprays in a high-temperature and high-pressure environment. The design temperature and pressure are 500°C and 4.1 MPa, respectively. Electrical resistance heaters are used to maintain the temperature of the bomb and the inert nitrogen atmosphere which was used to prevent ignition at the higher temperatures.

A jerk pump plunger and barrel (8.5 mm diameter) was installed in a special drive system. The drive system consisted of a pump cam driven at constant speed by an electric motor. A latching mechanism on the cam follower made it possible to bring the cam up to speed before engaging the follower. The number of injections was variable from 2 to 10. Both nozzles were equipped with needle-lift and line-pressure transducers. The transducer signals were used to trigger the various diagnostic systems and to verify that the system dynamics were similar to those of the equivalent systems installed on the test engine.

Two different systems were used to examine the injection characteristics of the various test fuels. A high-speed motion-picture camera was used to determine the global characteristics of the fuel jets while a high-resolution camera system was used to examine the micro-structure of the jets.

5.2 HIGH-SPEED MOVIES - High-speed movies were taken using a Hycam II, 16 mm high-speed motion-picture camera equipped with a Com-Nikor lens (focal length of 88 mm f/2.0, fixed magnification of 0.2X) and a quarter framing head which allowed framing rates of up to 44,000 quarter frames per second. The camera was positioned

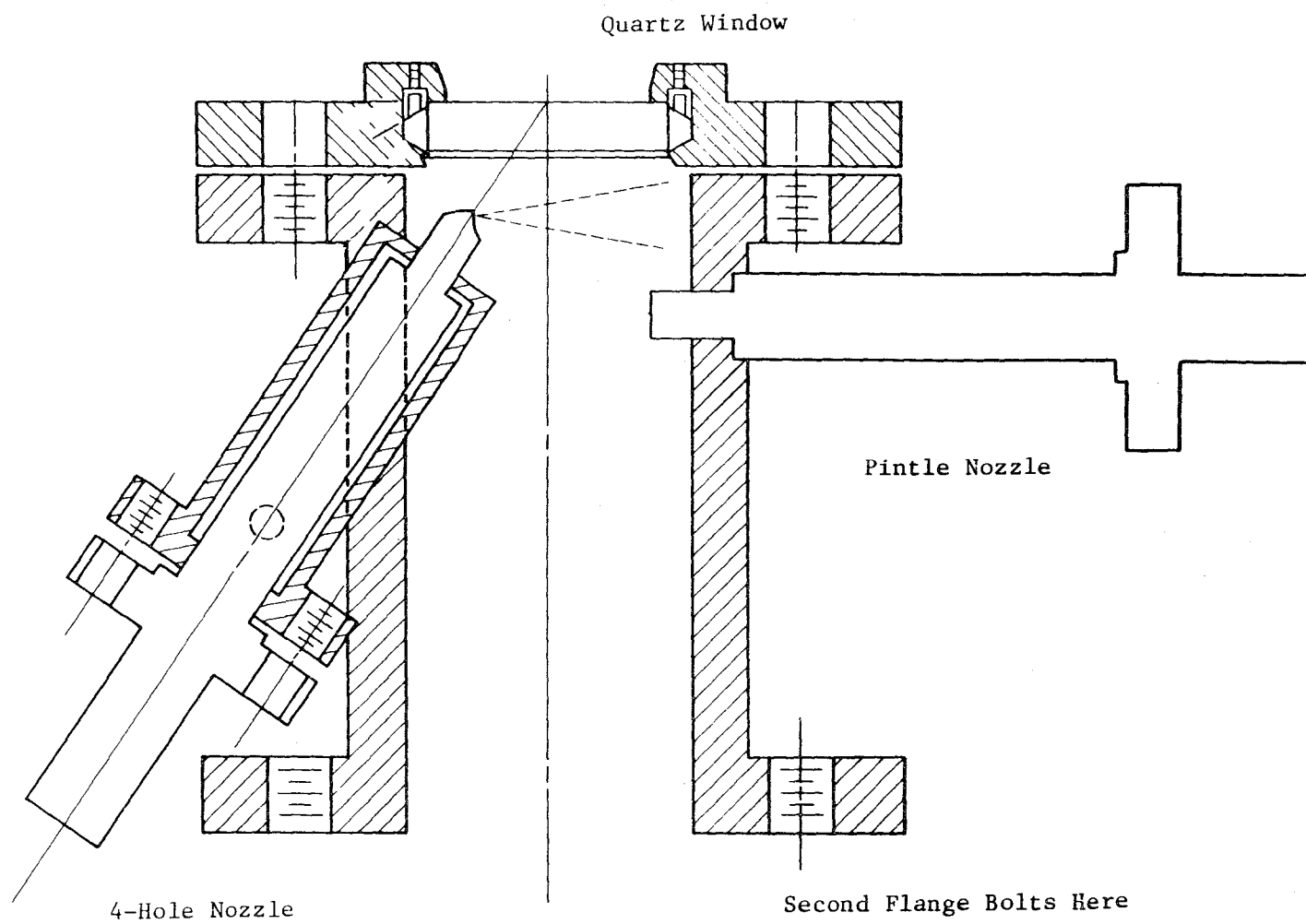


FIGURE 2. INJECTION AND ATOMIZATION BOMB

such that the lens was focused on the center of the spray. Back-lighting was provided using a 1000w Tungsten-Halogen light. All movies were taken at 25,000 quarter frames per second providing a temporal resolution of $40 \mu\text{s}$. (Examples of several frames of high-speed movie can be seen in Reference 9.)

Data obtained from the movies consisted of the penetration distance versus time and the spray cone angle. Penetration rate is defined as the time rate at which the tip of the spray advances away from the injection nozzle. Cone angle is defined in terms of the angle encompassed by the spray with the apex located inside the injection nozzle due to the fact that the jet has a finite diameter at the nozzle exit. The data was reduced from the movies using a Vanguard motion analyzer. The penetration data was reduced in terms of the length of the spray in each quarter frame. The cone-angle data was obtained by averaging over 10 to 15 frames, the angle formed by two lines drawn tangent to the nozzle orifice and edge of the spray at approximately 13 mm from the nozzle.

High-Speed Movie Data - The conditions at which each of the fuels were tested in the spray bomb are outlined in Table 6. The table is also a summary of the cone angle data for the various test conditions and test fuels. As can be seen, the higher concentration slurries were all tested using the pintle nozzle. Attempts to run the Otisca-T and k-fuel slurries through the four-hole nozzle during tests in the DI engine were unsuccessful due to problems with deposit formation on the inside of the nozzle orifice and due to sticking of the needle valve in the nozzle. As will be described in more detail in another section, one or the other of these problems would appear within minutes of switching to fuels formulated using either of these solids. The pintle nozzle performed much better with these fuels but nozzle failures were still a problem which made it impossible to obtain either spray or engine data for fuels formulated with either the Otisca-T or k-Fuel. The experiences with the fuels did, however, indicate that the pintle nozzle was much more tolerant of the slurries. It was for this reason that the second group of fuels, the higher concentration slurries, were tested using the pintle nozzle and the IDI engine.

General characteristics of the sprays produced by each of the nozzles were readily apparent in the movies. The four-hole nozzle produced a flow which is typical of the classic jet break-up, with a solid core of fuel issuing from the orifice. Moving away from the nozzle, the jet widens due to air entrainment and the jet ultimately (25 to 40 mm from the nozzle) breaks up into what could be described as a spray with no

Table 6. Spray Cone Angle at 13 mm from Nozzle;
 $P_{\text{Bomb}}=\text{MPa}$, $T_{\text{Bomb}}=^{\circ}\text{C}$

<u>Fuel</u>	<u>Bomb Conditions</u>					
	<u>P=4.23</u> <u>T=470</u>	<u>P=2.17</u> <u>T=470</u>	<u>P=1.67</u> <u>T=26</u>	<u>P=0.55</u> <u>T=470</u>	<u>P=0.1</u> <u>T=470</u>	<u>P=0.1</u> <u>T=26</u>
<u>4-Hole Nozzle</u>						
Base	10.7	8.6	9.7	5.1	5.4	-
10% Mogul L	-	-	9.1	-	-	-
20% Mogul L	7.9	8.2	8.0	-	4.9	-
10% SRC-I	-	-	8.4	-	-	-
20% SRC-I	9.2	-	7.5	-	-	-
<u>Pintle Nozzle</u>						
Base	-	-	12.4	-	-	21.7
30% Mogul L	-	-	8.2	-	-	22.6
30% Fairless Coke	-	-	8.0	-	-	17.1
30% Eureka	-	-	6.0	-	-	14.1
30% Petroleum Coke	-	-	5.7	-	-	14.6
30% Clean Coal	-	-	5.9	-	-	14.7
20% Mogul L	-	-	8.8	-	-	19.3

obvious core of liquid. The movies of the pintle nozzle revealed characteristics typical of inward-opening, throttling pintle nozzles.⁽²⁶⁾ The initial jet issues from the nozzle with little or no break-up as it travels away from the nozzle. As the pintle moves in, a second spray develops at the nozzle which appears to be a hollow cone spray with sheets of fluid traveling for several millimeters from the nozzle before breaking into a dispersed spray.

Examination of the cone-angle data presented in Table 6 reveals several facts. For the four-hole nozzle, the density of the environment has a stronger effect on the cone angle than temperature. This is indicated by the very similar results for corresponding tests at $P=4.23$ MPa, $T=470^{\circ}\text{C}$ and $P=1.67$ MPa, $T=26^{\circ}\text{C}$, conditions at which the densities of the environment are nearly equivalent. On the other hand, holding the temperature constant while decreasing the pressure (and therefore the density) of the environment results in a very apparent decrease in the cone angle, as shown for both the baseline fuel and the 20 percent Mogul L slurry. This is in agreement with theory, which indicates that as the density of the environment is increased the cone angle increases and the penetration rate decreases. The penetration-rate data for the base fuel is presented in Figure 3 for the same temperature at three different pressures. The results do show that the penetration decreased with increases in the density of the environment.

At the higher temperature, the 20 percent SRC-I slurry had a larger cone angle than the corresponding Mogul L slurry, even though the apparent viscosity of the SRC-I slurry was higher than the Mogul L slurry. It is difficult, however, to interpret the results based on viscosity because of the non-Newtonian behavior of the slurries combined with the fact that it is difficult, if not impossible, to define the characteristic shear stress encountered by the fuels in the injection system.

As indicated previously, the pintle nozzle performed much differently than the four-hole nozzle. The cone-angle data presented in Table 6 for the pintle nozzle is the data for the second jet, the one which resembled a hollow cone spray. For this nozzle, the cone angle decreased with increasing pressure (density), the opposite of the results observed for the four-hole nozzle. Swirl atomizers produce sprays which are affected the same way by increases in the density of the environment. The effect of density on penetration rate is shown in Figure 4 for the baseline fuel. Increasing the density resulted in a decrease in penetration rate, a result which is also noted in swirl atomizers where the change is observed as a decrease in the volume of the spray. The

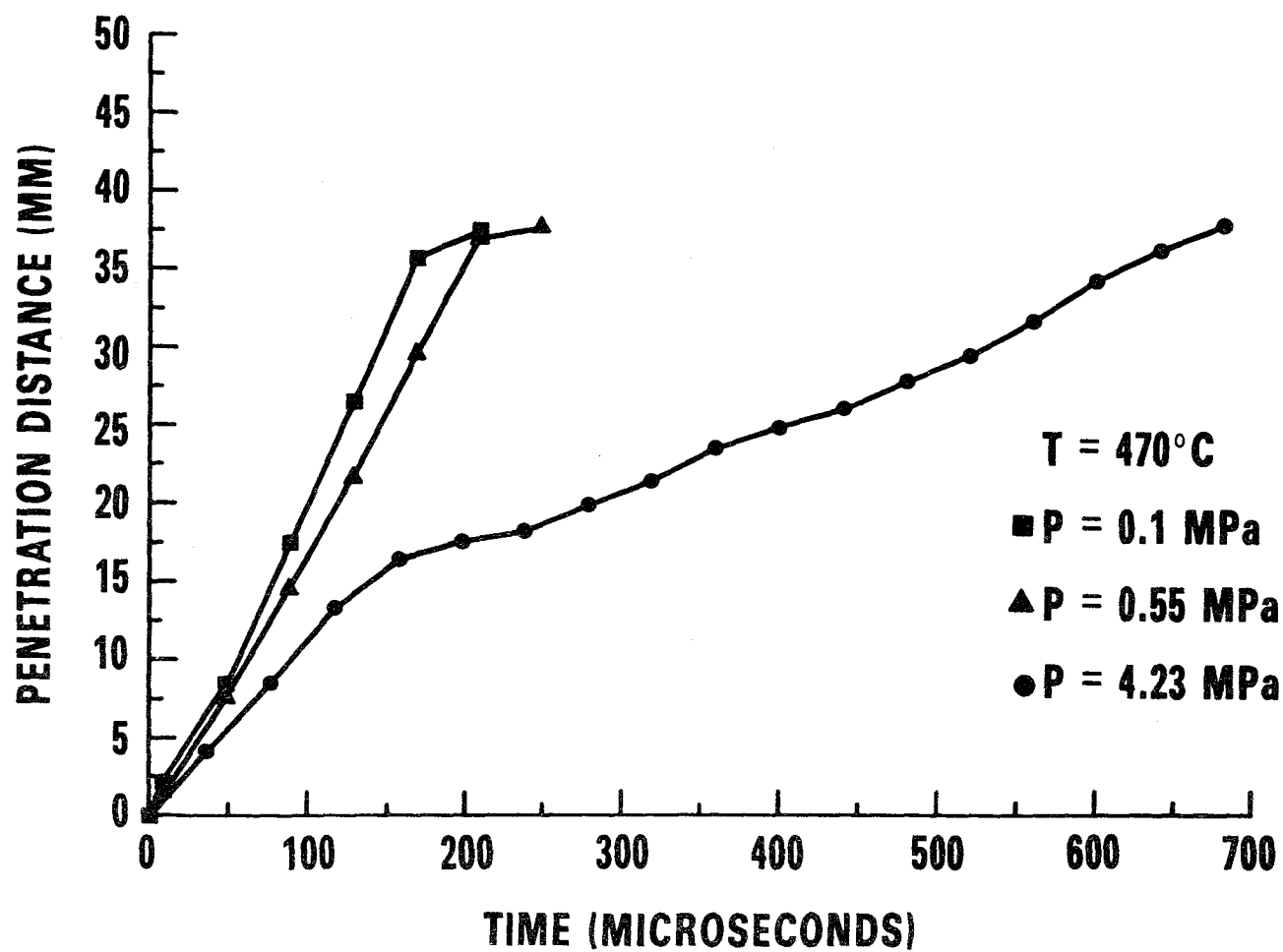


FIGURE 3. PENETRATION DISTANCE VERSUS TIME, BASELINE FUEL, FOUR-HOLE, THREE DIFFERENT PRESSURES, $T = 470^{\circ}\text{C}$

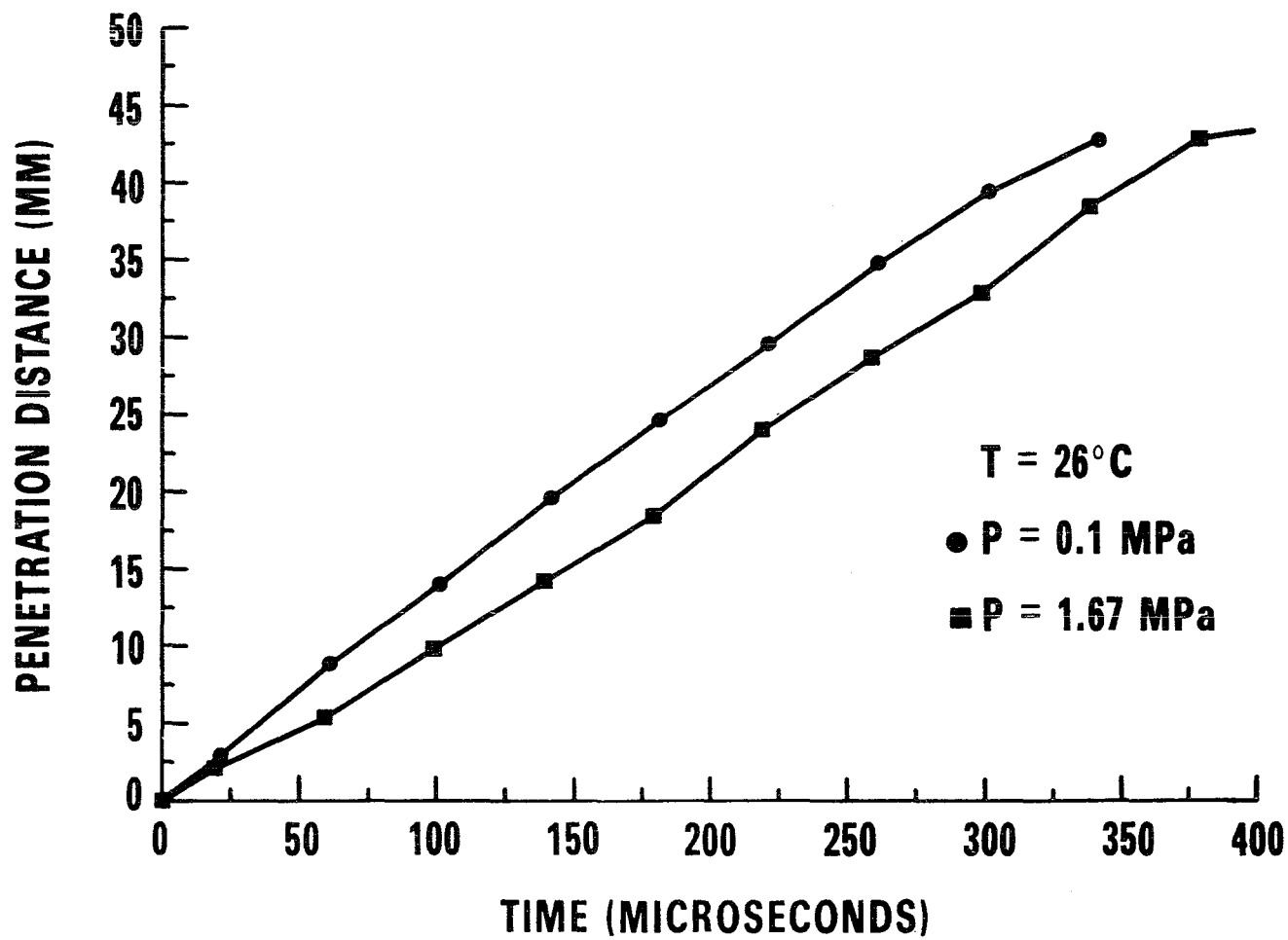


FIGURE 4. PENETRATION DISTANCE VERSUS TIME, PINTLE NOZZLE, TWO DIFFERENT PRESSURES, $T = 26^{\circ}\text{C}$

implications of these observations as they relate to spray modelling are discussed in other sections.

The penetration rates of the slurries were always slightly higher than the base fuel in the four-hole nozzle. The results do not appear to be strongly affected by concentration, as shown in Figure 5, for the SRC-I slurries; the Mogul L slurries showed very similar results. For the baseline fuel, there was some temperature dependence, with an apparent decrease in the penetration rate with an increase in the temperature of the environment. The result is most probably due to vaporization and thus disappearance of the liquid fuel. The slurries did not exhibit the temperature dependence because the solid component would remain and be visible even if the liquid component vaporized.

At the lower environment density, the penetration rate for the pintle nozzle was affected by the composition of the fuel, as shown in Figure 6, for the 30-percent slurries. There does appear to be some relationship between apparent viscosity, the cone angle, and the penetration rate in the pintle nozzle. The 30-percent Mogul L had the lowest apparent viscosity (Figure 1), the lowest penetration rate (Figure 6), and the largest cone angle. The 30-percent petroleum coke, on the other hand, had the highest apparent viscosity, the highest penetration rate, and the equivalent of the smallest cone angle. The other slurries follow approximately the same trends with an increase in apparent viscosity resulting in an increase in penetration rate and a decrease in the cone angle. The penetration-versus-time data is presented in Appendix B for all of the fuel/test condition combinations.

5.3 HIGH-RESOLUTION PHOTOGRAPHY - The diesel spray was "frozen" with the use of a laser strobe and a large format 4" x 5" camera. The camera consisted of a Sinar system with extra bellows arranged for 5X magnification using a Com-Nikor 88 mm focal length f/2.0 high-resolution lens. The camera was shutterless and operated in a dark room with a laser as a strobe. An aperture of f/2.8 or f/4.0 was employed for most photos, representing a compromise between the best modulation transfer function (MTF) and sufficient energy to expose the film. Survey-type work was performed with Polaroid Type 55 Positive/Negative film, and high resolution images were recorded with KODAK SO-253 holographic type film. Normal processing was used except that the SO-253 was push-processed in a few cases. The Polaroid Type 55 film is the highest resolution "instant film", while the SO-253 has substantially more resolving capabilities but requires full processing.

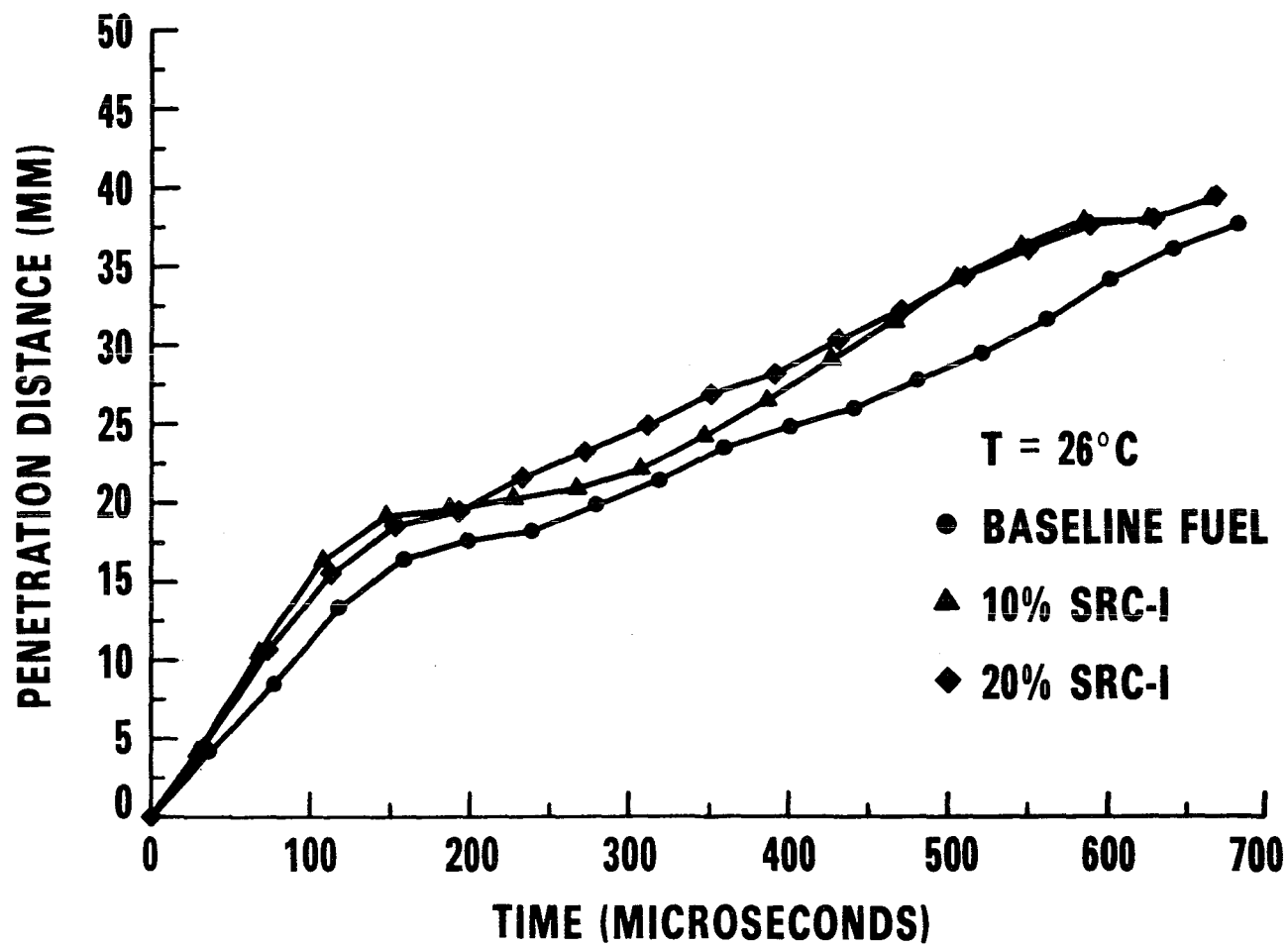


FIGURE 5. PENETRATION DISTANCE VERSUS TIME, FOUR-HOLE NOZZLE, BASELINE AND SRC-I SLURRIES, $P = 1.67 \text{ MPa}$, $T = 26^\circ\text{C}$

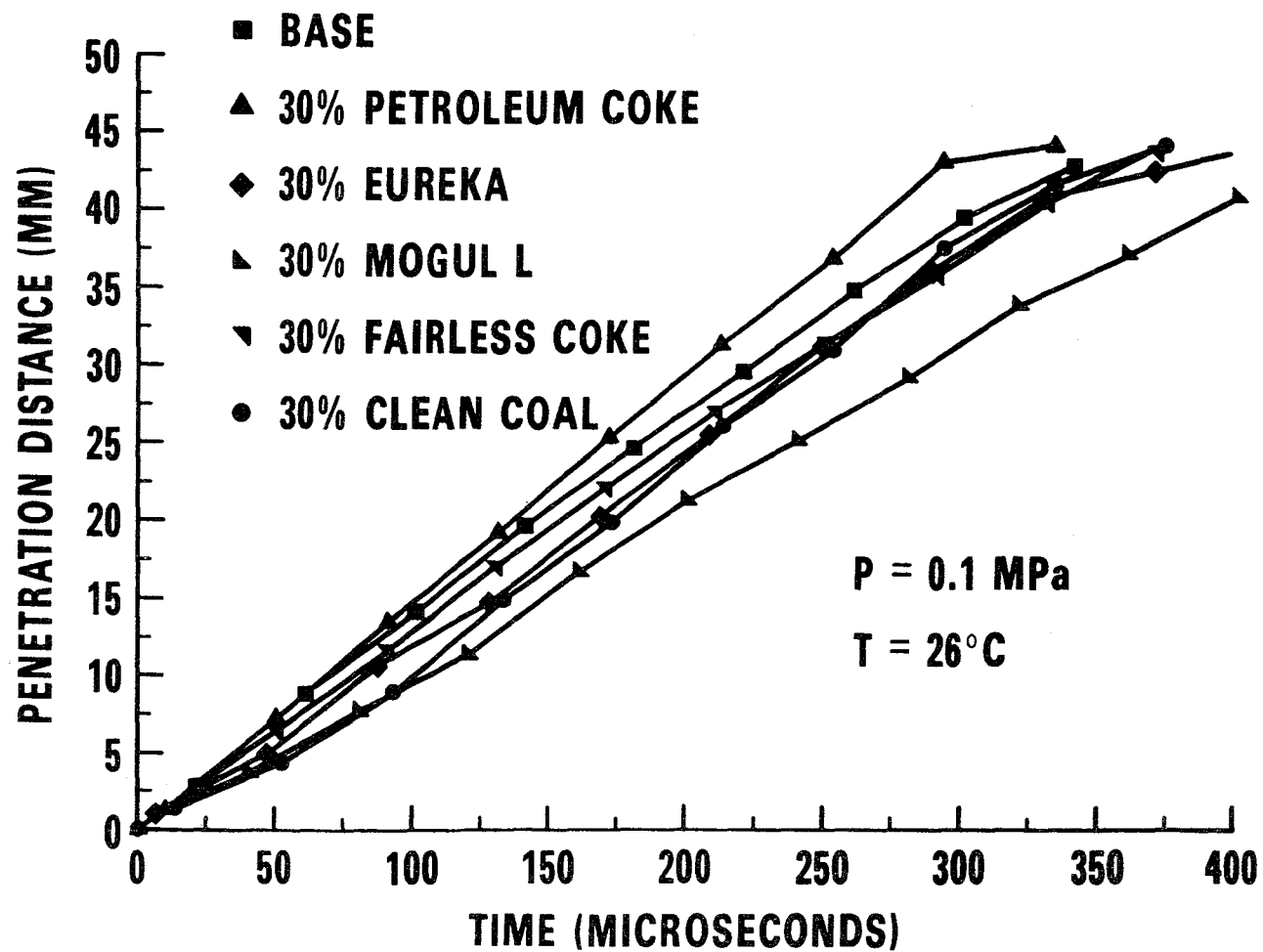


FIGURE 6. PENETRATION DISTANCE VERSUS TIME, PINTLE NOZZLE, BASELINE AND 30% SLURRIES, $P = 0.1 \text{ MPa}$, $T = 26^\circ\text{C}$

A Nd:YAG laser model DCR-1 manufactured by Quanta-Ray was used as the laser strobe. It was frequency-doubled from a wavelength of 1064 nm (near infrared) to 532 nm (green) using standard crystals and the 1064 nm pump beam was separated and dumped while the 532 nm was used for the photography. Q-switch operation with a single pulse was used for all pictures. Flashlamp energies of 60 Joules were used with the Polaroid film, while full flashlamp energies of 90 Joules were used for the high resolution film, producing a laser pulse of 6 ns and 22 MW. The 6 ns pulse was sufficiently fast to stop all spray movement. The laser beam was expanded with a negative lens and diffused with a ground glass and used as back-lighting.

Synchronization electronics were constructed which allowed for the proper timing of the laser pulse relative to the injection event. The laser operates most reliably and with the most power if pulsed regularly at about 10 Hz. With the Q-switch off, the flash lamps were pulsed at 10 Hz (100 ms between pulses) until a button was manually pushed to begin the timing process. A 100 ms delay after the button was activated allowed the flash lamp capacitors to fully recharge, and then a pulse was sent to the injection system to initiate injection at the next cam rise. Needle lift was detected electronically and a signal was sent back to the electronic synchronization box. After a delay adjustable in 0.1 ms increments from 0 to 9.9 ms, the flashlamps were fired, followed after 0.27 ms by the Q-switch and laser pulse. Thus, the minimum delay between the onset of needle lift and the laser strobe flash was 0.27 ms and the maximum was 10.17 ms.

High-Resolution Photography Data - As mentioned previously, two types of injectors were used in the engine experiments and these were duplicated in the spray photography. The spray characteristics were very different. Some of the observations described in this section and based on the still photographs are very similar to those described in the previous section which were based on high-speed movies. The four-hole nozzle produces a solid jet that breaks up into a fairly narrow cone angle of about 12° . Most of the cone is composed of ligaments and large drops which break into smaller drops on the order of 10 micrometers in diameter at the edge of the spray. The spray is mostly uniform in cone angle and appearance during the injection process. The throttling pintle nozzle, on the other hand, is not uniform but has two separate types of spray action. At the beginning of injection, the fuel comes out as a jet which, at atmospheric conditions, does not disperse or break-up at all. As the air density is increased to that typical of an engine, the jet does disperse somewhat. During the main part of the injection process, where most of the fuel is injected, the

spray is a hollow cone type with a cone angle of about 30° . Most of the fluid appears to be concentrated near the outer edges of the cone. As was the case for the four-hole nozzle injector, the majority of the fuel in the 25 mm long region of the photograph was in the form of ligaments and large drops. As air was entrained and mixed with the spray, these ligaments would leave the main body of the spray and break into small drops. For the throttling pintle nozzle, these drops were mostly in the size range from 5 to 25 micrometers. The slurries, particularly Mogul L, exhibited some much larger drops or particles which escaped the main spray region.

For each fuel type, high-resolution pictures were recorded at atmospheric conditions, and at an environment pressure of 1.67 MPa and a temperature of about 25°C . This elevated pressure condition produced an air density equivalent to that of engine compression conditions, with air compressed to 483°C and 4.23 MPa. For the four-hole nozzle, photographs were also recorded at this elevated temperature and pressure condition. High-speed movies indicated that penetration was determined by the air density alone with the temperature increase from 25°C to 470°C only affecting vaporization of the tip. This implies that in this high Reynolds number regime the increased air viscosity, by a factor of about 1.6, at the higher temperatures does not affect penetration rates. Increased temperature did have an effect on the drop-size distribution.

Three fuels, the base fuel (#2 diesel), a 20 percent Mogul L slurry, and a 20 percent SRC-I slurry were tested with the four-hole nozzle. At all conditions, the sprays appeared to be constant in terms of cone angle and form throughout the spray process with this nozzle. At atmospheric conditions, the air density was sufficiently low to examine some of the spray cone over the 25 mm region shown on the photographs. Contrary to the predictions made by some workers modelling diesel injection processes⁽²⁷⁾, the cone was not composed solely of very fine drops on the order of three micrometers in diameter, but rather consisted of ligaments and large drops with dimensions on the order of tens and hundreds of micrometers, as shown in Figure 7. The spray was a solid cone with an angle of about 12° , and along the edge of the cone the ligaments and drops seemed to shear into smaller drops. Examining the drop-size distribution along the edge of the spray by number (rather than weight or volume) showed that the great majority, approximately 75 to 95 percent of the drops, to be in the range of 5 to 10 micrometers. Drops smaller than five micrometers could not be resolved. Outside the dense central spray, there were few, if any, drops larger than 15 micrometers. Drop-size data are reported here only along the periphery of the



FIGURE 7. HIGH-RESOLUTION PHOTOGRAPH, FOUR-HOLE NOZZLE

spray because the central spray was too dense to record images of individual drops, and because ignition occurs along the edge of the spray where the fuel and air are well mixed.

At atmospheric temperature (25°C), but elevated pressure 1.67 MPa, all fuels showed an increase in drop sizes along the edge of the spray. For the base fuel and 20-percent SRC-I, the majority of the drops were still in the 5- to 10-micrometer range, but there were more drops in the larger size classes, but few if any, larger than 25 micrometers. For the 20-percent Mogul L, the majority of the drops or particles were larger, in the 10- to 15-micrometer range, and a few drops were as large as 50 micrometers.

At elevated temperatures, 470°C and pressure 4.25 MPa, the base fuel and 20-percent SRC-I showed about 85 to 90 percent of the drops along the periphery of the spray to be in the size range of 5 to 10 micrometers. For the 20-percent Mogul L, the size distribution was similar to that at 1.67 MPa, with a peak in the 10- to 15-micrometer range, but with no drops larger than 25 micrometers.

Seven fuels were tested with the pintle nozzle, the baseline fuel, 30-percent Mogul L, 20-percent Mogul L, 30-percent Fairless coke, 30-percent petroleum coke, 30-percent Eureka, and 30-percent clean coal. As mentioned previously, the throttling pintle nozzle operates in two distinct modes. This is demonstrated in Figures 8-10, which show the beginning of injection for 30 percent Mogul L slurry. As the pintle begins to retract into the nozzle, the spray comes out as a narrow stream, with surface tension forces probably limiting the dispersion. At an engine speed of 750 rpm, the initial jet lasts about 0.4 ms and then the spray abruptly changes into a hollow cone spray with a cone angle of about 30°. The hollow cone spray exhibits much better dispersion than the central jet, but large ligaments are still evident as shown in Figure 11. The base fuel appears to atomize more finely than the slurries during the hollow cone portion of the spray, as shown in Figure 12, comparable in time and bomb conditions to those of Figure 9 for the 30-percent Mogul L.

The break-up of ligaments into drops at the edges of the spray occurs for all the fuels studied at both atmospheric air density and the density at injection in an engine. Some examples at atmospheric density are shown for 30-percent Fairless coke in Figure 13, where the enlargement is of an area located 1.4 cm from the nozzle on the fringe of the spray. At densities equivalent to those in the engine at the time of injection, the spray is much denser, most being too opaque to see any details within the spray, but the edges still show ligament breakup into drops as shown in Figure 14

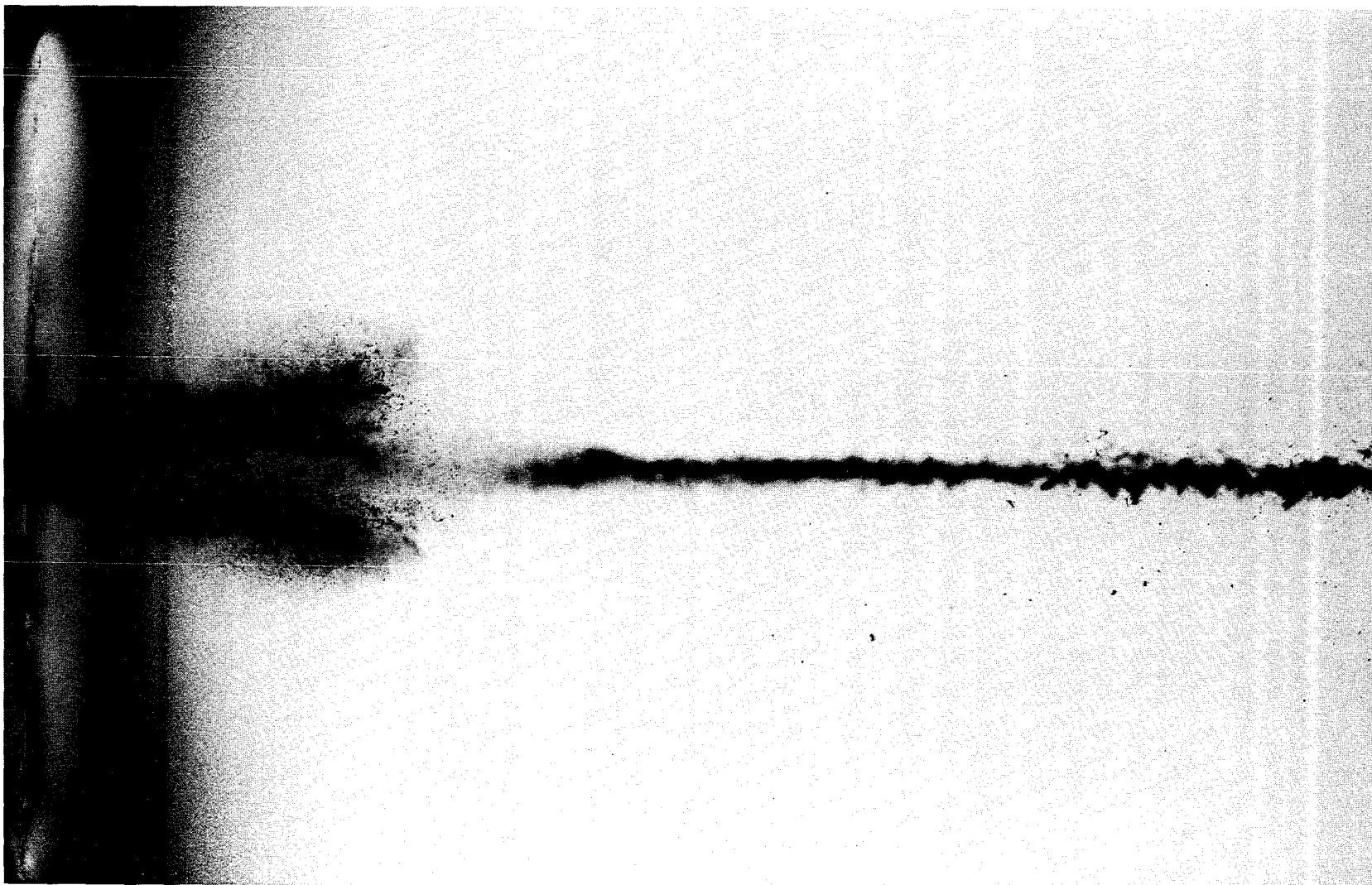


FIGURE 8. HIGH-RESOLUTION PHOTOGRAPH, PINTLE NOZZLE, $P = 0.1$ MPa,
 $T = 26^{\circ}\text{C}$, at 0.27 ms, 30% MOGUL L

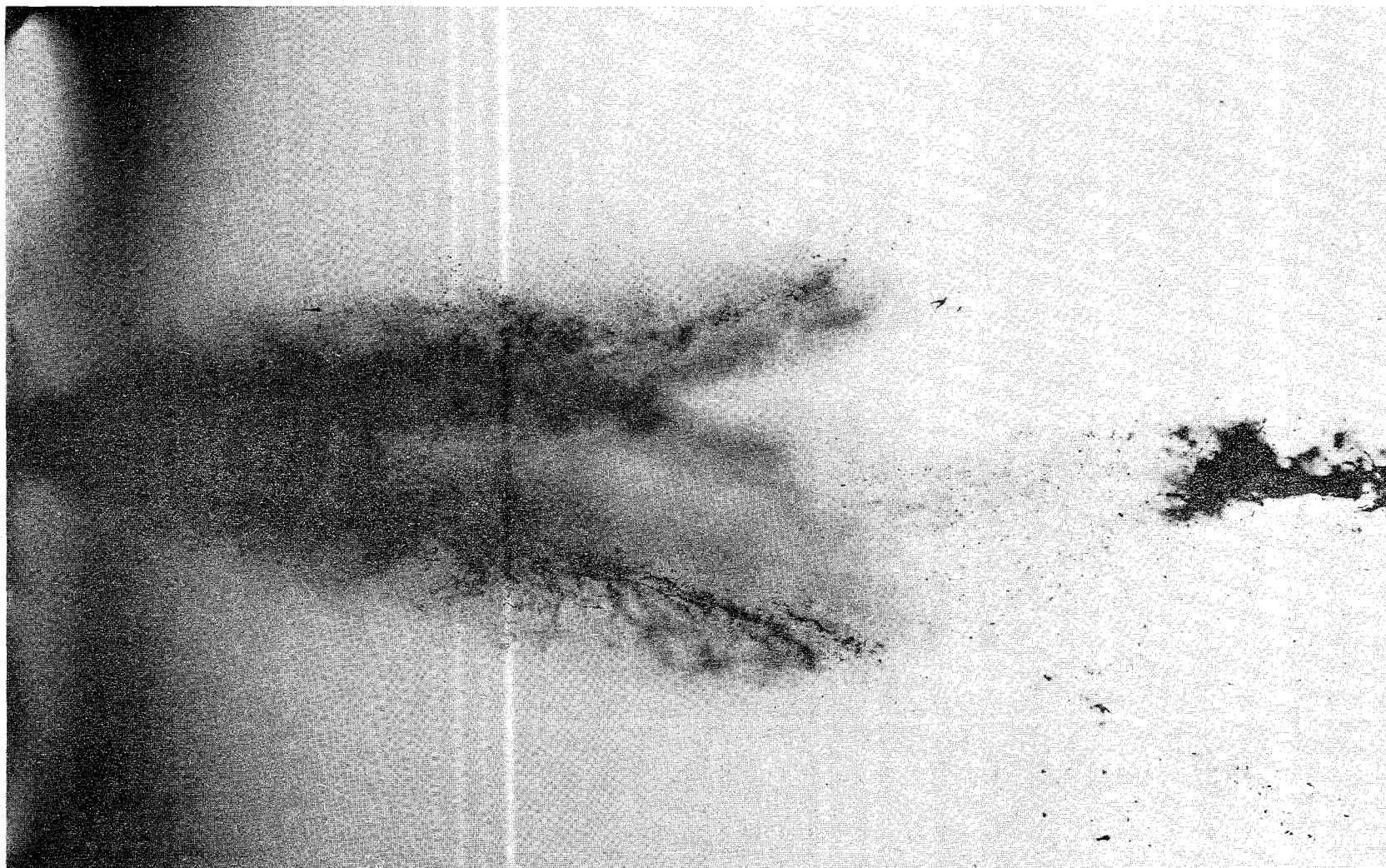


FIGURE 9. HIGH-RESOLUTION PHOTOGRAPH, PINTLE NOZZLE, $P = 0.1$ MPa,
 $T = 26^{\circ}\text{C}$, at 0.37 ms, 30% MOGUL L

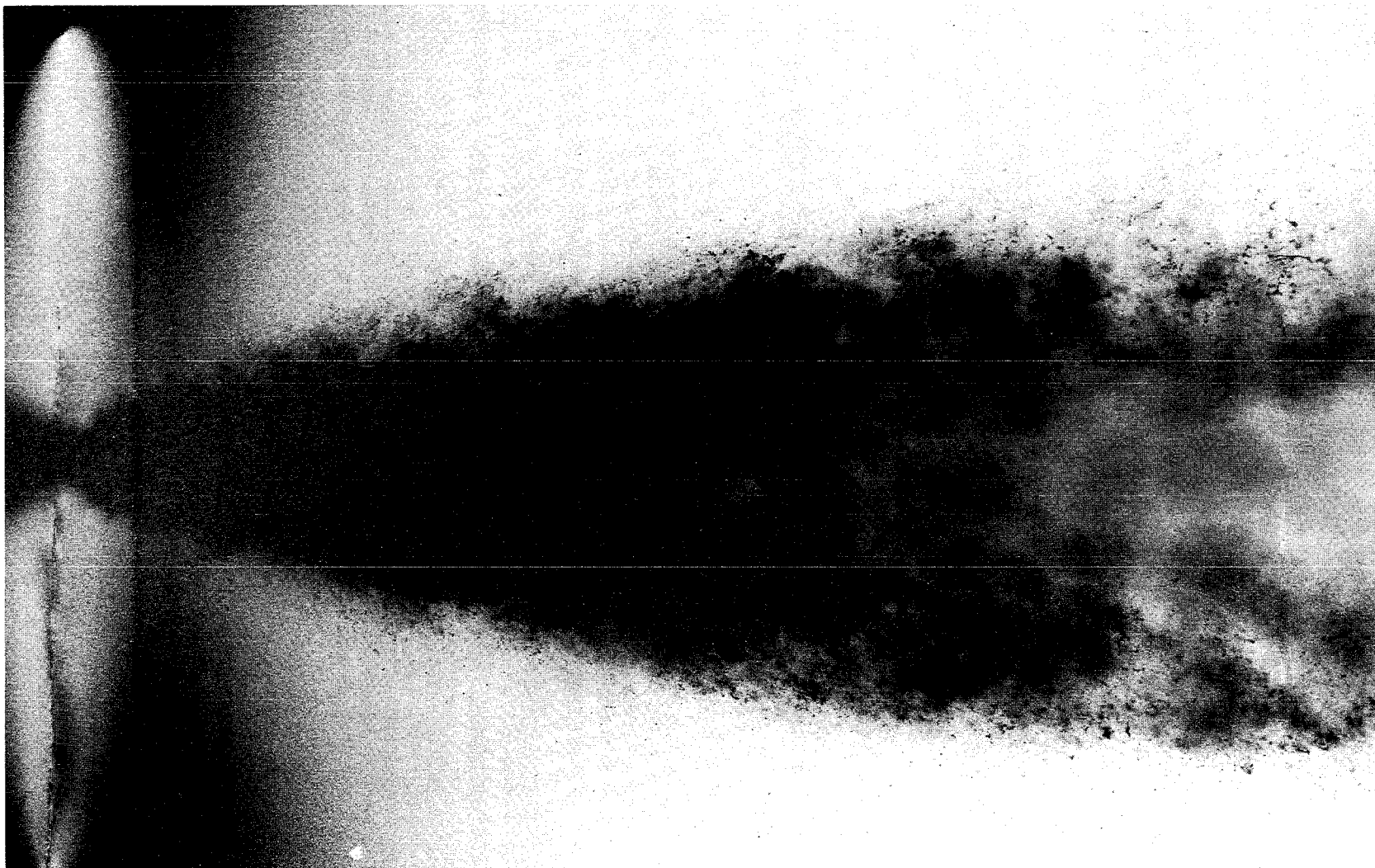


FIGURE 10. HIGH-RESOLUTION PHOTOGRAPH, PINTLE NOZZLE, $P = 0.1$ MPa,
 $T = 26^{\circ}\text{C}$, at 0.47 ms, 30% MOGUL L

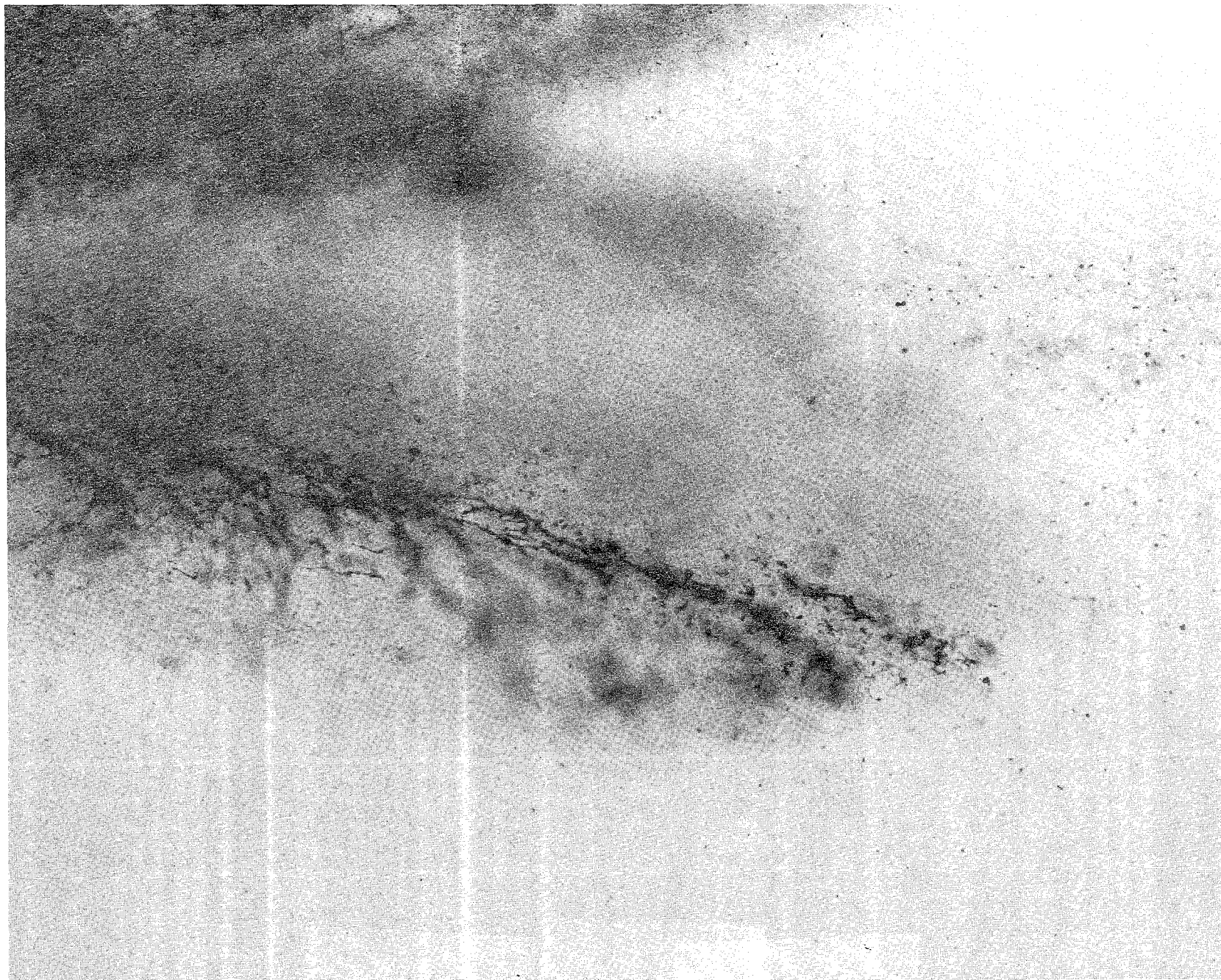


FIGURE 11. HIGH-RESOLUTION PHOTOGRAPH PINTLE NOZZLE, 5X MAGNIFICATION
OF FRINGE, $P = 0.1$ MPa, 26°C at 0.37 ms, 30% MOGUL L

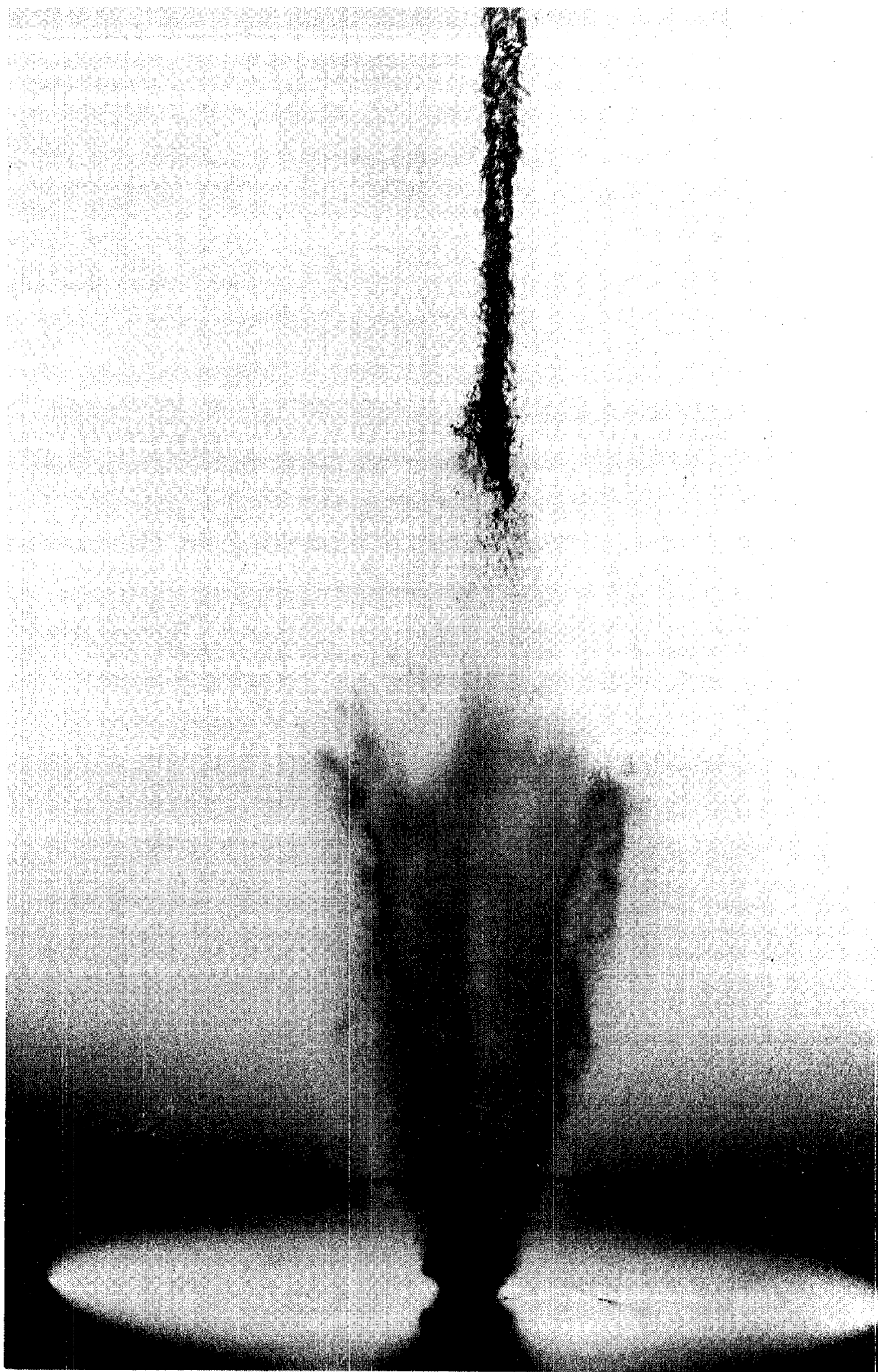


FIGURE 12. HIGH-RESOLUTION PHOTOGRAPH, PINTLE NOZZLE, $P = 0.1$ MPa,
 $T = 26^{\circ}\text{C}$, at 0.27 ms, BASELINE FUEL

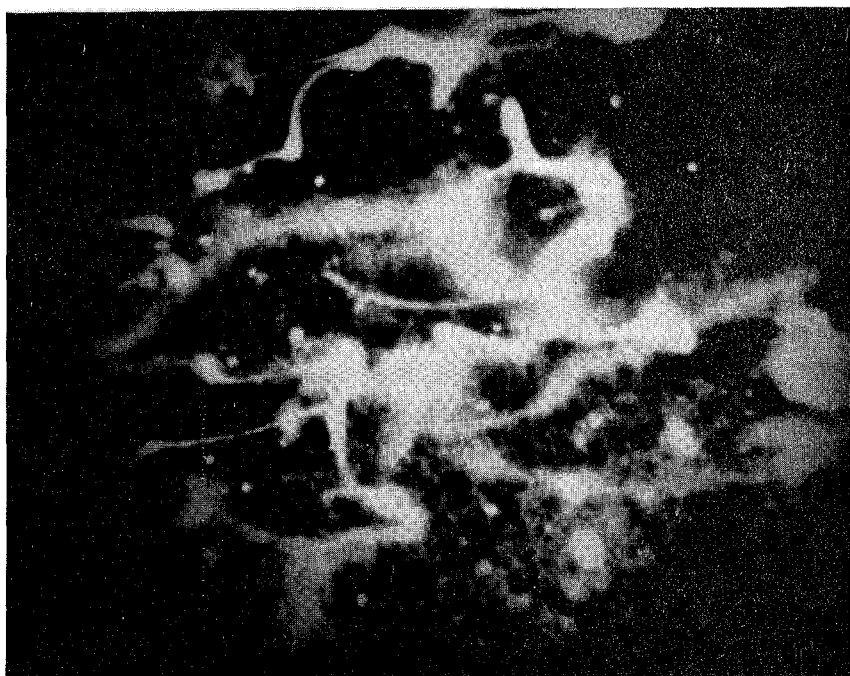


FIGURE 13. HIGH-RESOLUTION PHOTOGRAPH, 187X 30% PETROLEUM
COKE SLURRY, $P = 0.1 \text{ MPa}$, $T = 26^{\circ}\text{C}$

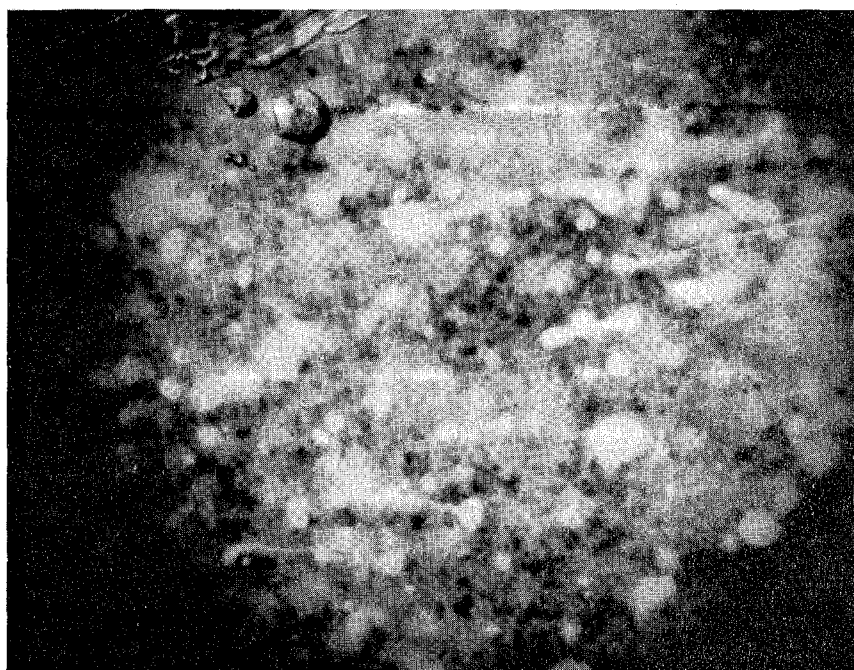


FIGURE 14. HIGH-RESOLUTION PHOTOGRAPH, 197X, 30% FAIRLESS
COKE SLURRY, $P = 167 \text{ MPa}$, $T = 26^{\circ}\text{C}$

for 30-percent Fairless coke 1.4 cm from the nozzle exit. Theoretical models for spray processes should recognize the existence of these ligaments.

Outside the most dense part of the spray, the pintle nozzle produces drops or particles that range in size from 5 to 25 micrometers with some larger structures evident but apparently unstable as they are generally parts of ligaments or double drops undergoing fragmentation. Detailed size analysis has not been performed to compare the fuels, but the two Mogul L slurries show some larger structures than the other fuels.

VI. ENGINE EXPERIMENTS

As indicated previously, the engine experiments were performed using two different configurations of the CLR single-cylinder research engine. The objectives of the engine experiments were to determine combustion characteristics, the performance characteristics, and the operational characteristics of each of the test fuels. The performance characteristics relate to the efficiency of conversion of the fuel chemical energy to mechanical work. The operational characteristics relate mainly to the ability to deliver the fuel to the combustion chamber. The equipment used in these experiments are described and the results and observations are presented and discussed in the following sections.

6.1 TEST EQUIPMENT AND PROCEDURES - A single-cylinder, four-stroke CLR research engine was used for these experiments. Two different heads and pistons were available for the engine so that it was possible to assemble it as a direct-injection engine or as a prechamber, or indirect-injection, engine. In the direct-injection configuration, a four-hole injection nozzle was installed in the head such that the sprays were located symmetrically in the "Mexican hat" combustion chamber machined in the piston. The head for the indirect-injection configuration was equipped with a Caterpillar-type prechamber, and an inward opening, throttling pintle injection nozzle was used in this configuration. The piston had a shallow dish machined in the crown and located symmetrically at the discharge from the prechamber. The specifications for both configurations are listed in Table 7.

The same (jerk-pump type) injection pump (CAV Minimec P4862/9A) was used for both engine configurations. An 8.5 mm diameter barrel-and-plunger assembly was used for all tests. Both nozzles were equipped with needle-lift sensors and line-pressure transducers which were used to monitor the performance of the injection system during the tests.

The engine was directly coupled to a motoring eddy-current dynamometer which was used to start, motor, and control the engine. The dynamometer controller was designed for speed control to within ± 5 rpm of the set point. Torque was measured using a strain gage load cell.

Fuel flow rate to the engine was measured gravimetrically using an electronic weighing platform. Inlet air was supplied through a pressure regulator from a large

Table 7. CLR Engine Specification

	<u>DI</u>	<u>IDI</u>
Bore (cm)	9.65	9.65
Stroke (cm)	9.53	9.53
Rod Length (cm)	17.46	17.46
Displacement (cm ³)	697.4	697.4
Compression Ratio	14:1	20:1
Combustion Chamber	"Mexican Hat"	Pre-Chamber
Injection Pump	CAV-8.5 mm	CAV-8.5 mm
Injection Nozzle	Bosch 4-hole	Bosch Pintle
Opening Pressure (MPa)	27.6	20.7
Injection Timing (°BTDC)	16.0	7.5

tank connected to the shop compressed air system. The pressure and temperature of the air was controlled for constant mass flow rate, which was monitored using a precision rotameter. The relative humidity of the inlet air was limited to 30 percent.

A water-cooled piezoelectric pressure transducer was installed in the head of the test engine to monitor the instantaneous cylinder pressure. The cylinder pressure signal was supplied to a high-speed A/D which was triggered every 0.7 degrees of crank shaft rotation using an optical rotary switch. The pressure records from 10 cycles were averaged and used to compute the heat release rate, the indicated power, and various combustion parameters (Q_t , $\bar{\theta}$, \bar{Q}) described in previous papers.^(9,25) Briefly, Q_t provides a measure of combustion efficiency while $\bar{\theta}$, \bar{Q} , the center of area of the heat release diagram, provides an indication of the timing and duration of the combustion process.

The gas phase emissions (CO , CO_2 , O_2 , NO/NO_x , and unburned hydrocarbons) were measured mainly as a diagnostic of the combustion process. The emissions data was used to calculate the overall air-fuel ratio. These calculations were generally within five percent of agreeing with the air-fuel ratio determined from the fuel and air flow measurements.

The amount of filterable material in the exhaust was determined by measuring the weight change of a filter through which a measured volume of exhaust was passed. The objective of the determination was solely to provide an indication of the amount of unburned solids in the exhaust not as an absolute measure of the particulate emissions.

All of the fuels were tested at three different steady-state conditions -- three loads at 1500 rpm. The loads were defined as 50, 75, and 100 percent, where 100 percent was the load at 20:1 air-fuel ratio using the baseline fuel. The engine was started and warmed-up using the baseline fuel before switching to the test fuel. The engine was allowed to run on the test fuel for at least one hour before taking data. It was during this period that operational problems were observed and corrected when possible.

The data set consisted of fuel consumption, air flow, exhaust emissions, and cylinder pressure data. The heat release rates and the combustion diagnostic parameters were calculated on-line during the data acquisition process. The fuel and

energy consumption data was reported on a brake as well as an indicated specific basis.

6.2 EXPERIMENTAL RESULTS - As indicated previously, the baseline fuel and six slurries, 10- and 20-percent Mogul L, 10- and 20-percent SRC-I, 20-percent k-Fuel, and 20-percent Otisca-T, were tested in the DI engine. Operational problems with Otisca-T and k-Fuel could not be overcome, therefore combustion and performance data are not available for these fuels.

The slurries produced using both of these materials all exhibited the same types of operational problems. In the standard injection system, the needle valve would begin to stick shortly after switching to the test fuels. This would be followed immediately by sticking of the injection pump plunger in the barrel. These problems were overcome by increasing the clearances in these two areas, thus allowing higher leakage rates which tended to prevent sticking of the parts. The increased leakage rate was overcome by using a larger diameter barrel and plunger. Tests with the modified system were only slightly longer in duration than the previous experiments due to the onset of rapid deposit formation on the inside of the holes of the injection nozzle; deposits typical of those of thermally unstable fuels. Based on the results of the pentane insoluble tests (Table 5), it appears that very little of these solid components went into solution with the baseline fuel. It is possible that some components did go into solution and greatly reduced the overall thermal stability of the fuel. It is more likely, however, that the problems are associated with melting of the solid components (possibly at temperatures as low as 350°C).

The SRC-I and Mogul L slurries were tested using the standard barrel-and-plunger and a nozzle in which the needle valve clearance had been increased by 0.025 mm, a clearance found to be acceptable in previous experiments.⁽⁹⁾ Under these conditions, the operational characteristics of these slurries were excellent. A standard gear pump was used to transfer fuel from the fuel tank to the injection pump at the standard supply pressure of 0.74 MPa. This type of pump was subsequently found to be inadequate for the higher concentration slurries which were tested in the IDI engine.

As indicated previously, the switch to the inward opening pintle nozzle was an attempt to use a system which, because of its design, appeared to be self-cleaning. This necessitated switching to the IDI-engine configuration, a configuration which in

previous work⁽²⁵⁾ was shown to be more fuel tolerant than the DI configuration. The k-Fuel and Otisca-T slurries would run slightly longer in the pintle nozzle/IDI engine configuration, but the nozzle deposit problem was still severe enough to stop the test. All of the 30-percent slurries were tested in this configuration with no apparent operational problems.

The performance and emissions data for both engines are presented in Appendix C. The heat-release diagrams for all of the test fuels and both engines are presented in Appendix D.

DI Engine Test Results - Examination of the data for each fuel over the load range revealed that the performance data for each fuel could be compared based on the averages over the load range. The indicated specific energy consumption (ISEC), defined as the time rate of fuel energy consumption per unit power (indicated) produced, is used as an indication of the overall efficiency. Figure 15 is a bar chart comparing the SRC-I and the Mogul L slurries to the baseline fuel. The 10 percent slurries compared very well with the base fuel. The 20-percent slurries, however, had average specific energy consumptions which were slightly higher (5 percent for Mogul L and 4 percent for SRC-I) than the baseline fuel. As in previous experiments⁽⁹⁾, the Mogul L slurry did have lower specific energy consumption than baseline fuel at some operating conditions.

The heat-release rate diagrams indicated that there were some differences in the combustion of the slurries as compared to the baseline fuel. Deviations from the baseline fuel performance are due to either lower overall combustion efficiency, incomplete combustion of the solids, or burning late in the cycle.

The total heat release shown in Figure 16 was, on the average, very similar for all of the fuels. In addition, the apparent combustion efficiency, which is based on the total heat release, was very similar for all of the fuels. The angular center of area of the heat release rate diagram, $\bar{\theta}$, is a good indicator of the timing of the combustion event. This is obvious in Figure 17, heat-release rate diagrams for the SRC-I slurries and the baseline fuel, where the 20-percent SRC-I is burning much later in the cycle than the base fuel, $\bar{\theta}$ of 378 degrees for the 20-percent SRC-I as compared to 373 degrees for the baseline fuel.

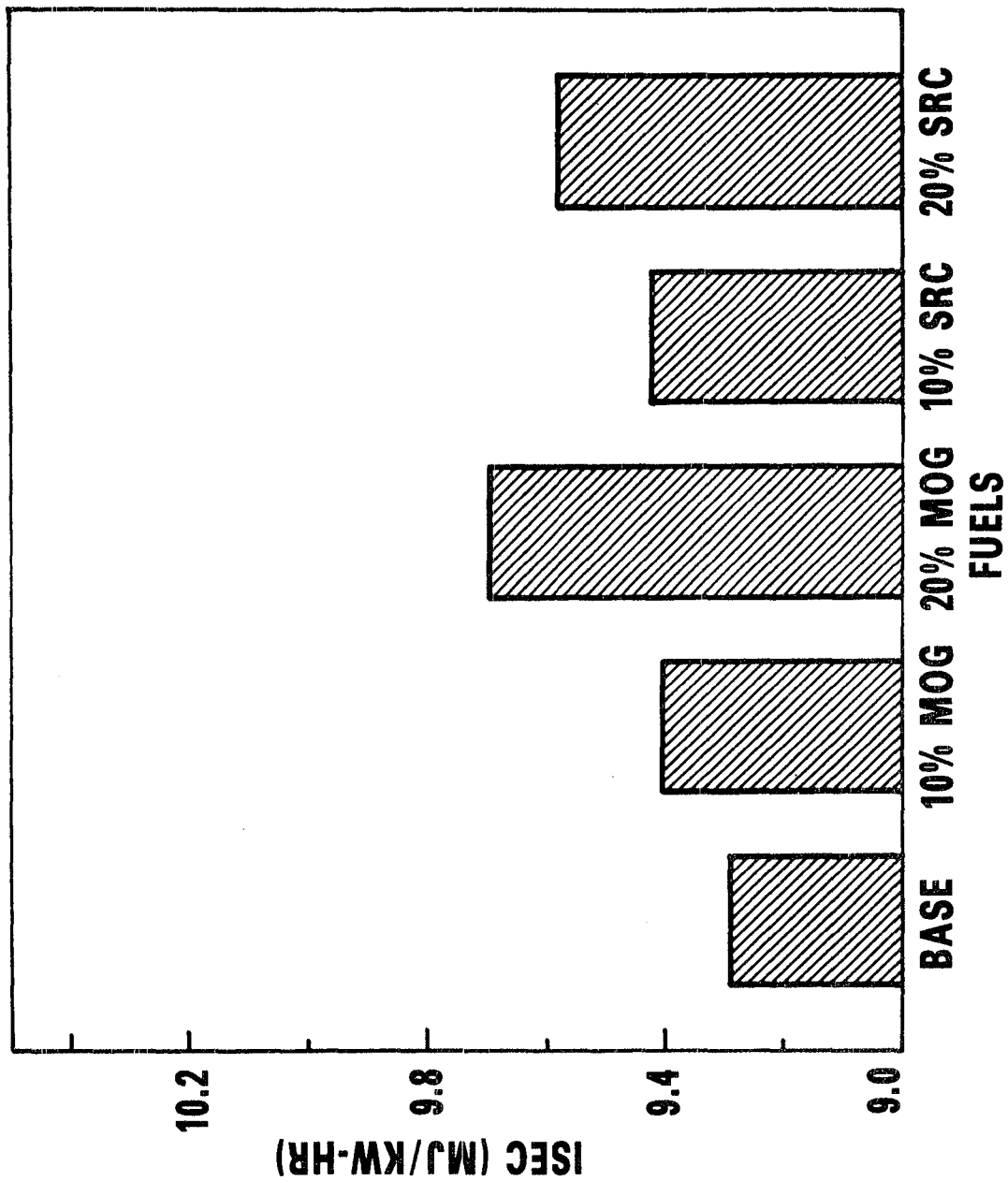


FIGURE 15. AVERAGE ISEC DATA FOR THE DI ENGINE TESTS

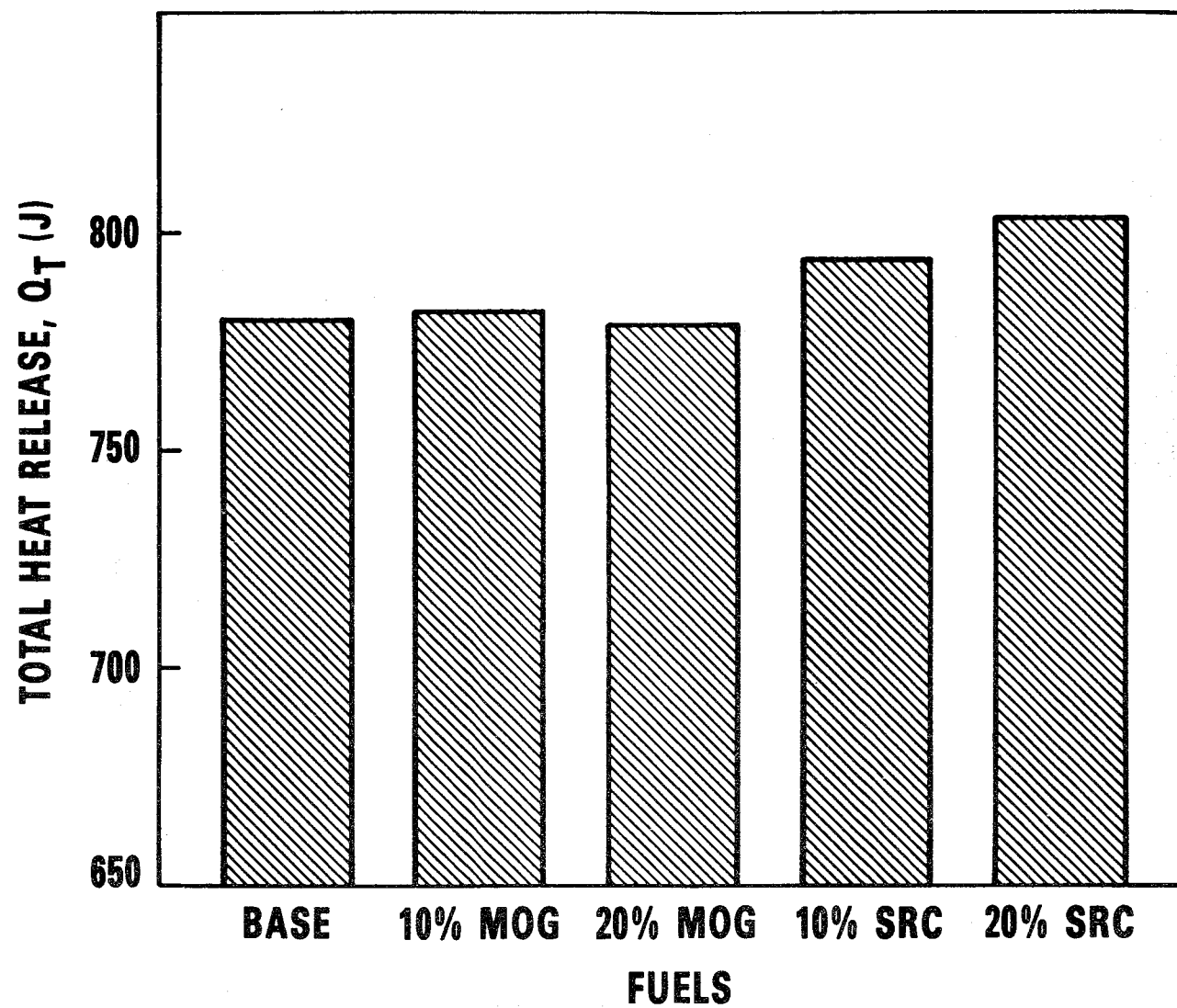


FIGURE 16. AVERAGE TOTAL HEAT RELEASE FOR THE DI ENGINE TESTS

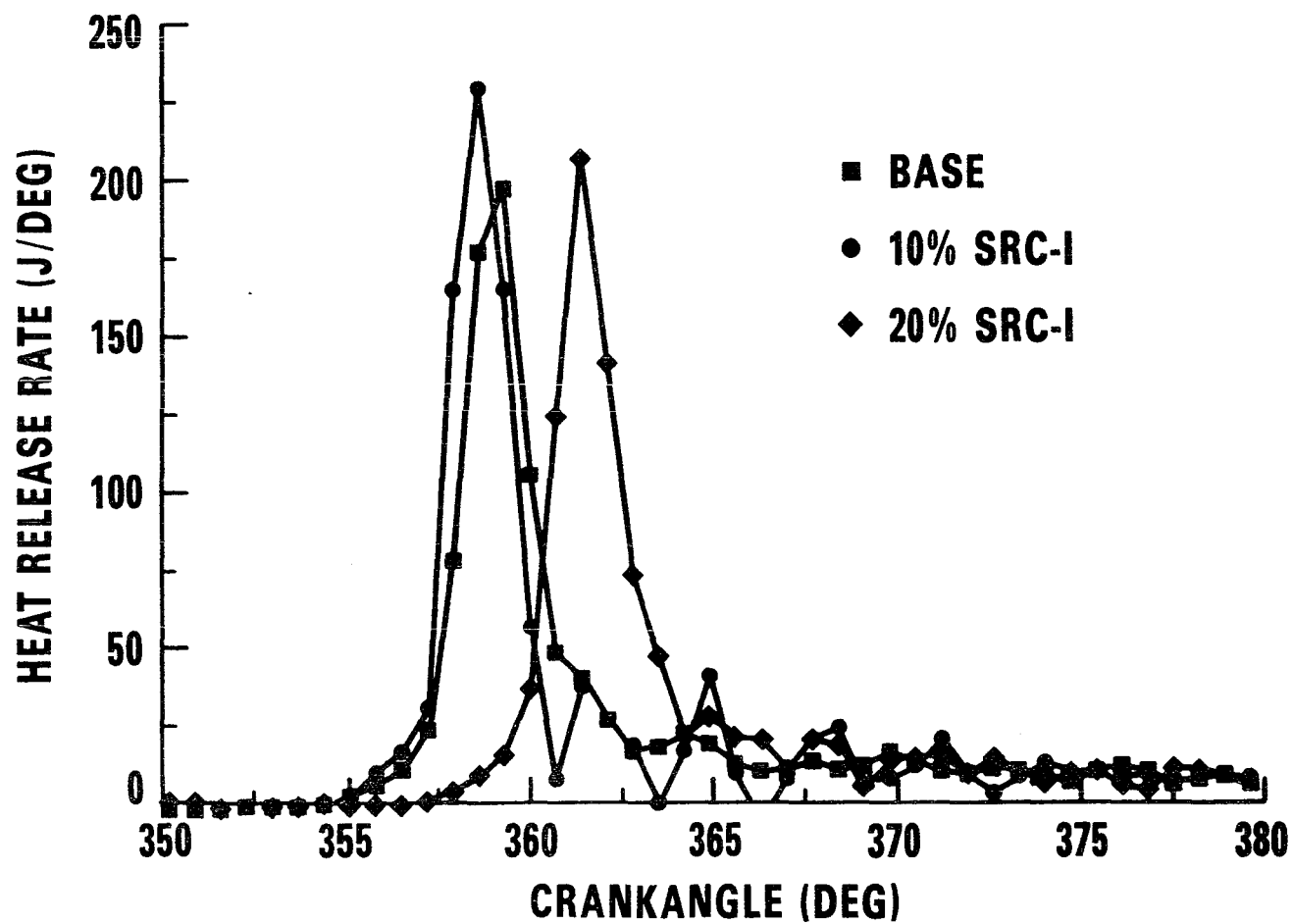


FIGURE 17. HEAT-RELEASE RATE VERSUS CRANKANGLE,
DI ENGINE, FULL LOAD

On the average, the emissions of solids in the exhaust were higher for the slurries than for the baseline fuel, the most notable increases occurring with the SRC-I slurries. The solid emissions in all cases represent a small fraction (less than six percent in the worst case) of the total mass of solid introduced into the engine in the fuel slurry. The small mass fraction, in turn, represents less than one percent of the total fuel energy content, a change too small to be reflected in the combustion efficiency or the specific energy consumption. The emissions data for all tests are tabulated in Appendix C. Based on these considerations, it appears that most of the solid components is burning in the engine. Therefore, deviations from the baseline fuel performance are most probably due to late burning of either or both components of the fuel, with incomplete combustion of the solid contributing in a minor way to lowering the thermal efficiency.

IDI Engine Test Results - As with the DI engine results, averaging the IDI engine performance and efficiency data provides a good indication of the overall performance of the test fuel. The average ISEC data for all of the fuels tested in the IDI engine are presented in Figure 18. The 30-percent Fairless coke had an overall efficiency equivalent to that of the baseline fuel. All of the other slurries performed, on the average, less efficiently (higher ISEC) than the baseline fuel, as shown in the figure. The apparent combustion efficiencies of all of the test fuels, except the 30-percent petroleum coke, were very similar to that of the baseline fuel. The low combustion efficiency for petroleum coke slurry is reflected in the low total heat release as shown in Figure 19. The total heat release was very similar for all of the other fuels. The solid emissions in the exhaust were also highest with the petroleum coke slurry, approximately three times as much solid in the exhaust as with the baseline fuel (see Appendix C). Even with the worst case condition for the petroleum coke slurry, the solid loading in the exhaust is less than 10 percent of the total solids introduced in the fuel slurry. This, in turn, represents less than three percent of the total energy content, not enough to account for a 15-20 percent lower combustion efficiency observed with the petroleum coke slurry. This indicates that the combustion efficiency of the liquid component of the fuel was affected by solids.

The timing of the combustion process, as indicated by $\bar{\theta}$, was somewhat advanced for the petroleum coke. This approach toward constant volume combustion may have somewhat offset the other effects and prevented a more dramatic difference in the overall efficiency, as indicated by ISEC.

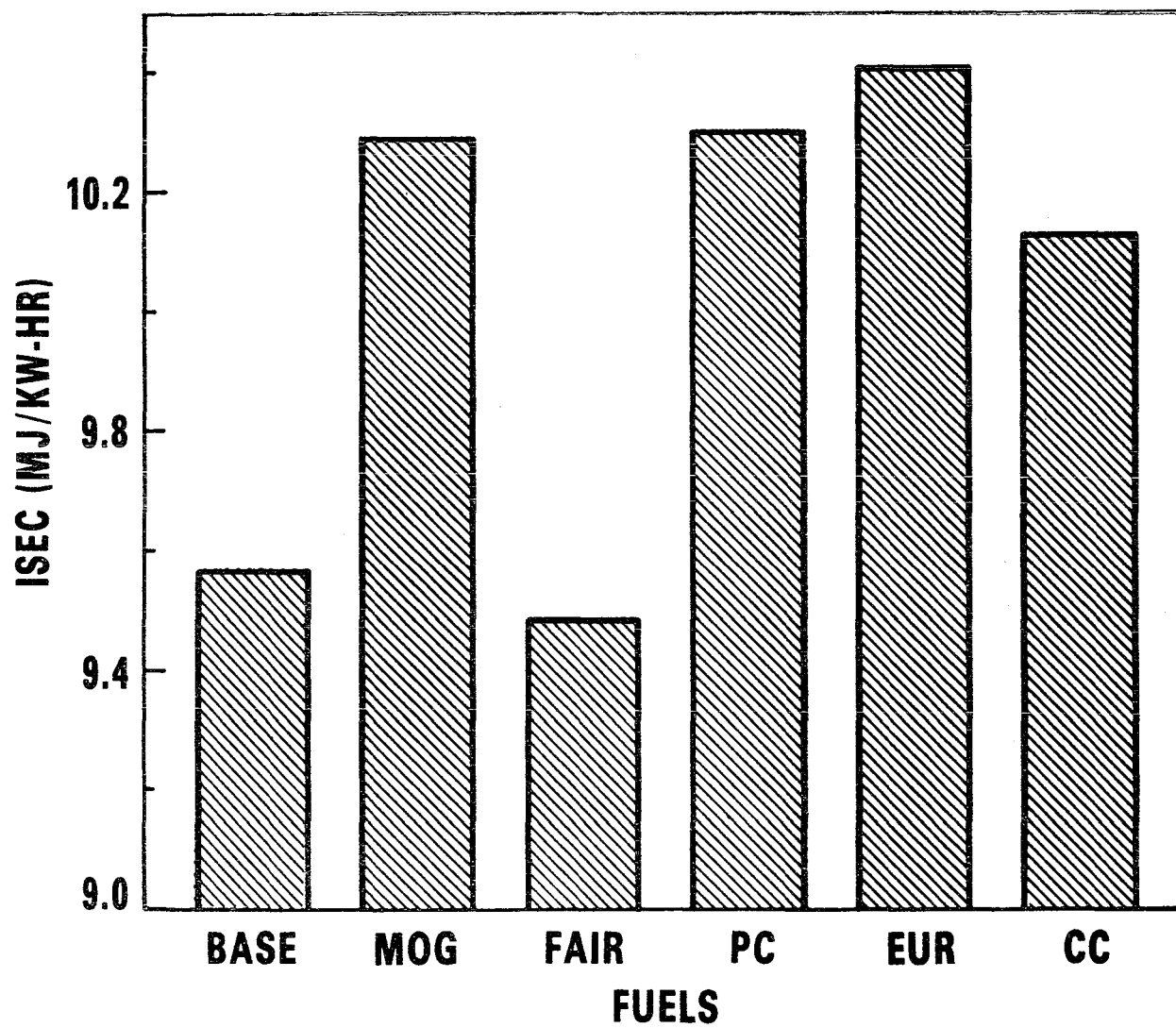


FIGURE 18. AVERAGE ISEC DATA FOR THE IDI ENGINE TESTS

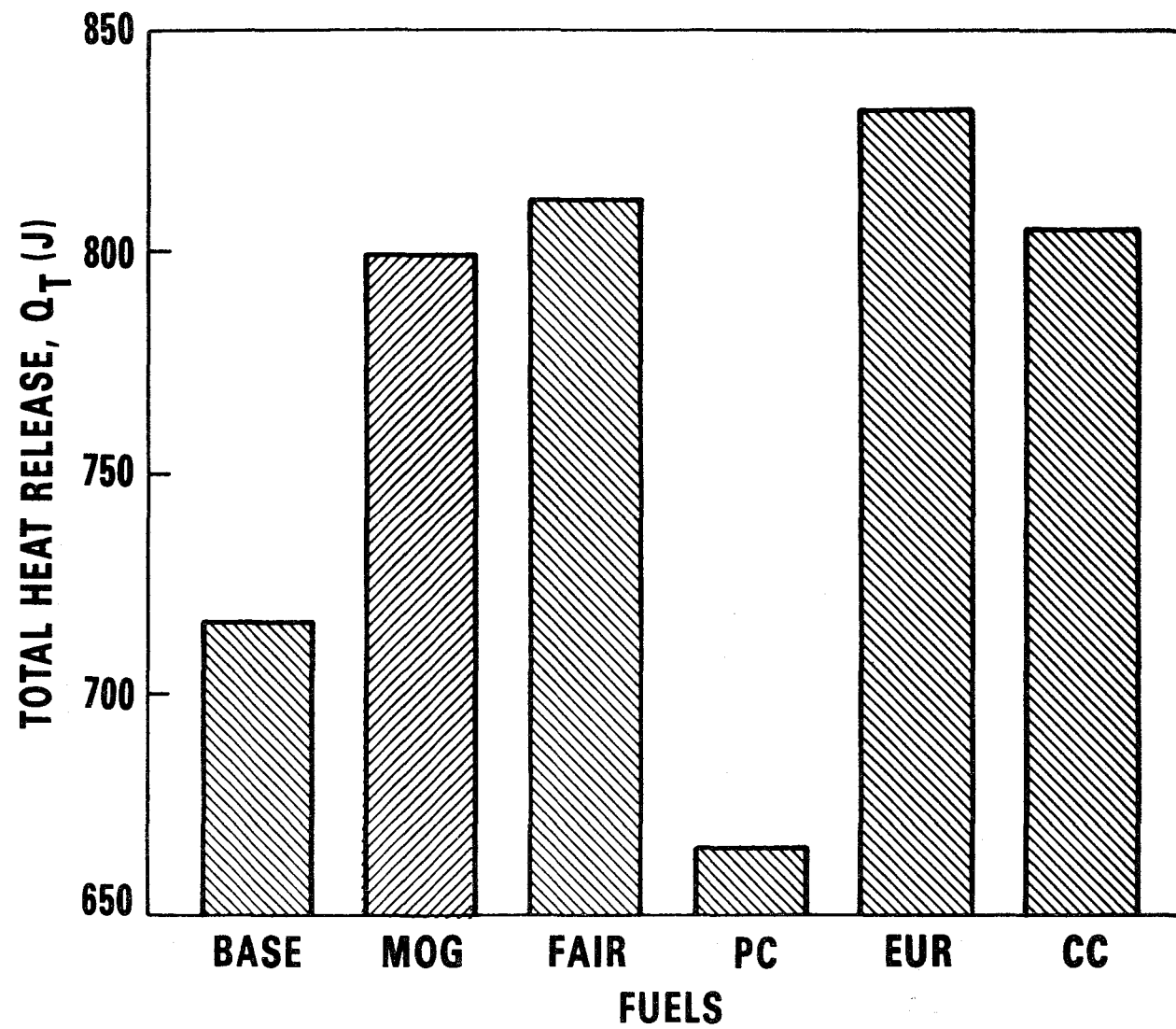


FIGURE 19. AVERAGE TOTAL HEAT RELEASE FOR THE IDI ENGINE TESTS

The Fairless coke slurry had the highest overall efficiency, being equivalent to the baseline fuel. As would be expected, the combustion characteristics and solid emissions were similar for both fuels.

The heat release rate diagrams for the baseline fuel, the 30-percent petroleum coke, and the 30-percent Fairless coke are presented in Figure 20 for the full load test condition. As can be seen, the Fairless coke and the baseline fuel have the same ignition delay time and similar premixed combustion and diffusion combustion phases. The petroleum coke, on the other hand, had a longer ignition delay time followed by a very large premixed phase with very high heat release rates, approaching constant volume combustion. The combustion characteristics of the other test fuels were similar to those of the baseline fuel. Differences in performance (as indicated by ISEC) could generally be attributed to variations in the combustion timing, as indicated by value of $\bar{\theta}$.

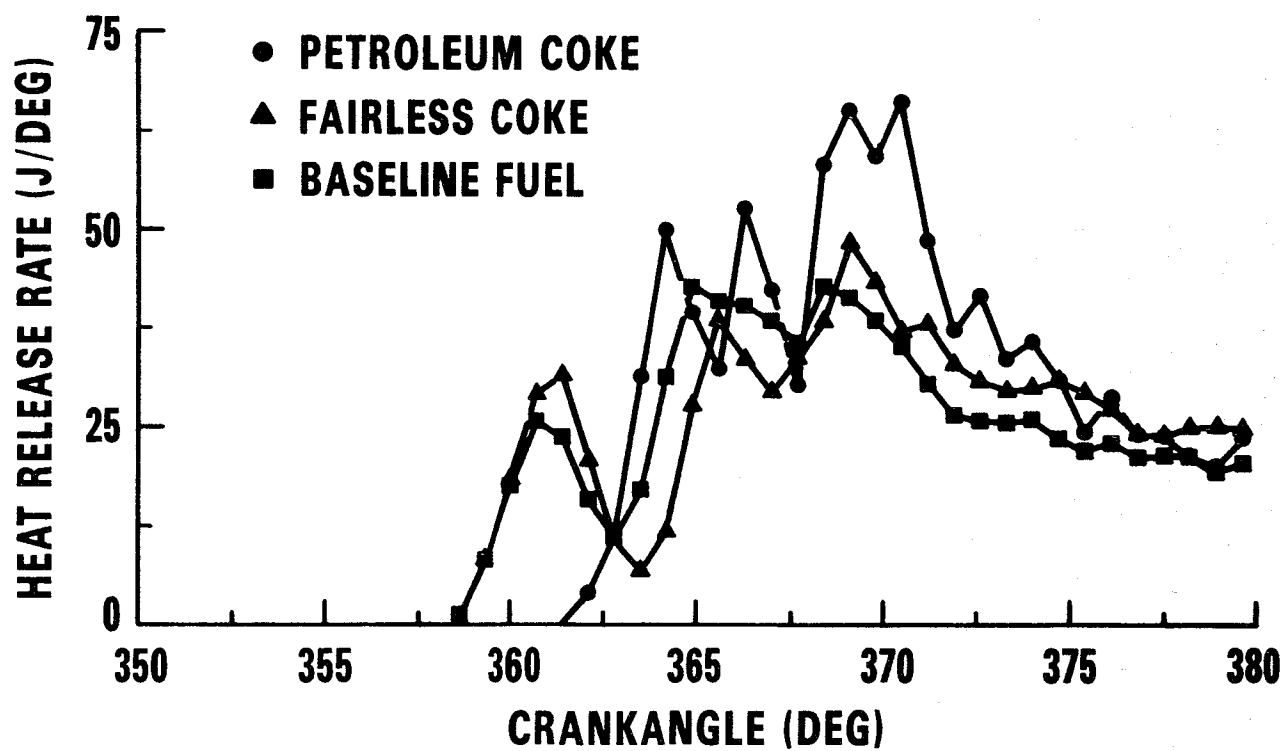


FIGURE 20. HEAT RELEASE RATE VERSUS CRANKANGLE,
IDI ENGINE, FULL LOAD

VII. DISCUSSION

7.1 COMPONENT SELECTION - The solid fuel materials used in this program were selected as representative of the large family of high-carbon content solid fuels. Guidelines used in the selection process included economic potential, abundance of supply, and quality of the material. The last criteria stemmed from the fact that the fuels were to be developed for, and tested in existing, or slightly modified equipment, thus placing limitations on the sulfur and ash content of the test fuels. It is realized that there are other processes in various stages of development which could result in solid fuel components which have as much, or more, potential as those tested. It is also envisioned that advancements in engine design, especially in the fuel injection area, would greatly extend the list of materials and could possibly reduce the processing requirements.

7.2 FUEL FORMULATION - The fuel formulation and engine test experience has pointed out a number of fuel properties which are important. The hardness of the solid component must be considered in the design and operation of the grinding/fuel processing procedures. In addition, the hardness could be directly related to fuel system and engine durability. The internal injection system deposits observed during the engine experiments with some of the fuels indicates that the fusion temperature and solubility of the solid component in the base liquid are important properties. The pentane insolubles determination (ASTM D893) could possibly be used to provide a measure of the solubility of the solid component. The ASTM procedure for determining the fusibility of coal and coke ash (D1857-68) could possibly be adapted to provide a measure of the fusibility of the solid component of slurries. It appears that proper specification of the fusibility and solubility of solids could prevent the deposit problem.

As indicated previously it appears that an SMD of less than 0.5 microns is necessary for proper operation of slurry fuels. There is some question, however, concerning the applicability of currently available particle sizing procedures due to the high dilutions required for these techniques. It is conceivable that the dilution, in some cases up to 1,000,000:1 dilution ratio, could result in changes in the size distribution. These considerations apply equally for optical microscopy and the various laser techniques. Based upon the results of these experiments, however, an SMD of 0.5 microns (using a Hiac-Royco PC-320 analyzer) corresponds to finding nothing larger than 5.0 microns using optical microscopy, and appears to be a reasonable limit for

proper operation in existing engine systems. The optical microscopy technique is a convenient and rapid means of monitoring the size distribution as the slurry is being processed.

As indicated previously, the particle-to-particle and liquid-to-particle interactions greatly complicate the relationship between shear stress and shear rate, even in the simple flow field encountered in a rotational viscometer. Since the apparent viscosities of the slurries are both time and shear rate dependent, it is important that slurries be handled in a standard fashion so that all are exposed to the same shear history before characterizing the flow properties. It is apparent that non-Newtonian behavior stems from structure formation and destruction. It is possible that these structure-forming tendencies could be indirectly assessed by measuring porosity and surface area of the solid particles, if such measurement could be made with the particles still in the slurry. Currently, the procedures are designed for dry powders. Another problem area involves characterization of the shear history of a fuel in a diesel injection system; this information is required in order to specify the appropriate apparent viscosity.

7.3 INJECTION AND ATOMIZATION - Briefly considering some general observations of the injection process, it became apparent from these studies that the four-hole nozzle produces a jet which appears to interact with the environment as a classical jet break-up. Observations also indicated that the transients, in terms of tip velocity, cone angle, and drop size, die out very quickly, within the first 150 microseconds, and the jet then behaves in steady-state manner for several milliseconds. In the pintle nozzles, the transient nature is even less apparent, as shown in Figure 4 by the fact that the penetration distance is nearly linear with time. In addition, the cone angle and penetration rate both decrease with the pintle nozzle as the density of the environment is increased, effects which are also observed in swirl atomizers. In the four-hole nozzle, the cone angle increases and the penetration rate decreases as the density of the environment is increased.

The results of the high-speed movies and the high-resolution work may point out the best approaches for modelling diesel injection. The differences in the spray characteristics of the two nozzles are related to the fact that two different mechanisms are controlling in the atomization process. It appears that the atomization process in the four-hole nozzle would best be modelled as a jet break-up problem, where the jet issues from the orifice as a solid core of liquid. Atomization occurs

away from the nozzle due to air entrainment in the fringes of the jet. Fuel in droplet form is observed only in the fringes, at some distance from the nozzle and late in the injection event far down stream of the nozzle. It appears that the pintle nozzle behaves and could be modelled as a swirl atomizer where a sheet of fluid leaves the nozzle, breaking into ligaments which ultimately break into drops. It appears that both nozzle types can be modelled as steady-state systems.

The high-resolution photographic data indicates that the drop sizes produced by both nozzles are similar, 5-25 microns, and that both are affected somewhat by the fuel type, although correlations between the drop/particle size and specific fuel properties were not apparent. In general appearance, there appeared to be more "debris" in the fringes and the surroundings of the slurry sprays. These particles appeared to have sharp corners indicating that there is some separation of the liquid and solid particles occurring with the slurries.

Although the injection and atomization processes are normally thought to be affected by fuel viscosity, it did not appear that the injection characteristics of the four-hole nozzle were strongly related to the apparent viscosity. It is possible, however, that the poor correlation results from the inability to characterize the flow field encountered by fuel in the injection system.

There does appear to be a correlation between the apparent viscosity of the slurries and the spray characteristics in the pintle nozzle. As indicated previously, there are apparent differences in the basic processes involved in the operation of the two nozzles.

7.4 ENGINE EXPERIMENTS - The performance of the slurry fuels are governed by the interaction of a large number of parameters including the fuel properties, the injection and atomization characteristics, and the ignition and combustion characteristics of the fuels. The global performance, in terms of thermal efficiency or specific energy consumption, is controlled not only by the combustion efficiency but also by the rate and phasing of the combustion process. These considerations also involve the assumption that the injection system is not malfunctioning due to deposits, sticking of parts, or wear.

In the DI engine, the performance of the slurries was very similar to that of the baseline fuel. The slightly lower thermal efficiencies (higher ISEC) most probably

resulted from late burning of both components of the fuel, as reflected by differences in the rate of heat release and in the angular center of area (timing) of the heat release diagrams. These differences could, in turn, be related to differences observed in the drop size distributions of the slurries and the baseline fuel, where the larger drops with the slurries increased the overall burning time. Differences between the slurries were small and could not be related to specific properties of the solid components.

In the IDI engine, there appeared to be both a best (30-percent Fairless coke) and a worst (30-percent petroleum coke) fuel. Differences between the other fuels were small, and compared to the baseline fuel, were apparently due to small variations in the combustion phasing. The degraded performance of the petroleum coke could be related to poor fuel atomization (narrow cone angle and high penetration) which, in turn, appeared to be related to a high apparent viscosity.

In all cases, it should be noted that the combustion efficiency of the solid components of the slurries were very high, typically higher than 90 percent. One factor which has not been discussed is the possibility of increased heat transfer to the cylinder walls due to increased flame radiation from the burning solids. This does not appear to be a major factor, however, since many of the fuels performed very similar to the baseline fuel and slurry-to-slurry differences in radiative heat transfer are probably small.

The operational problems with the slurries can be overcome by proper design and selection of the fuel handling system and components. Some general "rules of thumb" developed in this work include:

1. Avoid dead volumes and attempt to streamline all flow passages; this will prevent separation and packing of the solids.
2. Use pumps with large clearances to prevent wear.
3. The fuel supply pressure to the injection pump should be increased above normal to insure that the increased pressure drop at the fill port is overcome.

Most of these requirements can be met by using a large capacity transfer pump in which the clearances have been increased. The same rules apply to the fuel injection pump where increased clearances, higher flow rates, increased leakage rates, and increased capacity have been successfully used to overcome injection pump problems.

Although durability tests were not performed in this study, injection pump and engine wear were not observed during the performance tests of the slurries.

7.5 PRELIMINARY SPECIFICATION - As indicated previously, specifications involving details of the structure of the solid particles in the slurries, such as surface area or porosity, would be prohibitive due to the difficulties involved in making the measurements and in controlling these properties during the grinding process. In addition, it is felt that stringent compositional requirements would be unacceptable because of the large variations in the composition of coals. It appears that a reasonable specification would involve such properties as ash content, sulfur content, metals content, particle size distribution, stability, particle hardness, particle abrasiveness, particle fusion temperature, solubility of the solids, the slurry viscosity, and the slurry lubricity. Several of these properties were found to be important during this study. As a results of the fact that this is new information, very little data is available for formulation of a specification. The properties which fall into this category are particle hardness, abrasiveness, fusion temperature, and solubility in diesel fuel.

The viscosity and lubricity requirements are dependent on the hardware which is used. In addition, it is envisioned that the most efficient utilization of the slurry fuels will involve modifications to the fuel transfer and injection equipment. It is felt that specification of these slurry fuel properties will change considerably as the systems are developed specifically for the slurries. Future specifications could even involve some guidelines for acceptability in terms of limitations on the shear thickening tendency (non-Newtonian behavior) of the slurries.

Table 8 is a listing of a preliminary specification for slurry fuels. It should be noted that the limitations are based on slurries formulated using diesel fuels which meet the DF-2 specification, and for use in conventional engine systems. It is felt that the specification can be applied to fuel slurries in which other carrier fluids are used. It should also be realized that the various requirements are subject to the limitation discussed above and that the specification will be modified considerably in the future as additional information is developed.

The first three requirements in Table 8 deal with the contaminant level of the solid components. The limitations represent large deviations from the current diesel-fuel specification (ash = 0.01 percent, sulfur = 0.5 percent). It should be noted that the

Table 8. Slurry-fuel Specification

Solids Specification

Ash Content (wt% - max) (D 3180)	1.0
Sulfur Content (wt% - max) (D 3177)	1.0
Metal Content (wt% - max) (X-Ray)	0.2
Hardness (Hardgrove Index - min) (D 409)*	70
Abrasiveness (D 409 (min) or D 3402 (max) or * D 1367 (max))	70/20.0%/50 mg
Solubility (wt% - max) (ASTM D 893)	1.0
Fusion Temperature (°C - min) (ASTM D 1857-68)**	350

Slurry Specification

Stability (wt% - max in 48 hrs)***	0.1
Lubricity (mg - max) (D 1367)	50 mg
Particle-Size Distribution (microns SMD)	0.5
Viscosity (cSt at 40°C and 100 _{s-1})	300

* These three requirements may not be compatible for some materials.

** Based on the maximum expected temperature of injection nozzle.

*** Two-day quiescent storage in fuel tank.

metals content represents a part of the ash limit and is not meant to be added to it. The limitations were selected based on observations made in this study, and also based on the fact that the solids will be blended with liquid carriers which will have much lower concentrations of these contaminants, resulting in a dilution of the concentration of the contaminants in the solids.

The hardness and abrasiveness limitations are designed to minimize the grinding or particle-size reduction requirements and also to limit or prevent wear in the injection system. The limits presented are somewhat arbitrary, being in the mid-ranges of various ratings. ASTM D 409 and D 3402 are grinding tests in which the particle size reduction in a specified grinding apparatus is determined by sieve procedures. ASTM D 409 is designed specifically for coal, while D 3402 is designed for coke. As indicated, the limits listed in Table 8 represent moderate ratings in terms of hardness or abrasiveness. It should be realized that the actual specification of these properties will require extensive durability testing.

Specification of the solubility and fusion-temperature limitations are based mainly on experience developed in this project, although the data is very limited. The solubility requirement allows some solubilization of the solids, but not to the extent observed with the SRC-I slurries. The fusion-temperature requirement is based on reported fusion temperature of SRC-I. It is felt that this would also represent the maximum sac-volume temperature that would be encountered in an injection nozzle in an operating engine.

It is felt that the specification of the slurry properties will be expanded as additional experience is gained with these fuels. The properties and limitations listed in Table 8 for the slurries are viewed as minimum requirements for successful testing in conventional equipment.

The stability requirement consists of a maximum settling rate over 48 hours. This accounts for the 24-hour soak period required for proper wetting of most powders, and an additional 24 hours for testing. Future stability requirements will be governed mainly by the constraints of the fuel transport and storage systems.

The lubricity requirement was included mainly to handle those situations in which non-diesel fuel carriers are used. ASTM D 1367 is suggested as a basis for development of a new standard procedure for assessing the lubricating qualities of the

slurry fuels. It is felt that the 50-mg limitation, listed in Table 8, represents a fairly stringent requirement for slurry fuels.

The particle-size distribution requirements, listed in Table 8, have been discussed extensively in previous sections. Based on experience developed in this project, refinement of this specification will consist of, or result from, improvements in rapid in situ particle-sizing instrumentation.

The viscosity requirement is based on the use of fairly conventional fuel-tank and fuel-pump designs. It should be realized that the use of flow-improving and stability additives will necessitate refinements of this requirement. It appears that major advancements in slurry-fuel technology will occur with the development of an understanding of the flow properties and the interactions of the various components of the slurries. This information will be useful in controlling stability in maintaining a fluid state for transport, and in controlling the injection and atomization characteristics of the slurry fuels.

VIII. SUMMARY

As in the other sections of the paper, the results of the different types of experiments are summarized by experiment.

8.1 FUEL FORMULATION - The important observations of the fuel formulation experiments can be summarized as follows:

1. Several properties of the solid components are important for both fuel formulation and performance; these include hardness, fusion temperature, and the ash and sulfur contents.
2. The particle-size distribution in the slurry is important for proper performance in the engine. A limit on the Sauter mean diameter (SMD) of 0.5 microns appears to be an acceptable limit. There is some question concerning the accuracy of existing sizing techniques, but it is felt that they do provide a good relative measurement.
3. The rheological properties of the slurries are very complex with the apparent viscosities being both time and shear rate dependent.
4. The slurries have higher volumetric energy contents than the base liquid. This means that engine derating does not necessarily result from the use of slurries.

8.2 INJECTION AND ATOMIZATION - The injection and atomization studies produced both general results as well as results specific to slurries.

1. The spray from a multihole nozzle behaves as a jet break-up problem.
2. A pintle nozzle produces a spray which resembles and behaves in the same fashion as a swirl atomizer.
3. The transient part of the injection represents a small fraction, in both time and mass of fuel injected, of the total injection process.
4. The spray characteristics (cone angle and penetration rate) of the four-hole nozzle were not as fuel dependent as those of the pintle nozzle.
5. The drop size distribution of both nozzle types was affected by the presence of slurry although specific property relationships were not apparent.
6. In general, the drop sizes for the baseline fuel range from 5 to 10 microns while the drop sizes for the slurries range from 5 to 25 microns.

8.3 ENGINE EXPERIMENTS - The results of the engine experiments can be summarized as follows:

1. Fuel delivery problem can be prevented by system design changes which allow for higher leakage rates, minimum dead volumes, increased supply pressures, and increased clearances.
2. It appears that a large percentage (90 percent or more) of the solid component of the slurries is burning in the engine.
3. The performance of properly formulated slurry fuels is very similar to that of the baseline fuel. Proper fuel formulation involves meeting the requirement described previously.
4. It appears that the combustion of both components of the slurries are coupled such that incomplete combustion and late burning involve both components rather than just the solid.
5. It appears that slurry fuels are technically viable with proper formulation and using fuel delivery systems designed specifically for slurries.

IX. REFERENCES

1. Rich, L.L. and Walker, M.L., "Pulverized Coal-Burning Diesel Engines," Report No. 46, Office of Coal Research, U.S. Department of the Interior, 1969.
2. Pavolikowski, R., "The Coal-Dust Engine Upsets Tradition," Power, July, 1928.
3. Morrison, L.H., "The Coal-Dust Engine. Details of the Design," Power, Nov. 1928.
4. Soehngen, E.E., "Development of Coal-Burning Diesel Engines in Germany," Final Report No. FE/WAPO/3387-1 for ERDA Contract No. WA76-3387, August 1976.
5. Ryan, T.W., III, Likos, W.E., Moses, C.A., "The Use of Hybrid Fuel in a Single-Cylinder Diesel Engine," SAE paper 801380, Oct. 1980.
6. Marshall, H.P., and Walters, O.C., "An Experimental Investigation of a Coal-Slurry Fueled Diesel Engine," SAE paper No. 770795, September 1977.
7. Tataiah, K., Wood, C.D., "Performance of Coal Slurry Fuels in a Diesel Engine," SAE paper No. 800329, February 1980.
8. Marshall, H.P., Bhat, S.M., Mulvancy, S.T., Sevelli, J.F., "Performance of a Diesel Engine Operating on Raw Coal-Diesel Fuel Slurries," SAE paper No. 810253, February 1981.
9. Ryan, T.W., III, Callahan, T.J., Dodge, L.G., Moses, C.A., "Injection, Atomization and Combustion of Carbon Slurry Fuels," SAE paper No. 821199.
10. Essenhigh, R.H., "Combustion and Flame Propagation in Coal Systems: (A Review)," The Sixteenth International Combustion Symposium, The Combustion Institute, Pittsburgh, PA, August 1976.
11. A Carbon Black Primer, Cabot Corp., Boston, MA.
12. Murray, R.G., "Stable High Energy Solid Fuel From Lignite," presented at AICHE 71st Annual Meeting, Miami, FL, Nov. 1978.
13. Phillips, R.C., Koppelman, E., Murray, R.G., "Upgrading Lignite by the Koppelman Process," presented at Coal Technology 1978, Houston, TX, Oct. 1978.
14. Murray, R.G., "Development of the Koppelman Process for the Manufacture of Metallurgical Coke," Research Brief, SRI International, Menlo Park, CA.
15. Murray, R.G., "Preliminary Tests on Upgrading Australian Brown Coal by the Koppelman Process," prepared for Edward Koppelman, SRI Project 4478-2, SRI International, Menlo Park, CA.
16. Murray, R.G., "Production of High Value Solid Fuels From Cellulosic Feed Materials by the Koppelman Process," presented at The Biomass Energy Conversion Session of the 1979 International Gas Turbine Conference and Products Conference, San Diego, CA, March 1979.

17. Phillips, R.C., Murray, R.G., Koppleman, E., "Peat Dewatering and Upgrading by the Koppleman Process," prepared for IGT Executive Conference, Management Assessment of Peat as an Energy Resource, Arlington, VA, July 1979.
18. SRI International "k-Fuel," SRI International, Menlo Park, CA.
19. Rygiel, R., U.S. Steel, Pittsburgh, PA, personal communication.
20. Otisca Industries, Ltd., "Otisca-T-Process," Otisca Industries, Ltd., Syracuse, NY, Clay D. Smith President, 1982.
21. Tao, J.C., Malhotra, R.K., Sukel, T.M., Foster, E.P., Morris, S.M., "Solvent-Refined Coal (SRC-I). Technology, Product Markets, and Economics," presented at the Third International Coal Utilization Exhibition and Conference, Houston, TX, Nov. 1980.
22. Aiba, T., Sumida, Y., Hozuma, H., Kojima, T., and Bailey, R.T., "Upgrading of Canadian Oil Sands by Eureka Process," presentation at the 1982 NPRA Annual Meeting, San Antonio, TX, March 1982.
23. Mannheimer, R.J., "Effect of Slip on Flow Properties of Cement Slurries can Flaw Resistance Calculations," *Oil & Gas Journal*, pg. 144, December 1983.
24. Eirich, F.R., Rheology - Theory and Applications, Volume 1, Academic Press, NY, 1956.
25. Ryan, T.W., III, Dodge, L.G., Callahan, T.J., "The Effects of Vegetable Oil Properties on Injection and Combustion in Two Different Diesel Engines," 74th Annual AOCS Meeting, Chicago, May, 1983, to be published JAOCS, 1984.
26. Obert, E.F., Internal Combustion Engines, 3rd Edition, pg. 448, International Textbook Co., Scranton, PA, 1970.
27. Kuo, T.W., Bracco, F.V., "Computations of Drop Sizes in Pulsating Sprays and of Liquid Core Length in Vaporizing Sprays," SAE paper No. 820133, Feb. 1982.
28. Ryan, T.W., III, Callahan, T.J., Moses, C.A., "Combustion of Fourteen Different Vegetable Oils in Two Different Diesel Engines," paper No. CSS/CI83-18, Spring Meeting Central States Section, Combustion Inst., Lexington, KY, March 1983.

ACKNOWLEDGEMENT

The authors wish to express their thanks to Mr. Milan Maymar for his assistance in performing the experiment and to Mr. T.J. Callahan for his assistance in processing the data.

APPENDIX A

Process Synopses and Supplemental References

Table of Contents

	<u>Page</u>
SRC-1 PROCESS	A-3
HYDROTHERMAL PROCESS (BATTELLE)	A-4
HIGH GRADIENT MAGNETIC SEPARATION	A-5
KOPPELMAN PROCESS	A-6
TSL SOLIDS (SOLVENT REFINED COAL)	A-7
TRW MEYERS PROCESS FOR DESULFURIZATION	A-8
EUREKA PROCESS	A-9
TRW GRAVIMELT PROCESS	A-10
DRY TABLE	A-11
OTISCA MEDIA PROCESS	A-12
OTISCA T-PROCESS	A-13
MICROWAVE PROCESS	A-14
CHEMICAL COMMUNUTION	A-15
IGT FLASH DESULFURIZATION	A-16
COAL DESULFURIZATION BY LOW-TEMPERATURE CHLORINOLYSIS	A-17
MAGNEX	A-18
FROTH FLOTATION	A-19
OXIDATIVE DESULFURIZATION	A-20
CONVERTOL PROCESS	A-21
PETROLEUM COKE VIA DELAYED COKING	A-22
SUPPLEMENTAL REFERENCES	A-24

SRC-1 PROCESS (1)

The coal is pulverized to less than 1/8", mixed with a process-derived solvent, and fed into the reactor systems as a slurry. The slurry is mixed with hydrogen (450°F; 2000 psig), then heated to near the desired reaction temperature (700-750°F) in a preheater. The coal apparently swells and softens very rapidly during its short stay in the preheater, becoming a viscous gel and transforming bituminous coal into pyridine soluble or cresol soluble materials.

The mixture is then sent to the reactor vessel (dissolver) which is maintained at an optimum temperature of 840°-870°F for 20-60 minutes. The coal is hydrogenated and thus depolymerized here in the reactor, causing the dissolution of the coal. Hydrogen is transferred from the solvent to the coal. The coal molecule is cleaned due to the heat and the hydrogen transfer. The organic sulfur reacts to form hydrogen sulfide. The solvent is also subjected to hydrocracking during this time, yielding lower molecular weight hydrocarbon ranging from light oil to methane. The hot effluent from the reactor is sent to a series of high-pressure separators, where gases and low molecular weight hydrocarbons are removed as vapor. The liquid slurry stream which remains is suitable as solvent. Liquid hydrocarbons are recovered from the vapor stream by condensation. The liquid slurry goes through a mineral separation step which removes the undissolved solids with the process solvent being recovered from the coal via distillation, after which it is recycled to slurry additional coal feed. The residue remaining is SRC-1.

HYDROTHERMAL PROCESS (BATTELLE)(2)(3)(42)

The raw coal is crushed or ground to a particle size suitable for desulfurization (usually 70 percent - 200 mesh or 100 percent - 28 mesh). A physical beneficiation step can be inserted here to remove some of the mineral matter present, including a portion of the pyritic sulfur.

The coal is sent directly to a mixing tank where it is slurried with the leachant (usually an aqueous solution of up to 10 percent sodium hydroxide and about 2 percent calcium hydroxide).

The slurry is heated in an autoclave to 250-350°C (steam pressure 600-2500 psig) in order to extract out a significant amount of the sulfur and mineral matter. After cooling, the slurry is pumped into a receiving tank where the desulfurized coal is separated from the leachant and is water-washed. Drying of the desulfurized coal is optional.

The spent leachant can be regenerated for recycle by several methods.

HIGH GRADIENT MAGNETIC SEPARATION⁽¹⁵⁾⁽¹⁶⁾⁽¹⁷⁾⁽²⁵⁾

The principle of the process is that most mineral impurities in coal that contribute to the pyritic sulfur, sulfate sulfur, and ash content, are paramagnetic. If liberated as discrete particles, they can be separated from the diamagnetic coal by magnetic techniques. This has been successfully done in the processing of kaolin. A typical system is capable of a field intensity of 20 kOe distributed uniformly throughout the working volume. When the ferromagnetic packing materials are placed in the field, thus increasing and distorting the field around them, large field gradients of the order 1-10 kOe/ m can be produced.

The feed containing the magnetic contaminants are pumped through the stainless-steel wool packing of the separator from the bottom while the magnet is on. The magnetic materials (mags) are "captured" and retained inside the separator matrix while the nonmagnetic material (tails) pass through the separator matrix and are collected from the top of the magnet as the beneficiated product. When the separator matrix is filled to its loading capacity, the feed is stopped and the separation matrix is washed with water. The magnet is turned off and the mags in the separator matrix are backwashed and collected and the procedure continues in a cyclic manner.

This process is very similar to the process High Extraction Magnetic Filtration (HEMP).

KOPPELMAN PROCESS (5)(6)(7)(8)(9)(10)(11)

This process converts low grade carbonaceous or cellulosic materials to high heating value, stable solid fuels with considerable energy value enhancement.

The cellulosic material (biomass) is fed as a slurry into the reactor. Under intense heat and pressure (to 100 atmosphere), the feedstock is converted to a solid, clean-burning fuel resembling coal, and containing low ash and low sulfur.

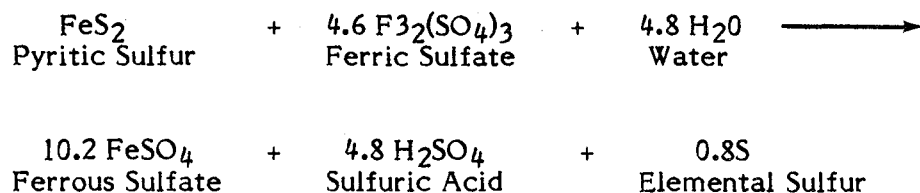
The feedstock can be wood waste, peat, lignite and brown coal, coal fumes, subbituminous, seaweed, etc. The process is essentially one of advanced pyrolysis where the feedstock is restructured under controlled conditions of high temperature and pressure. The cost of the process makes it competitive with conventional sources of energy.

TSL SOLIDS (SOLVENT REFINED COAL)(1)

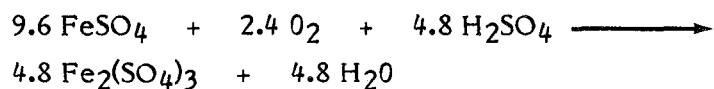
A SRC-I Demonstration Plant being built in Newman, Kentucky and scheduled to be operational in later 1984, incorporates a first-stage liquefaction section (SRC-I), followed by an LC-Finer referred to as two-stage liquefaction (TSL), and a delayed coker and calciner. The plant will produce two types of SRC-I solids. The "Classic" SRC solid, similar to those described in synopsis No. 1, and TSL solids. The TSL solids are those solids remaining after ther molten SRC solid has been processed through the expanded-bed hydrocracking (LC-fining) stage. They contain lower sulfur and lower ash.

TRW MEYERS PROCESS FOR DESULFURIZATION(22,23,38,45)

This process has application for converting coals with relatively high pyritic sulfur and low organic sulfur content, such as those found in Appalachian coals, to coals that have sulfur levels that will meet governmental sulfur oxide emission standards when used as a fuel. The pyrite sulfur in the coal is oxidized selectively using an aqueous ferric sulfate solution at 90-130°C, to ferrous sulfate and free elemental sulfur.



The ferrous sulfate dissolves in solution and the free sulfur is removed from the coal matrix by either solvent extraction or by vaporization. The oxidizing agent is regenerated at similar temperature with air or oxygen and thus can be recycled.



The ferrous sulfate can be removed by liming and/or crystalization. In a survey of 35 coals, the average coal contained 2.02 percent pyrite sulfur and 3.05 percent total sulfur. In regard to trace element removal, the results varied greatly from coal to coal, but some general conclusions can be stated.

- (a) As, Cd, Mn, Ni, Pb, Zn were removed to a greater extent by the Meyers Process than by the physical cleaning process.
- (b) Li and F are partitioned better by the physical separation procedures; Ag and Cu removal had a slight preference for the float-sink separation.
- (c) Cr and V removal was about the same by both processes.

EUREKA PROCESS⁽¹⁴⁾

The feed is usually vacuum resid, although the process has possible application to Canadian oil sands. After the feed is preheated, it enters the bottom of the fractionator and mixed with the recycle oil that comes from the above. This mixture is transferred to the charge heater and fed via an automatic switching valve to the reactor system. This system consists of two reactors, operating alternately. The cycle time is about four hours. Superheated steam is injected into the reactor and supplies approximately 20 percent of the required heat for the reaction. The steam also strips the cracked product out of the reactor. As the reaction proceeds, the pitch (bottom material) becomes viscous due to a poly-condensation reaction and the degree of this reaction is measured by the softening point (SP). At a predetermined SP, the reaction is quenched with water. The pitch is still a viscous liquid and can be transferred to the pitch stabilizer (usually every two hours). The pitch is pumped to the flaker where it is solidified and flaked. The effluent from the reactor goes to the lower section of the main fractionator and the small amount of entrained pitch is removed. The upper section is ordinary fractionator, where the heavy cracked oil (CHO) is removed. The lighter cracked oil (CLO) fraction is usually obtained from the overhead drum.

TRW GRAVIMELT PROCESS~~(51)(52)(53)(61)~~

In the Gravimelt Process, molten sodium hydroxide and potassium hydroxide are used for the removal of organic sulfur from coal. The laboratory runs were made in stirred reactors, the dimensions of which were 3 inches in diameter and 12 inches in height. Kentucky No. 11 coal was reduced in sulfur content to a level of 0.10 lbs of sulfur/ 10^6 BTU with an ash content of 0.21% in a cumulative reaction time of 60 minutes. This process is under development and is being funded by DOE.

DRY TABLE (4)

Coarsely-ground coal is fed into a wedge-shaped shaker table. As the coal is fed into the longest side of the unit, it is moved toward the backwall by the conveying force. With a large pile of particles formed against the backwall and filling all of the trough, the particle on the pile's surface is moved down the open slope by gravity. The underlying material is still driven against the backwall and causes a continuous overturning of the bed. As the incoming feed causes the overturning of the bed and flow across the deck away from the feed, a helical motion results. As these actions are taking place, size- and bulk-density separations are occurring in the bed, with the low-density and large particles moving into a spiralling path. The particles migrate toward the toe of the pile while the high-density or small particles move into a smaller spiral. These particles tend to concentrate towards the backwall. The particles that are both low density and large (coal) move past the large and high-density particles (rock and pyrite) and concentrate at the toe of the pile. The small particles of pyrite tend to concentrate at the backwall in preference to small coal particles. There is also a "discharge lip", an attached downward sloping surface to the nearly horizontal deck from which the particles are discharged. This lip causes further separation based on the particle shape, resiliency, and surface roughness. Thus the tabular rock and pyrite particles are stable when the unit is vibrating and the cubical coal particles are unstable. The latter will be discharged by rolling off the lip; the tabular rock and pyrite are taken back up the lip and into the pile. The roughness of the rock and pyrite causes them to be conveyed back into the deep particle bed while the rather smooth surface coal slips off the lip. Since the coal also has more resiliency, the conveying vibrations cause them to bounce and assure their instability on the discharge lip.

OTISCA MEDIA PROCESS⁽⁵⁷⁾

The process exploits the gravimetric differences between the coals and the impurities contained in the coal. A static bath containing a low-viscosity organic liquid is employed. Depending on the coal treated, BTU recoveries greater than 90 percent have been achieved and with reductions in the sulfur content exceeding 60 percent.

OTISCA T-PROCESS (58)

The coal is ground to 15 microns by conventional means. It is then agglomerated with the almost 100-percent recovery of the BTU's in the coal feed and with less than 1-percent ash. The ground coal can be recovered as a dry powder or in a water or oil slurry.

MICROWAVE PROCESS⁽⁵⁴⁾⁽⁶¹⁾

A laboratory-size flow reactor (100 g per batch) is being used, and with modification, can run continuously (500 g to 1000 g per minute). The coal ($\frac{1}{8}$ " size particles) are subjected to microwave radiation which results in the conversion of pyrite to FeS, the latter having strong magnetic properties. If the coal is crushed further (30-100 mesh) and subjected further to microwaves combined with a NaOH treatment, the sulfur content can be reduced 80-90%.

CHEMICAL COMMINUTION(19)

Chemical comminution is the pulverizing, or reducing, to powder by chemical means. Studies at Syracuse University Research Corporation indicate that liquid ammonia is probably the most effective chemical found thus far for this task.

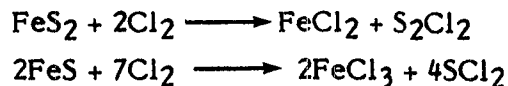
When coal is treated with liquid ammonia it is fractured in a highly selective manner, with the breaks occurring in those internal boundaries that were previously weakened by infiltration of pyrite, ash, and other mineral constituents. Analyses of the sink-float products after chemical comminution show that the float fraction had about 55 percent less ash and 73 percent less pyrite sulfur.

IGT FLASH DESULFURIZATION⁽³²⁾

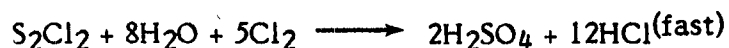
The process is based on both chemical and thermal treatment of the coal to be desulfurized. The coal is subjected to hydrogen treatment at elevated temperatures and near-atmospheric pressure. The coal had a pretreatment to prevent it from coking and to enhance the overall sulfur removal.

COAL DESULFURIZATION BY LOW-TEMPERATURE CHLORINOLYSIS⁽³³⁾

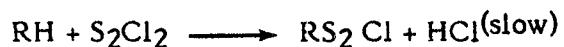
The reaction of pyritic sulfur with chlorine is shown by the reactions:



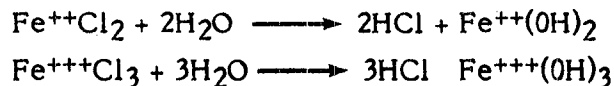
If water is present and the temperature is 750°C, the S_2Cl_2 formed in the first reaction can readily be converted to H_2SO_4 and HCl



If no moisture is present and the temperature is 50°C, the S_2Cl_2 may react with other organic compounds to form organo-sulfur compounds.

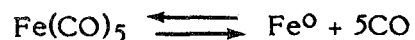


The chlorinated coal can be heated (300° - 550°C) to remove hydrogen chloride.



MAGNEX (56)

The "Magnex" process is a four-step process involving crushing, heating, carbonyl treating, and magnetic separation. The coal is crushed to minus 14 mesh, followed by heating to 170°C. To improve the selectivity, the coal can be exposed to steam during the heating process. The coal is then exposed to vapors of iron pentacarbonyl. This decomposes in the presence of the hot coal as represented by the simplified equation

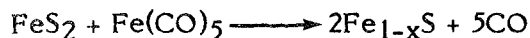


The reaction between iron pentacarbonyl and the ash in the coal has been difficult to establish, but it is believed that atomic iron forms crystallites which are attached to the ash particles.



Measurements of the magnetic susceptibility show the presence of super paramagnetic iron crystallites in the magnetic refuse.

The reaction between the iron pentacarbonyl and the pyrite can be represented by the equation below.



The iron pentacarbonyl decomposes when it comes in contact with the pyrite surface and is thought to be converted into a pyrite-like material.

The pyrite and ash can be separated from the clean coal by commercial low-to-medium intensity induced magnetic-roll separations having field strengths between 8000 to 12,000 gauss.

FROTH FLOTATION (21)(26)

The froth flotation process uses the differences in the surface properties of the coal and the refuse particles in its operation. The coal is usually sized down to particles $1/32$ of an inch or smaller and placed in water in a large mixing tank (flotation cell). The contents of the tank are mixed, usually by pneumatic or mechanical stirring, followed by addition of special reagents to promote bubbling and the attachment of coal particles to these bubbles. When this is accomplished and is introduced into the flotation cell, the coal particles attach themselves to the bubbles. The bubbles with the coal particles attached rise to the surface where the coal is removed. The pyrite and ash are left behind in the suspension.

The process has not been developed to a point where the ash and pyrite sulfur particles are rejected completely while all the coal particles are caused to float; but research continues.

OXIDATIVE DESULFURIZATION (24)

Of the several techniques for removing sulfur from coal by oxidative means, the one using air and water appears to be the most feasible. It removes both pyrite sulfur (90%) and organic sulfur (40%).

An aqueous slurry of coal is contacted with air at pressure up to 1000 psi and temperatures of 140-200°C. Table 1 shows the organic sulfur removal from various coals using oxidative desulfurization.

**Table 1. Organic Sulfur Removal from Representative
Coals by Oxydesulfurization**

<u>Seam</u>	<u>State</u>	<u>Temp (°C)</u>	<u>Organic Sulfur (wt %)</u>	
			<u>Untreated</u>	<u>Treated</u>
Bevier	Kansas	150	2.0	1.6
Mammoth ^a	Montana	150	0.5	0.4
Wyoming No. 9 ^a	Wyoming	150	1.1	0.8
Pittsburgh	Ohio	180	1.5	0.8
Lower Freeport	Pennsylvania	180	1.0	0.8
Illinois No. 6	Illinois	200	2.3	1.3
Minshall	Indiana	200	1.5	1.2
^a Subbituminous				

CONVERTOL PROCESS^(#1)

In this process, droplets of dispersed oil are intimately contacted with the solids suspended in the coal slurry. As a result, the oils displace the water on the surface by preferential wetting, after which the coal particles are allowed to agglomerate. This permits their removal from the slurry using centrifugal filtration. Since clay and other particles of mineral matter that are suspended in the slurry do not have the affinity for oil that the coal particles have, the oil treatment is preferential to the coal particles. These coal particles are permitted to agglomerate by gentle stirring in a conditioner to form flocs. The agglomerated coal is washed and partially dewatered by using a vibrating screen. The washed flocculate is further dewatered using a high speed screen basket centrifuge or a solid bowl centrifuge.

PETROLEUM COKE VIA. DELAYED COKING⁽⁵⁰⁾

Coking has been described as a severe thermal cracking process. The heaters are designed to raise the temperature of the residual stock above the point at which coking occurs by having a minimum retention time. This is achieved by having high velocities in the heaters. An insulated surge drum on the heater effluent permits a time delay sufficient enough to allow (delayed) coking to occur before subsequent processing takes place.

In the delayed coking process, the hot fresh liquid feed enters the fractionator two to four trays above that of the vapor zone. This allows the hot vapors from the coke drum to be quenched by the cooler feed liquid and thus prevent any sizable amount of coke formation. At the same time, this permits the high boiling material to be condensed and recycled. If any undesirable light boiling material is present, it can be vaporized from the feed which is further preheated in the fractionator. The remaining fresh feed liquid is combined with the condensed recycle and pumped from the bottom of the fractionator to the coker heater. It is partially vaporized and sent to one of the two coke drums.

The velocities are usually controlled by the introduction of steam in the heater tubes, thus keeping the coke deposition at a minimum. The unvaporized portion from the heater effluent settles out in the coke drum because of temperature and retention time effects, thus resulting in coke formation. The gaseous material consisting of thermally cracked products (gas oils, naphtha, gas) and steam from the top of the coke drum are sent to the bottom of the fractionator and travel upward through the quench trays. Above where the fresh feed enters the fractionator there are several additional trays below the gas oil drawoff tray. These are refluxed with partially cooled gas oil in order that a fine control of the gas oil end point can be maintained and entrainment of any fresh feed liquid or recycle liquid into the gas oil product can be minimized. The conventional six-to-light-tray stripper is used on the oil side draw. Steam is introduced under the bottom tray to vaporize the light end in order to control the initial boiling point of the gas oil. The steam carrying the vaporized light ends are sent from the top of the stripper to the fractionator about two trays above the draw tray. Once the coke drum is filled, it is isolated from the system, steamed to remove hydrocarbon vapors, cooled by filling with water, opened, and the coke is removed.

14. Aiba, T., Sumida, Y., Hozuma, H., Kojima, T., and Bailey, R.T., "Upgrading of Canadian Oil Sands by Eureka Process", presentation at the 1982 NPRA Annual Meeting, San Antonio, TX March 21-23, 1982.
15. Liu, Y.A. and Lin, C.J., "High-Gradient Magnetic Separation in Coal Beneficiation" Vol. IV., Coal Processing Technology, American Institute of Chemical Society, Washington, D.C., (1979).
16. Murray, H.H., "Magnetic Desulfurization of Some Illinois Basin Coals" in Coal Desulfurization, T.D. Wheelock, Editor, ACS Symposium Series 64, American Chemical Society, Washington, D.C. (1979).
17. Elliott, M.A. (Editor), "High-Gradient Magnetic Separation" and "Magnex Process" in Chemistry of Coal Utilization. Second Supplementary Volume Wiley-Interscience Publication, New York, (1981).
18. Stambaugh, E.P., Miller, J.F., et al, "Clean Fuels From Coal", Vol. IV, Coal Processing Technology, American Institute of Chemical Engineers, New York, 1977.
19. Howard, P., Hanchett, A., and Aldrich, R.G., "Chemical Comminution for Cleaning Bituminous Coal", in Coal Desulfurization, T.D. Wheelock, Editor, ACS Symposium Series 64, American Chemical Society, Washington, D.C., (1977).
20. Howard, P.H., and Datta, R.S., "Chemical Comminution: A Process for Liberating the Mineral Matter From Coal" in Coal Desulfurization, T.D. Wheelock, Editor, ACS Symposium Series 64, American Chemical Society, Washington, D.C., (1977).
21. Aplan, F.F., and Luckie, P.T., "Methods of Processing Coal to Remove Sulfur", Earth and Mineral Science, The Pennsylvania State University, Vol. 51, No. 3., Jan/Feb. 1982. (Subjects: By Gravity Concentrations; Heavy-Media Cycloning; Fine Jigging; Tabling; Water-only Cyclone; Pneumatic or Dry Cleaning Processes; Froth Flotation; other methods.
22. Hammersma, J.W., Kraft, M.L., and Meyers, R.A., "Applicability of the Meyers Process for Desulfurization of U.S. Coal (A Survey of 35 Coals)", in Coal Desulfurization, T.D. Wheelock, Editor, ACS Symposium Series 64, American Chemical Society, Washington, D.C., (1977).
23. Elliott, M.A. (Editor), "TRW Meyers Process" in Chemistry of Coal Utilization. Second Supplementary Volume. Wiley-Interscience Publication, New York, (1981).
24. Friedman, S., Lacorent, R.B., and Warzinski, R.P., "Oxidative Desulfurization of Coal", in Coal Desulfurization, T.D. Wheelock, Editor, ACS Symposium Series 64, American Chemical Society, Washington, D.C., (1977).
25. Lin, C.J., and Liu, Y.A., "Desulfurization of Coals by High-Intensity High-Gradient Magnetic Separation: Conceptual Process Design and Cost Estimation", in Coal Desulfurization, T.D. Wheelock, Editor, ACS Symposium Series 64, American Chemical Society, Washington, D.C., (1977).

26. Aplan, F.F., "Use of the Flotation Process for Desulfurization", *ibid.*
27. Cavallaro, J.A., and Deurbrouck, A.W., "An Overview of Coal Preparation", *ibid.*
28. Miller, K.J., "Coal-Pyrite Flotation in Concentrated Pulp. A Pilot Plant Study", Report of Investigations 8239, Bureau of Mines, U.S. Department of Interior, 1977.
29. Miller, K.J., "Flotation Study of Refractory Coals", Report of Investigations 8224, *ibid.*
30. Elliott, M.A., (Editor), "Coal-Pyrite Flotation Process", in Chemistry of Coal Utilization. Second Supplementary volume, Wiley-Interscience Publication, New York, (1981).
31. Min, S. and Wheelock, T.D., "A Comparison of Coal Beneficiation Methods", in Coal Desulfurization, T.D. Wheelock, Editor, ACS Symposium Series 64, American Chemical Society, Washington, D.C, (1977), (methods evaluated were roll crushing, pulverizing, ball milling, chemical comminution, gravity separation, froth flotation, and oil agglomeration).
32. Fleming, D.K., Smith, R.D., and Aquino, M.R.Y., "Hydrodesulfurization of Coal", *ibid.* (paper on Institute of Gas Technology's Flash Desulfurization).
33. Hsu, G.C., Kalvinskas, J.J., Ganguli, P.S., and Gavalas, G.R., "Coal Desulfurization by Low-Temperature Chlorinolysis", *ibid.*
34. Tai, C.Y., Graves, G.V., and Wheelock, T.D., "Desulfurizing Coal with Alkaline Solutions Containing Dissolved Oxygen", *ibid.*
35. Sareen, S.S., "Sulfur Removal From Coal: Ammonia/Oxygen System", *ibid.*
36. Tipton, A.B., "Improved Hydrodesulfurization of Coal Clear by Acid Leach", *ibid.*
37. Huang, E.T.K, and Pulsifer, A.H., "Coal Desulfurization during Gaseous Treatment", *ibid.*
38. Meyers, R.A., "Desulfurize Coal Chemically" Hydrocarbon Processing, June 1975. (Meyers Process).
39. Anon. "Vibrating Dry Table Speeds Removal of High-Ash Material From Coal", Coal Age, June 1976.
40. Iammartino, N.R., "New Task for Magnetism", Chemical Engineering, Jan 7, 1974.
41. Brisse, A.H., and McMOVUS, W.L., Jr., "Converal Process" Transactions AIME, Mining Engineering, Feb. 1958.
42. Stambaugh, E.P., "Batelle Develops Leaching Process to Desulfurize Coal", (Hydrothermal Coal Process), Coal Age, aug. 1975.
43. Reis, T., "To Coke, Desulfurize, and Calcine. Part 2: Coke Quality and Its Control", Hydrocarbon Processing, June 1975.

14. Aiba, T., Sumida, Y., Hozuma, H., Kojima, T., and Bailey, R.T., "Upgrading of Canadian Oil Sands by Eureka Process", presentation at the 1982 NPRA Annual Meeting, San Antonio, TX March 21-23, 1982.
15. Liu, Y.A. and Lin, C.J., "High-Gradient Magnetic Separation in Coal Beneficiation" Vol. IV., Coal Processing Technology, American Institute of Chemical Society, Washington, D.C., (1979).
16. Murray, H.H., "Magnetic Desulfurization of Some Illinois Basin Coals" in Coal Desulfurization, T.D. Wheelock, Editor, ACS Symposium Series 64, American Chemical Society, Washington, D.C. (1979).
17. Elliott, M.A. (Editor), "High-Gradient Magnetic Separation" and "Magnex Process" in Chemistry of Coal Utilization. Second Supplementary Volume Wiley-Interscience Publication, New York, (1981).
18. Stambaugh, E.P., Miller, J.F., et al, "Clean Fuels From Coal", Vol. IV, Coal Processing Technology, American Institute of Chemical Engineers, New York, 1977.
19. Howard, P., Hanchett, A., and Aldrich, R.G., "Chemical Comminution for Cleaning Bituminous Coal", in Coal Desulfurization, T.D. Wheelock, Editor, ACS Symposium Series 64, American Chemical Society, Washington, D.C., (1977).
20. Howard, P.H., and Datta, R.S., "Chemical Comminution: A Process for Liberating the Mineral Matter From Coal" in Coal Desulfurization, T.D. Wheelock, Editor, ACS Symposium Series 64, American Chemical Society, Washington, D.C., (1977).
21. Aplan, F.F., and Luckie, P.T., "Methods of Processing Coal to Remove Sulfur", Earth and Mineral Science, The Pennsylvania State University, Vol. 51, No. 3., Jan/Feb. 1982. (Subjects: By Gravity Concentrations; Heavy-Media Cycloning; Fine Jigging; Tabling; Water-only Cyclone; Pneumatic or Dry Cleaning Processes; Froth Flotation; other methods.
22. Hammersma, J.W., Kraft, M.L., and Meyers, R.A., "Applicability of the Meyers Process for Desulfurization of U.S. Coal (A Survey of 35 Coals)", in Coal Desulfurization, T.D. Wheelock, Editor, ACS Symposium Series 64, American Chemical Society, Washington, D.C., (1977).
23. Elliott, M.A. (Editor), "TRW Meyers Process" in Chemistry of Coal Utilization. Second Supplementary Volume. Wiley-Interscience Publication, New York, (1981).
24. Friedman, S., Lacorent, R.B., and Warzinski, R.P., "Oxidative Desulfurization of Coal", in Coal Desulfurization, T.D. Wheelock, Editor, ACS Symposium Series 64, American Chemical Society, Washington, D.C., (1977).
25. Lin, C.J., and Liu, Y.A., "Desulfurization of Coals by High-Intensity High-Gradient Magnetic Separation: Conceptual Process Design and Cost Estimation", in Coal Desulfurization, T.D. Wheelock, Editor, ACS Symposium Series 64, American Chemical Society, Washington, D.C., (1977).

26. Aplan, F.F., "Use of the Flotation Process for Desulfurization", *ibid.*
27. Cavallaro, J.A., and Deurbrouck, A.W., "An Overview of Coal Preparation", *ibid.*
28. Miller, K.J., "Coal-Pyrite Flotation in Concentrated Pulp. A Pilot Plant Study", Report of Investigations 8239, Bureau of Mines, U.S. Department of Interior, 1977.
29. Miller, K.J., "Flotation Study of Refractory Coals", Report of Investigations 8224, *ibid.*
30. Elliott, M.A., (Editor), "Coal-Pyrite Flotation Process", in Chemistry of Coal Utilization. Second Supplementary volume, Wiley-Interscience Publication, New York, (1981).
31. Min, S. and Wheelock, T.D., "A Comparison of Coal Beneficiation Methods", in Coal Desulfurization, T.D. Wheelock, Editor, ACS Symposium Series 64, American Chemical Society, Washington, D.C, (1977), (methods evaluated were roll crushing, pulverizing, ball milling, chemical comminution, gravity separation, froth flotation, and oil agglomeration).
32. Fleming, D.K., Smith, R.D., and Aquino, M.R.Y., "Hydrodesulfurization of Coal", *ibid.* (paper on Institute of Gas Technology's Flash Desulfurization).
33. Hsu, G.C., Kalvinskis, J.J., Ganguli, P.S., and Gavalas, G.R., "Coal Desulfurization by Low-Temperature Chlorinolysis", *ibid.*
34. Tai, C.Y., Graves, G.V., and Wheelock, T.D., "Desulfurizing Coal with Alkaline Solutions Containing Dissolved Oxygen", *ibid.*
35. Sareen, S.S., "Sulfur Removal From Coal: Ammonia/Oxygen System", *ibid.*
36. Tipton, A.B., "Improved Hydrodesulfurization of Coal Clear by Acid Leach", *ibid.*
37. Huang, E.T.K, and Pulsifer, A.H., "Coal Desulfurization during Gaseous Treatment", *ibid.*
38. Meyers, R.A., "Desulfurize Coal Chemically" Hydrocarbon Processing, June 1975. (Meyers Process).
39. Anon. "Vibrating Dry Table Speeds Removal of High-Ash Material From Coal", Coal Age, June 1976.
40. Iammartino, N.R., "New Task for Magnetism", Chemical Engineering, Jan 7, 1974.
41. Brisse, A.H., and McMOVUS, W.L., Jr., "Converal Process" Transactions AIME, Mining Engineering, Feb. 1958.
42. Stambaugh, E.P., "Batelle Develops Leaching Process to Desulfurize Coal", (Hydrothermal Coal Process), Coal Age, aug. 1975.
43. Reis, T., "To Coke, Desulfurize, and Calcine. Part 2: Coke Quality and Its Control", Hydrocarbon Processing, June 1975.

44. O'Brien, E.J., "Water-only Cyclones: Their Functions and Performance", Coal Age, Jan. 1976.
45. Lorenzi, L., Jr., Land, J.S., Van Nice, L.J., Koutsoukos, E.P., and Meyers, R.A., "TRW Zeroes in on Leaching Method to Desulfurize Pyritic coals", Coal Age, Nov. 1972. (Meyers Process).
46. Hucko, R.E., "Beneficiation on Coal by Selective Flocculation, A Laboratory Study", Report of Investigations 8234, Bureau of Mines, U.S. Department of the Interior, 1977.
47. Haldipur, G.B., and Wheelock, T.D., "Desulfurization of Coal in a Fluidized-Bed Reactor", in Coal Desulfurization, T.D. Wheelock, Editor, ACS Symposium series 64, American Chemical Society, Washington, D.C., (1977).
48. Green, N.W., "Synthetic Fuels From Coal. The Garrett Process", presented at the Clean Fuels From Coal Symposium II, Chicago, June 23-27, 1975.
49. Jones, J.E., "Project COE Char-Oil-Energy Development", *ibid.*
50. Gary, J.H., and Handwerk, G.E., "Delayed Coking" in Petroleum Refining, Marcel Dekker, Inc., New York, (1975).
51. Department of Energy, "Laboratory Study For Removal of Organic Sulfur From Coal" U.S. DOE Contract No. DE-AC22-80PC30141, Quarterly Technical Progress Report, July 15, 1980.
52. *Ibid.*, Quarterly Technical Progress Report, Oct. 15, 1980.
53. *Ibid.*, Quarterly Technical Progress Report, Jan. 15, 1981.
54. Zavitanos, P.D., Golden, J.A., Bleiler, K.W., and Jacobs, I.S., "Coal Desulfurization by a Microwave Process", work performed under Contract No. DE-AC22-80PC30142, General Electric Company, Research and Engineering, Re-Entry Systems Division, Philadelphia, PA., March 1981.
55. Hise, E.C., "Sulfur and Ash Reduction in Coal by Magnetic Separation", Engineering Technology Division, Oak Ridge National Laboratory, Oak Ridge, TN.
56. Porter, C.R., and Goens, D.N., "Magnex, Pilot Plant Evaluation - A Dry Chemical Process for the Removal of Pyrite and Ash From Coal", SME preprint 78-F-352, SME Fall Meeting, St. Louis, MO, Oct. 1977.
57. Otisca Industries, Ltd., "Otisca Media Process", Otisca Industries, Ltd., Syracuse, N.Y., Clay D. Smith President, 1982.
58. Otisca Industries, Ltd., "Otisca T-Process", *ibid.*
59. Maize, K., "Sulfur-Munching Microbes May Cure Ailing Ohio Coal", The Energy Daily, March 18, 1982.

60. Zavitsanos, P.D., Golden, J.A., and Bleiler, K.W., "Coal Desulfurization by a Microwave Process", work performed under Contract No. DE-AC22-80PC30142, General Electric Company, Research and Engineering, Re-Entry Systems Division, Philadelphia, PA., Technical Progress Report, Feb. 1981 - May 1981.
61. Berry, R.I., "Guide to Coal-Cleaning Methods", Chemical Engineering, Jan. 26, 1981.
62. Romey, I., and Hein, M., "Carbon Fibers From Coal-Tar Pitch", Fuel, Vol. 60, 849, Sept. 1981.
63. Stadelhofer, J.W., Marrett, R., and Gemmeke, W., "The Manufacture of High-Value Carbon From Coal-Tar Pitch", Fuel Vol. 60, 877, sept. 1981.
64. Leonard, J.W., and Mitchell, D.R., Editors, Coal Preparation, Third Edition, The American Institute of Mining, Metallurgical, and Petroleum Engineers, Inc., New York, 1968.
65. Anon, "Cleaning Pulverized Coal-Dust Free", Chemical Week, Dec. 23, 1981.
66. Detz, C.M., and Barvinchak, G., "Microbial Desulfurization of Coal", Mining Congress Journal, July, 1979.
67. Santhanam, C.J., "Development of Coal/Liquid CO₂ Slurry Transportation", presented at the Seventh International Technical Conference on Slurry Transportation, Lake Tahoe, NV., March 1982.
68. Rich, S.R., "Pilot Plant Program for the AED Advanced Coal Cleaning System", prepared by Advanced Energy Dynamics, Inc., Natick, MA, Contract No. 80-69, Interim Final Report, Aug. 1980.
69. Anon, "Introduction to Advanced Energy Dynamics, Inc.", Coal Cleaning Systems, Natick, MA.
70. Anon, "Economic Analysis of the Coal-Cleaning System Developed by Advanced Energy Dynamics, Inc., at an Electric Utility, Synfuel Plant on Coal-Oil-Mixture Facility", Advanced Energy Dynamics, Inc., March 27, 1981.
71. Mason, R.B., "Hydrodesulfurization of Coke", Chemical Engineering Progress, Vol. 51, No. 9, 1027, (1959).
72. Barr, F.T., and Kakning, C.E., "Fluid Coking and Fluid Coke", Chemical Engineering Progress, Vol. 51, No. 4, 167, (1955).
73. Nelson, W.L., "Heating Value of Petroleum Coke", Questions on Technology, The Oil and Gas Journal, June 22, 1950.
74. Nelson, W.L., "Sulfur Content of Petroleum Coke", Questions on Technology, The Oil and Gas Journal, March 9, 1953.
75. Nelson, W., "Properties of Petroleum Coke", Questions on Technology, The Oil and Gas Journal, Nov. 28, 1955.
76. Dunlay, J., "Coal: Diesel Fuel of the Future?", Power, March 1981.

77. Hardcastle, J.R., "Low-Cost Route to New Liquid Slurry", Popular Science, March 1982.
78. Shea, F.L., "Production of Coke From Petroleum Hydrocarbons", U.S. Patent 2,775,720, Sept. 13, 1966.
79. Peet, N.P., "Coking Process", U.S. Patent 3,272,720, Sept. 13, 1966.
80. Schlinger, W.G., Slater, W.L., Delle, R.M., And Tassoney, J.P., "Slurries of Solid Carboniferous Fuels", U.S. Patent 3,764,547, Oct. 8, 1973.
81. Theodore, F.W., Wasson, G.E., Jasulaitis, W.A., and Gorin, E., "Process for Making Metallurgical Coke", U.S. Patent 4,201,655, May 6, 1980.
82. Havoresen, W.J., "Integrated Coal Cleaning and Slurry Preparation Process", U.S. Patent 4,244,530, Jan. 13, 1981.
83. Venaty, J., "Process for Micronizing of Solid Carbonaceous Matter and Preparation of Carbon-Oil Mixtures", U.S. Patent 4,244,528, Jan. 13, 1981.
84. Bender, H., Hasse, W., Pfeiffer, R., and Unkelbach, K.H., "Method for the Desulfurization of Coal", U.S. Patent 4,252,638, Feb. 24, 1981.
85. Wynne, F.E. Jr., Lopez, J., and Zaborowsky, E.J., "Coke From Coal and Petroleum", U.S. Patent 4,259,178, March 31, 1981.
86. Rose, K.E., "Delayed coking --- What You Should Know", Hydrocarbon Processing, July 1971.
87. Ramirez, R., "Novel Process Makes Coke From Coal Tar Pitch", Chemical Engineering, Feb. 24, 1969.
88. Stormont, D.H., "Delayed Coking Techniques Fuel Effect of Increased Needle-Coke Demand", The Oil and Gas Journal, March 17, 1969.
89. Schowalter, K.A., and Boodman, N.S., "The Clean-Coke Process for Metallurgical Coke", Chemical Engineering Progress, Vol. 70, No. 6, 76, (1974).
90. McDonald, J. and Rhys, C.O. Jr., "The Fluid Coking Process - Commercial Experience to Date", Refining Engineer, Sept. 1959.
91. Liu, Y.A. and Lin, C.J., "Assessment of Sulfur and Ash Removal From Coals by Magnetic Separation", IEEE Transactions on Magnetics, Vol. Mag.-12, No. 5, 538, Sept. 1976.
92. Murray, H.H., "Beneficiation of Selected Industrial Minerals and Coal by High-Intensity Magnetic Separations", IEEE Transactions on Magnetics, Vol. Mag.-12, No. 5, 498, Sept. 1976.
93. Iannicelli, J., "Development of High Extraction Magnetic Filtration by the Kaolin Industry in Georgia", IEEE Transactions on Magnetics, Vol. Mag.-12, No. 5, 489, Sept. 1976.

94. Cohen, H. and Good, J.A., "The Principles and Operation of a Very High Intensity Magnetic Mineral Separator", IEEE Transactions on Magnetics, Vol. Mag-12, No. 5, 552, Sept. 1976.
95. Kemnitzer, W.J., and Edgerton, C.D. Jr., "Petroleum Coke on the West Coast of the United States", Information Circular 8259, United States Dept. of the Interior Bureau of Mines, May 1964.
96. Lewis, D. and Wellington, T.D., "Some Old and New Concepts in Magnetic Separation", IEEE Transactions on Magnetics, Vol. Mag-12, No. 5, 480, Sept. 1976.
97. Oder, R.R., "High-Gradient Magnetic Separation Theory and Applications", IEEE Transactions on Magnetics, Vol. Mag-12, No. 5, 428, Sept. 1976.
98. Iannicelli, J., "New Developments in Magnetic Separation", IEEE Transactions on Magnetics, Vol. Mag-12, No. 5, Sept. 1976.
99. Koppelman, E., "Process for Making Coke From Butuminous Fines and Fuels Produced Therefrom", U.S. Patent 4,127,391, Nov. 28, 1978.
100. Koppelman, E., "Process for Making Coke From Cellulosic Materials and Fuels Produced Therefrom", U.S. Patent 4,129,420, Dec. 12, 1978.
101. Trent, W.E., "Process of Purifying Materials", U.S. Patent 1,420,164, June 20, 1922.
102. Murray, R.G., "Apparatus and Method for Thermal Treatment of Organic Carbonaceous Material", U.S. Patent 4,126,519, Nov. 21, 1978.
103. Koppelman, E., "Process for Upgrading Lignitic-Type Coal as a Fuel". U.S. Patent 4,052,168, Oct. 4, 1977.
104. Mekler, V. and Brooks, M.E., "New Developments and Techniques in Delayed Coking", Refining Engineer, Sept. 1959.
105. Worthy, W., "Hydrothermal Process Cleans Up Coal", Chemical and Engineering News, July 7, 1975.
106. Maxwell, E., Kelland, D.R., and Akoto, I.Y., "High-Gradient Magnetic Separation of Mineral Particulates From Solvent Refined Coal", IEEE Transactions on Magnetics, Vol. Mag-12, No. 5, 507, Sept. 1976.
107. Cohen, E., and Good, J.A., "The Application of a Superconducting Magnet System to the Cleaning and Desulfurization of Coal", IEEE Transactions on Magnetics, Vol. Mag-12, No. 5, 503, Sept. 1976.
108. Vives, D.L., Hirth, L.J., and Summerlin, W.H., "Direct Reduction and Magnetic Beneficiation of Alabama Brown Ore with Lignite", IEEE Transactions, Vol. Mag-12, No. 5, 490, Sept. 1976.
109. DeBiase, R. and Elliott, J.D., "Coking Process Reflects Trends, Innovations". Technology, Oil and Gas Journal, April 19, 1982.

110. Anon, "Fluid Coking", Hydrocarbon Processing.
111. Monteiro, J.L.F., Saddy, M., and Trindade, S.C., "Studies on Sulfur Recovery From Coal Wastes and Propective Magnetic Separation Applications", IEEE Transactions on Magnetics, Vol. Mag-12, No. 5, 522, Sept. 1976.
112. Good, J.A. and Cohen, E., "A Superconducting Magnet System for A Very High Intensity Magnetic Mineral Separator", IEEE Transactions on Magnetics, Vol. Mag-12, No. 5, 493, Sept. 1976.
113. Bienstock, D. and Jamgochian, E.M., "Coal-Oil Mixture Technology in the U.S.", Fuel, Vol. 60, 863, Sept. 1981.
114. Wilson, J., "Active Carbons From Coals", Fuel, Vol. 60, 823, Sept. 1981.
115. Cammack, P., "Coal Preparation for Conversion Process", Fuel, Vol. 60, 763, Sept. 1981.
116. Singer, L.S., "Carbon Fibers From Mesophase Pitch", Fuel, Vol. 60, 839, Sept. 1981.
117. Clayfield, E.J., Dorresteiijn, E., Lumb, E.C., Wilbraham, K.J, and Barratt, D.J, "COOLOIL Manufacture and Application", Fuel, Vol. 60, 865, Sept. 1981.
118. Veal, J.C. and Wall, D.R., "Coal-Oil Dispersions - An Overview", Fuel, Vol. 60, 873, Sept. 1981.
119. Jenkins, J.C. and Jenkins, G.W., "Study of the Extrusion of a Typical Pitch Mesophase and the Nature of the Cokes Derived Therefrom", Fuel, Vol. 60, 8883, Sept. 1981.
120. Beech, R.N., and Price, M.S.T., "The Manufacture of Artefacts From Coal", Fuel Vol. 60, 889, Sept. 1981.
121. Jordan, K.D., "Study of Precombustion Methods of Chemical Coal Cleaning", NTIS, DOE/PC/20083-T1, 1980 (University of Pittsburgh).
122. Keller, D.V. Jr. and Simmons, F.J., "Heavy-Liquid Beneficiation of Fine Coal", NTIS DOE/PC/30239-T*, 1980 (Otisca Industries).
123. Herkst, J.A., "Energy Requirements for Fine Grinding of Coal in a An Attritor", Final Report, Sept. etc, NTIS COO-4560-1, Nov. 1978, (Utah University).
124. Anon, "An Analysis of Chemical Coal Cleaning Processes. (Final Report)", NTIS, DOE/ET/10045-T1, June 19809, (BEC HTEL National, Inc.).
125. Anon, "Comparative Engineering and Cost Analysis of Coal Beneficiation Process", NTIS, FE-2344-T*, March 20, 1978, (Energy and Environmental Analysis, Inc.).
126. Murray, H.H., et al., "Beneficiation of Industrial Minerals, Ores, and Coal by High-Intensity Wet Magnetic Separation - A Survey", NTIS, NSF/RA-800286A; PB81-188385, 1980, (Indiana University at Bloomington).

127. Spaite, P.W., et al., "Environmental Assessment of Coal Cleaning Processes: Technology Overview", NTIS, EPA-600/7-79-073E; PB80-128143, Sept. 1979, (Battelle).
128. Holt, E.C. Jr., "An Engineering/Economic Analysis of Coal Preparation Plant Operation and Cost", NTIS EPA/600/7-78-124; PB-285251, July 1978, (Hoffman-Muntner Corp).

APPENDIX B
Spray Penetration Versus Time Data

Table B1. Data for Four Hole Nozzle
Using Basefuel.

T=470 C

P=4.23 MPa

Time (usec)	Distance (mm)
0.00	0.00
36.42	4.08
76.85	8.42
117.28	13.25
157.71	16.37
198.14	17.50
238.57	18.12
279.00	19.79
319.43	21.32
359.86	23.47
400.29	24.77
440.72	25.94
481.15	27.74
521.58	29.39
562.01	31.55
602.44	34.12
642.87	36.10
683.30	37.64

Table B2. Data for Four Hole Nozzle
 Using Basefuel.
 T=470 C
 P=2.17 MPa

Time (usec)	Distance (mm)
0.00	0.00
18.76	3.08
58.51	9.97
98.26	16.42
138.01	21.90
177.76	26.15
217.51	27.01
257.26	27.83
297.01	29.06
336.76	31.00
376.51	32.69
416.26	34.65
456.01	36.07
495.76	38.15
535.51	39.64

Table B3. Data for Four Hole Nozzle
Using Basefuel.

T=470 C

P=0.55 MPa

Time (usec)	Distance (mm)
0.00	0.00
7.93	1.43
48.18	7.53
88.43	14.44
128.68	21.61
168.93	29.55
209.18	36.87
249.43	37.60

Table B4. Data for Four Hole Nozzle
Using Basefuel.

T=470 C

P=0.10 MPa

Time (usec)	Distance (mm)
0.00	0.00
8.17	2.12
48.55	8.37
88.93	17.43
129.31	26.47
169.69	35.57
210.07	37.40

Table B5. Data for Four Hole Nozzle
Using Basefuel.

T=26 C

P=1.67 MPa

Time (usec)	Distance (mm)
0.00	0.00
18.76	2.13
59.21	6.99
99.66	11.54
140.11	15.27
180.56	18.20
221.01	20.18
261.46	23.10
301.91	25.63
342.36	27.88
382.81	29.70
423.26	31.01
463.71	32.92
504.16	34.63
544.61	35.59
585.06	36.60
625.51	36.98
665.96	37.05

.Table B6. Data for Four Hole Nozzle
Using 10% Mogul L.

T=26 C

P=1.67 MPa

Time (usec)	Distance (mm)
0.00	0.00
19.14	2.79
59.13	7.32
99.12	13.27
139.11	17.95
179.10	21.68
219.09	24.28
259.08	24.67
299.07	26.15
339.06	27.66
379.05	28.44
419.04	29.80
459.03	31.75
499.02	34.12
539.01	36.52
579.00	38.21
618.99	39.24

.Table B7. Data for Four Hole Nozzle
Using 20% Mogul L.

T=470 C

P=4.23 MPa

Time (usec)	Distance (mm)
0.00	0.00
13.74	1.78
54.06	8.14
94.38	13.26
134.70	14.45
175.02	16.80
215.34	19.69
255.66	22.51
295.98	24.63
336.30	26.33
376.62	27.47
416.94	29.14
457.26	31.75
497.58	34.05
537.90	35.48
578.22	36.63
618.54	37.75

Table B8. Data for Four Hole Nozzle
Using 20% Mogul L.
T=470 C
P=2.17 MPa

Time (usec)	Distance (mm)
0.00	0.00
7.53	1.15
47.86	7.01
88.19	13.08
128.52	18.98
168.85	21.71
209.18	25.19
249.51	27.65
289.84	30.44
330.17	32.71
370.50	35.40
410.83	37.00
451.16	38.29

Table B9. Data for Four Hole Nozzle
Using 20% Mogul L.

T=470 C

P=0.10 MPa

Time (usec)	Distance (mm)
0.00	0.00
17.95	2.63
58.37	9.57
98.79	15.28
139.21	21.54
179.63	26.47
220.05	34.55
260.47	38.05

Table B10. Data for Four Hole Nozzle
 Using 20% Mogul L.
 T=26 C
 P=1.67 MPa

Time (usec)	Distance (mm)
0.00	0.00
18.21	1.34
58.67	4.46
99.13	7.41
139.59	11.70
180.05	15.32
220.51	19.29
260.97	22.76
301.43	25.05
341.89	26.47
382.35	27.54
422.81	27.97
463.27	29.07
503.73	29.73
544.19	31.73
584.65	33.91
625.11	35.58
665.57	36.18
706.03	37.30

Table B11. Data for Four Hole Nozzle
 Using 10% SRC-I.
 T=26 C
 P=1.67 MPa

Time (usec)	Distance (mm)
0.00	0.00
28.02	4.18
67.91	10.52
107.80	16.31
147.69	19.15
187.58	19.55
227.47	20.22
267.36	20.90
307.25	22.13
347.14	24.23
387.03	26.55
426.92	29.08
466.81	31.49
506.70	34.25
546.59	36.30
586.48	37.85
626.37	38.07
666.26	39.32

Table B12. Data for Four Hole Nozzle
Using 20% SRC-I.

T=470 C

P=4.23 MPa

Time (usec)	Distance (mm)
0.00	0.00
9.61	1.35
50.06	4.76
90.51	9.81
130.96	14.58
171.41	18.14
211.86	20.69
252.31	22.29
292.76	23.46
333.21	25.59
373.66	27.85
414.11	29.55
454.56	31.58
495.01	33.21
535.46	35.02
575.91	36.77
616.36	37.63
656.81	38.36

Table B13. Data for Four Hole Nozzle
 Using 20% SRC-I.
 T=470 C
 P=2.17 MPa

Time (usec)	Distance (mm)
0.00	0.00
28.23	3.72
67.90	8.78
107.57	14.06
147.24	18.25
186.91	20.98
226.58	23.81
266.25	26.06
305.92	27.75
345.59	28.87
385.26	31.13
424.93	33.33
464.60	35.78
504.27	38.13
543.94	39.40

Table B14. Data for Four Hole Nozzle
Using 20% SRC-I.

T=470 C

P=0.10 MPa

Time (usec)	Distance (mm)
0.00	0.00
17.95	3.51
57.52	11.09
97.09	18.86
136.66	23.99
176.23	32.39
215.80	39.32

Table B15. Data for Four Hole Nozzle
Using 20% SRC-I.

T=26 C

P=1.67 MPa

Time (usec)	Distance (mm)
0.00	0.00
12.92	1.91
52.92	8.27
92.92	14.17
132.92	18.63
172.92	21.44
212.92	23.61
252.92	25.58
292.92	26.79
332.92	28.56
372.92	29.64
412.92	30.37
452.92	31.60
492.92	32.68
532.92	34.11
572.92	34.67
612.92	36.10
652.92	38.07
692.92	38.66

Table B16. Data for Four Hole Nozzle
 Using 20% SRC-I*.
 T=26 C
 P=1.67 MPa

Time (usec)	Distance (mm)
0.00	0.00
33.64	4.49
73.40	10.66
113.16	15.51
152.92	18.51
192.68	19.41
232.44	21.55
272.20	23.20
311.96	24.94
351.72	26.83
391.48	28.12
431.24	30.31
471.00	32.19
510.76	34.25
550.52	35.97
590.28	37.58
630.04	37.88
669.80	39.40

* indicates duplicate data.

Table B17. Data for Pintle Nozzle
Using Basefuel.

T=26 C

P=1.67 MPa

Time (usec)	Distance (mm)
0.00	0.00
17.78	1.37
57.87	5.03
97.96	7.98
138.04	12.80
178.13	16.17
218.22	20.16
258.30	24.51
298.39	29.43
338.48	34.71
378.57	39.53
418.65	44.00

Table B18. Data for Pintle Nozzle
Using Basefuel.
T=26 C
P=0.10 MPa

Time (usec)	Distance (mm)
0.00	0.00
27.12	3.52
67.14	9.23
107.17	14.22
147.20	19.72
187.22	23.94
227.25	28.17
267.28	32.96
307.31	38.82
347.33	42.74
387.36	44.00

Table B19. Data for Pintle Nozzle
Using 30% Clean Coal.

T=26 C

P=1.67 MPa

Time (usec)	Distance (mm)
0.00	0.00
4.72	1.17
45.06	1.92
85.41	5.75
125.75	8.37
166.10	10.66
206.44	13.62
246.79	16.60
287.14	19.86
327.48	22.96
367.83	26.69
408.17	30.05
448.52	33.76
488.86	36.58
529.21	39.77
569.55	42.27
609.90	44.00

Table B20. Data for Pintle Nozzle
Using 30% Clean Coal.

T=26 C

P=0.10 MPa

Time (usec)	Distance (mm)
0.00	0.00
22.51	1.15
62.86	2.33
103.20	4.46
143.55	6.17
183.90	10.34
224.25	15.50
264.60	21.46
304.95	27.85
345.30	31.43
385.65	39.29
426.00	44.00

Table B21. Data for Pintle Nozzle
 Using 30% Eureka.
 T=26 C
 P=1.67 MPa

Time (usec)	Distance (mm)
0.00	0.00
14.38	1.51
54.93	2.79
95.48	6.41
136.03	9.70
176.57	13.36
217.12	17.78
257.67	22.06
298.22	28.42
338.77	34.56
379.32	39.71
419.86	44.00

Table B22. Data for Pintle Nozzle
Using 30% Eureka.

T=26 C

P=0.10 MPa

Time (usec)	Distance (mm)
0.00	0.00
7.88	1.72
48.24	5.57
88.61	12.44
128.97	17.65
169.34	23.26
209.70	29.56
250.06	34.90
290.43	39.49
330.79	42.63
371.15	44.00

Table B23. Data for Pintle Nozzle
Using 30% Fairless Coke.

T=26 C

P=1.67 MPa

Time (usec)	Distance (mm)
0.00	0.00
16.46	1.44
56.67	4.52
96.88	8.06
137.09	12.02
177.30	16.53
217.52	21.51
257.73	26.39
297.94	31.50
338.15	37.17
378.36	42.18
418.57	44.00

Table B24. Data for Pintle Nozzle
 Using 30% Fairless Coke.
 T=26 C
 P=0.10 MPa

Time (usec)	Distance (mm)
0.00	0.00
11.09	1.42
51.26	6.56
91.44	11.70
131.61	17.17
171.78	22.25
211.96	27.11
252.13	31.51
292.30	35.86
332.48	40.51
372.65	44.00

Table B25. Data for Pintle Nozzle
Using 20% Mogul L.

T=26 C

P=1.67 MPa

Time (usec)	Distance (mm)
0.00	0.00
29.04	3.03
69.23	6.08
109.41	10.55
149.59	14.49
189.78	18.50
229.96	22.33
270.14	25.97
310.33	30.78
350.51	35.92
390.69	40.75
430.88	44.00

Table B26. Data for Pintle Nozzle
Using 20% Mogul L.

T=26 C

P=0.10 MPa

Time (usec)	Distance (mm)
0.00	0.00
30.21	2.88
70.38	6.74
110.56	10.54
150.73	14.33
190.90	19.68
231.08	22.72
271.25	30.30
311.42	33.95
351.60	38.59
391.77	42.38
431.94	44.00

Table B27. Data for Pintle Nozzle
Using 30% Mogul L.

T=26 C

P=1.67 MPa

Time (usec)	Distance (mm)
0.00	0.00
29.84	2.62
69.89	5.99
109.94	9.55
149.99	13.25
190.04	17.28
230.09	21.33
270.14	26.76
310.18	31.91
350.23	37.46
390.28	42.56
430.33	44.00

Table B28. Data for Pintle Nozzle
 Using 30% Mogul L.
 T=26 C
 P=0.10 MPa

Time (usec)	Distance (mm)
0.00	0.00
39.99	3.70
80.11	7.69
120.23	11.26
160.36	16.58
200.48	21.20
240.60	24.99
280.73	29.02
320.85	33.68
360.98	36.98
401.10	40.65
441.22	42.85
481.35	44.00

Table B29. Data for Pintle Nozzle
Using 30% Petroleum Coke.

T=26 C

P=1.67 MPa

Time (usec)	Distance (mm)
0.00	0.00
38.13	3.71
78.28	7.33
118.43	11.37
158.58	15.07
198.73	19.31
238.89	24.48
279.04	29.65
319.19	34.80
359.34	39.74
399.49	44.00

Table B30. Data for Pintle Nozzle
Using 30% Petroleum Coke.

T=26 C

P=0.10 MPa

Time (usec)	Distance (mm)
0.00	0.00
10.05	1.57
50.67	7.17
91.28	13.38
131.90	19.16
172.52	25.23
213.13	31.25
253.75	36.76
294.37	42.99
334.98	44.00

This Page Intentionally Left Blank

APPENDIX C

Engine Performance and Exhaust Emissions Data

NOMENCLATURE

Bhp	Brake Power
Ihp	Indicated Power
BSFC	Brake Specific Fuel Consumption
ISFC	Indicated Specific Fuel Consumption
BSEC	Brake Specific Energy Consumption
ISEC	Indicated Specific Energy Consumption
XBAR	Angular Center of Area of Heat Release
YBAR	Energy Center of Area of Heat Release
QTOT	Total Heat Release
EGT	Exhaust Temperature
AFIN	Air-Fuel Ratio Measured
AFEX	Air-Fuel Ratio From Exhaust Gases
BSNOX	Brake Specific NO _x Emissions
BSHC	Brake Specific HC Emissions
BSCO	Brake Specific CO Emissions
PART	Solids Loading in Exhaust

Table C1. Engine Performance Data for Direct-Injected Engine

Fuel	Run	Bhp	Ihp	Bsfc	Isfc	Bsec	Isec	Xbar	Ybar	Qtot
		(kW)	(kW)	(kg/kW-hr)		(MJ/kW-hr)		(CA deg)	(N-m/deg)	(N-m)
10%MOGUL L	33.000	4.9609	7.0199	.33379	.23590	13.948	9.858	372.60	41.893	967.5
10%MOGUL L	34.000	3.7300	5.6323	.33805	.22374	14.120	9.352	372.80	38.594	773.1
10%MOGUL L	35.000	2.4916	4.4536	.37878	.21219	15.830	8.862	371.00	28.663	602.7
10%MOGUL L	36.000	4.9609	6.8557	.32042	.23226	13.401	9.708	375.50	39.927	966.8
10%MOGUL L	37.000	3.7300	5.6621	.33987	.22374	14.205	9.360	374.40	34.877	776.6
10%MOGUL L	38.000	2.4916	4.4536	.39520	.22131	16.531	9.246	370.50	24.347	604.9
10%SRC 1	39.000	4.9609	6.9602	.32893	.23469	13.825	9.861	374.40	43.746	979.1
10%SRC 1	40.000	3.7300	5.7442	.33562	.21766	14.096	9.151	372.20	41.836	785.4
10%SRC 1	41.000	2.4916	4.4984	.39094	.21645	16.420	9.103	371.40	30.019	613.2
10%SRC 1	42.000	4.9609	6.7811	.32954	.24138	13.853	10.137	374.80	39.227	954.9
10%SRC 1	43.000	3.7300	5.6920	.33562	.22010	14.116	9.240	373.80	38.662	788.7
10%SRC 1	44.000	2.4916	4.6103	.39702	.21462	16.684	9.016	372.30	27.014	638.8
20%MOGUL L	27.000	4.9609	6.9676	.33440	.23834	13.667	9.742	373.50	44.492	964.2
20%MOGUL L	28.000	3.7300	5.7144	.35775	.23347	14.634	9.553	372.50	35.498	778.5
20%MOGUL L	29.000	2.4916	4.4014	.42621	.24138	17.424	9.871	369.50	30.561	576.8
20%MOGUL L	30.000	4.9609	6.8035	.33622	.24563	13.757	10.044	373.70	41.543	941.6
20%MOGUL L	31.000	3.7300	5.7218	.36298	.23651	14.850	9.683	372.60	35.114	788.2
20%MOGUL L	32.000	2.4916	4.6998	.42682	.22618	17.453	9.250	368.80	30.945	621.3
20%SRC1	15.000	4.9609	6.8408	.34838	.25293	13.833	10.018	378.70	34.493	972.8
20%SRC1	16.000	3.7300	5.7069	.36419	.23834	14.437	9.439	379.40	28.042	815.9
20%SRC1	17.000	2.4916	4.4089	.41283	.23347	16.415	9.270	377.50	20.506	620.1
20%SRC1	18.000	3.8792	5.7442	.35021	.23651	14.436	9.367	379.20	32.538	809.4
20%SRC1	19.000	4.9609	6.8632	.34899	.25232	13.857	10.018	379.70	32.696	986.7
BASELINE	2.000	4.9609	6.7811	.33926	.24806	14.375	10.511	378.20	19.094	963.0
BASELINE	3.000	3.7300	5.5950	.32832	.21888	13.912	9.274	373.90	23.183	762.6
BASELINE	4.000	2.4916	4.5357	.37453	.20550	15.871	8.708	367.10	25.319	595.6
BASELINE	5.000	2.4916	4.3939	.38547	.21888	16.333	9.274	370.60	24.133	617.4
BASELINE	6.000	3.7300	5.4010	.34534	.23834	14.634	10.099	376.10	24.234	774.4
BASELINE	7.000	4.9609	6.7513	.33622	.24746	14.246	10.485	377.10	20.122	969.3
BASELINE	8.000	4.9609	6.7364	.34109	.25110	14.453	10.639	378.40	19.410	952.6
BASELINE	9.000	3.7300	5.6696	.34413	.22618	14.582	9.584	374.50	23.918	776.6
BASELINE	10.000	2.4916	4.4760	.34413	.20854	15.896	8.837	366.40	23.760	583.7
BASELINE	11.000	2.4916	4.4909	.37149	.20611	15.740	8.733	371.60	22.065	610.0
BASELINE	12.000	3.7300	5.7964	.33513	.21566	14.170	9.069	374.50	23.861	794.1
BASELINE	13.000	4.9609	6.8334	.32893	.23882	13.938	10.124	378.00	17.817	971.7
BASELINE	20.000	4.9609	6.7513	.31190	.22922	13.242	9.738	377.10	29.974	951.8
BASELINE	21.000	3.7300	5.7218	.31738	.20672	13.448	8.759	372.30	32.606	787.7
BASELINE	22.000	2.4916	4.6177	.36541	.19760	15.510	8.373	367.90	30.561	613.3
BASELINE	23.000	4.9609	7.0273	.29914	.21098	12.676	8.940	373.40	38.221	965.1
BASELINE	24.000	3.7300	5.7517	.31373	.20368	13.294	8.630	370.00	36.696	764.9
BASELINE	25.000	2.4916	4.4909	.36541	.20246	15.510	8.605	368.70	35.363	599.6
BASELINE	26.000	4.9609	6.8334	.30157	.21949	12.779	9.274	374.40	36.673	945.0

Table C2. Engine Performance Data for Prechamber Engine

Fuel	Run	Bhp (kW)	Ihp (kW)	Bsfc (kg/kW-hr)	Isfc	Bsec (MJ/kW-hr)	Isec	Xbar (CA deg)	Ybar (N-m/deg)	Qtot (N-m)
20%MOGUL L	81.000	4.9236	7.2362	.36358	.24740	14.873	10.120	382.70	11.592	1005.2
20%MOGUL L	82.000	3.7300	6.1172	.39374	.24010	16.107	9.822	377.90	12.891	817.1
20%MOGUL L	83.000	2.5289	4.9161	.46798	.24077	19.144	9.848	373.40	13.987	633.7
30%CLEAN	101.000	4.9609	6.9900	.38164	.27086	15.217	10.799	383.20	10.055	999.6
30%CLEAN	102.000	3.7300	5.7591	.40949	.26521	16.326	10.574	376.10	11.292	766.9
30%CLEAN	103.000	2.4916	4.8714	.46938	.24010	18.715	9.572	373.80	12.270	644.0
30%CLEAN	104.000	4.9609	6.9080	.39210	.28156	15.633	11.227	383.60	10.134	977.2
30%CLEAN	105.000	3.7300	6.1097	.36820	.22478	14.681	8.963	375.50	12.304	801.4
30%CLEAN	106.000	2.4320	4.9236	.48780	.24095	19.449	9.606	372.60	12.835	644.6
30%EUREKA	93.000	4.9609	7.3556	.37276	.25177	15.182	10.255	383.00	10.914	1025.0
30%EUREKA	94.000	3.7300	6.0426	.40748	.25153	16.597	10.245	377.20	12.484	815.0
30%EUREKA	95.000	2.4916	4.8490	.49655	.25208	20.223	10.267	373.20	13.060	630.7
30%EUREKA	96.000	4.9609	7.3257	.40760	.27603	16.601	11.242	384.10	11.027	1052.7
30%EUREKA	97.000	3.7300	6.1396	.41380	.25141	16.854	10.239	375.50	12.450	820.0
30%EUREKA	98.000	2.4469	4.9460	.50276	.24946	20.476	10.160	373.90	12.292	649.6
30%FAIRLESS	84.000	4.9684	7.3481	.36516	.24691	14.381	9.724	382.60	11.761	1017.9
30%FAIRLESS	85.000	3.7300	6.1097	.37909	.23378	14.930	9.207	375.80	12.857	809.0
30%FAIRLESS	86.000	2.4916	4.7520	.45484	.23852	17.912	9.394	376.20	12.032	616.2
30%FAIRLESS	87.000	4.9609	7.2959	.37660	.25609	14.831	10.086	381.60	11.795	993.5
30%FAIRLESS	88.000	3.7300	5.9605	.36079	.22575	14.209	8.890	377.00	13.219	781.8
30%FAIRLESS	90.000	2.4916	5.0131	.48871	.24290	19.247	9.565	373.90	12.755	653.4
30%MOGUL L	75.000	4.9982	7.2362	.35799	.24727	14.045	9.701	380.50	13.535	981.3
30%MOGUL L	76.000	3.7225	5.9680	.41909	.26138	16.442	10.255	378.60	13.625	809.7
30%MOGUL L	77.000	2.4916	4.6998	.48421	.25670	18.998	10.071	374.80	13.942	620.7
30%MOGUL L	78.000	4.9609	6.9602	.40475	.28850	15.879	11.319	382.90	12.541	969.6
30%MOGUL L	79.000	3.7300	5.9158	.40912	.25797	16.052	10.121	379.60	13.659	806.6
30%MOGUL L	80.000	2.4916	4.7520	.49613	.26016	19.465	10.208	373.80	14.879	609.4
30%PETCOKE	53.000	4.9609	5.9904	.29524	.24466	11.709	9.703	310.40	30.708	299.3
30%PETCOKE	54.000	4.4014	6.7140	.33993	.22283	13.482	8.842	385.20	14.665	1045.7
30%PETCOKE	55.000	3.7300	6.3559	.38638	.22660	15.324	8.987	376.90	17.263	843.2
30%PETCOKE	56.000	2.4916	5.0952	.47491	.23238	18.835	9.216	356.70	31.216	498.1
30%PETCOKE	57.000	3.7300	5.9307	.40055	.25171	15.886	9.983	361.80	28.866	609.0
30%PETCOKE	58.000	4.9609	7.2511	.42998	.29445	17.052	11.678	377.30	15.727	890.1
BASELINE	59.000	4.9609	7.1765	.32935	.22788	14.058	9.727	367.40	14.134	790.3
BASELINE	60.000	3.7822	6.0202	.35434	.22265	15.125	9.503	355.80	21.059	598.2
BASELINE	61.000	2.4916	4.7147	.43685	.23098	18.645	9.858	346.10	31.928	422.7
BASELINE	62.000	4.9609	7.2586	.32723	.22368	13.967	9.547	368.90	16.224	800.4
BASELINE	63.000	3.7300	5.8934	.35094	.22143	14.979	9.451	359.60	23.771	601.2
BASELINE	64.000	2.4916	4.8042	.43533	.22605	18.580	9.649	350.40	34.289	434.1
BASELINE	65.000	4.9609	7.1019	.33258	.23244	14.195	9.921	378.10	12.168	951.7
BASELINE	66.000	3.7300	5.9605	.36054	.22557	15.390	9.628	375.50	12.710	780.7
BASELINE	67.000	2.4916	4.8117	.44074	.22818	18.812	9.739	372.90	14.518	629.8
BASELINE	69.000	4.9609	7.1914	.32759	.22605	13.983	9.649	378.30	12.688	964.0
BASELINE	70.000	3.7300	5.9829	.35246	.21973	15.044	9.379	376.60	14.043	790.1
BASELINE	71.000	2.4916	4.7893	.42688	.22222	18.221	9.485	372.80	15.072	622.6
BASELINE	72.000	4.9609	7.1094	.31701	.22131	13.530	9.447	379.70	11.829	966.7
BASELINE	73.000	3.7300	5.8710	.33774	.21444	14.416	9.154	375.50	12.970	780.2
BASELINE	74.000	2.4916	4.7595	.41460	.21700	17.696	9.263	373.10	13.433	605.9

Table C3. Emissions Data for Direct-Injected Engine

Fuel	Run	Bhp	E.G.T.	AFIN	AFEX	BSNOX	BSHC	BSCO	Part.
		(kW)	(deg C)				(g/kW-hr)		(g/liter)
10%MOGUL L	33.000	4.9609	482.22	19.900	20.940	4.155	2.145	17.292	.00163
10%MOGUL L	34.000	3.7300	410.00	26.400	26.800	4.155	2.011	9.383	.00128
10%MOGUL L	35.000	2.4916	337.78	35.640	37.140	4.290	2.279	1.072	.00126
10%MOGUL L	36.000	4.9609	482.22	20.550	21.160	3.887	1.877	13.539	.00168
10%MOGUL L	37.000	3.7300	412.78	26.090	26.540	3.619	2.011	10.054	.00165
10%MOGUL L	38.000	2.4916	337.78	33.840	33.970	3.753	2.011	9.517	-1.00000 *
10%SRC 1	39.000	4.9609	493.33	20.080	20.410	3.753	1.877	34.316	.00452
10%SRC 1	40.000	3.7300	412.78	26.460	26.380	4.290	1.475	12.064	.00163
10%SRC 1	41.000	2.4916	346.11	34.370	33.920	4.021	1.475	10.724	.00112
10%SRC 1	42.000	4.9609	487.78	19.980	19.990	3.619	1.877	43.298	.00214
10%SRC 1	43.000	3.7300	404.44	26.500	26.120	4.290	1.475	13.003	.00120
10%SRC 1	44.000	2.4916	346.11	33.700	33.290	3.887	1.609	10.456	.00067
20%MOGUL L	27.000	4.9609	482.22	19.850	20.780	4.021	2.681	13.137	.00200
20%MOGUL L	28.000	3.7300	407.22	24.950	26.370	4.290	2.413	9.383	.00174
20%MOGUL L	29.000	2.4916	337.78	31.800	33.000	5.094	3.083	11.796	.00171
20%MOGUL L	30.000	4.9609	487.78	19.760	20.480	3.619	2.547	15.147	.00285
20%MOGUL L	31.000	3.7300	410.00	24.730	25.440	4.155	2.279	10.188	.00215
20%MOGUL L	32.000	2.4916	337.78	31.750	33.010	4.290	2.547	11.260	.00210
20%SRC1	15.000	4.9609	504.44	18.820	19.320	3.351	.938	49.196	.00533
20%SRC1	16.000	3.7300	443.33	24.140	24.400	3.753	4.692	25.067	.00244
20%SRC1	17.000	2.4916	371.11	32.060	30.840	4.021	3.753	12.198	.00106
20%SRC1	18.000	3.8792	437.78	24.190	24.110	3.485	4.290	19.169	.00255
20%SRC1	19.000	4.9609	515.56	18.740	18.720	2.681	4.290	49.330	.00338
BASELINE	2.000	4.9609	504.44	19.730	20.070	2.279	1.475	63.941	-1.00000
BASELINE	3.000	3.7300	404.44	27.290	27.960	3.351	1.877	18.633	-1.00000
BASELINE	4.000	2.4916	321.11	36.150	37.360	4.021	2.145	10.456	-1.00000
BASELINE	5.000	2.4916	326.67	35.340	36.010	4.826	2.547	11.126	-1.00000
BASELINE	6.000	3.7300	415.56	26.040	26.370	3.485	2.145	24.933	-1.00000
BASELINE	7.000	4.9609	504.44	19.830	20.170	2.279	1.609	57.507	-1.00000
BASELINE	8.000	4.9609	504.44	19.580	19.640	2.145	5.496	67.694	.00262
BASELINE	9.000	3.7300	415.56	26.040	26.440	.804	3.217	26.810	.00111
BASELINE	10.000	2.4916	332.22	35.950	36.430	1.072	3.083	10.054	.00053
BASELINE	11.000	2.4916	326.67	36.340	35.070	.804	2.815	9.383	.00052
BASELINE	12.000	3.7300	421.11	26.650	26.740	.536	1.609	17.962	.00093
BASELINE	13.000	4.9609	515.56	20.020	21.220	2.860	1.340	68.633	.00209
BASELINE	20.000	4.9609	493.33	21.460	21.270	2.815	2.279	16.220	.00120
BASELINE	21.000	3.7300	398.89	28.250	28.280	3.753	2.011	7.641	.00045
BASELINE	22.000	2.4916	315.56	37.060	37.180	4.424	2.011	6.836	.00037
BASELINE	23.000	4.9609	471.11	22.270	22.050	3.619	2.011	15.818	.00060
BASELINE	24.000	3.7300	382.22	28.450	28.350	4.960	1.743	6.568	.00048
BASELINE	25.000	2.4916	310.00	36.870	37.080	4.155	1.877	10.992	.00049
BASELINE	26.000	4.9609	471.11	21.960	21.790	4.021	2.011	14.075	.00073

* -1.000 indicates missing data.

Table C4. Emissions Data for Prechamber Engine

Fuel	Run	Bhp (kW)	E.G.T. (deg C)	AFR	AFEX	BSNOX -----	BSHC (g/kW-hr) -----	BSCO -----	Part. (g/liter)
20%MOGUL L	81.000	4.9236	426.67	18.490	18.520	3.485	.402	1.743	.00157
20%MOGUL L	82.000	3.7300	326.67	22.740	23.730	5.094	.402	1.206	.00058
20%MOGUL L	83.000	2.5289	276.67	28.270	28.850	4.290	.536	1.475	-1.00000 *
30%CLEAN	101.000	4.9609	421.11	17.650	17.710	3.887	.268	4.021	.00136
30%CLEAN	102.000	3.7300	337.78	21.960	22.360	6.032	.536	3.619	.00019
30%CLEAN	103.000	2.4916	254.44	29.280	28.380	6.032	.536	3.887	.00077
30%CLEAN	104.000	4.9609	421.11	17.170	17.800	3.753	.536	4.021	.00044
30%CLEAN	105.000	3.7300	337.78	24.440	22.660	4.826	.804	3.351	.00027
30%CLEAN	106.000	2.4320	254.44	28.600	28.290	4.424	1.206	3.887	.00019
30%EUREKA	93.000	4.9609	426.67	17.900	17.270	3.351	2.011	3.485	.04168
30%EUREKA	94.000	3.7300	343.33	21.990	22.000	5.228	1.743	3.619	.00130
30%EUREKA	95.000	2.4916	276.67	27.660	27.560	5.764	1.609	4.290	.00090
30%EUREKA	96.000	4.9609	432.22	16.410	17.320	3.619	.938	4.021	.00183
30%EUREKA	97.000	3.7300	337.78	21.780	22.040	5.228	1.072	3.619	.00088
30%EUREKA	98.000	2.4469	271.11	27.410	27.850	5.362	1.206	4.290	.00021
30%FAIRLESS	84.000	4.9684	415.56	18.500	17.990	3.217	.268	1.072	.00117
30%FAIRLESS	85.000	3.7300	332.22	23.180	23.050	4.155	.268	1.206	.00068
30%FAIRLESS	86.000	2.4916	260.00	29.530	29.320	4.424	.268	1.340	.00047
30%FAIRLESS	87.000	4.9609	421.11	17.580	18.090	3.217	.268	1.475	.00150
30%FAIRLESS	88.000	3.7300	332.22	24.530	23.240	4.155	.268	1.072	.00063
30%FAIRLESS	90.000	2.4916	271.11	27.450	28.720	5.228	.536	1.206	-1.00000
30%MOGUL L	75.000	4.9982	415.56	18.390	17.930	3.753	.268	1.475	.00023
30%MOGUL L	76.000	3.7225	332.22	21.360	22.480	4.558	.268	1.743	.00008
30%MOGUL L	77.000	2.4916	260.00	27.680	28.450	4.692	.536	2.011	.00025
30%MOGUL L	78.000	4.9609	426.67	16.290	18.030	3.753	.402	1.877	.00094
30%MOGUL L	79.000	3.7300	337.78	21.650	22.840	4.155	.402	1.609	.00010
30%MOGUL L	80.000	2.4916	265.56	26.880	29.040	4.290	.268	2.145	.00004
30%PETCOKE	53.000	4.9609	498.89	21.730	15.500	1.340	.268	2.279	.00067
30%PETCOKE	54.000	4.4014	498.89	21.290	15.770	1.340	.268	7.105	.00188
30%PETCOKE	55.000	3.7300	498.89	22.590	18.630	1.609	.268	2.011	.00227
30%PETCOKE	56.000	2.4916	215.56	27.500	23.820	1.877	.268	2.279	-1.00000
30%PETCOKE	57.000	3.7300	354.44	21.300	19.140	2.145	.268	2.279	.00480
30%PETCOKE	58.000	4.9609	454.44	14.650	14.850	1.609	.134	4.826	-1.00000
BASELINE	59.000	4.9609	404.44	20.270	21.410	2.011	.536	1.609	.00065
BASELINE	60.000	3.7822	315.56	24.810	25.520	2.413	.402	1.877	.00061
BASELINE	61.000	2.4916	254.44	30.570	30.990	2.815	.402	2.279	.00048
BASELINE	62.000	4.9609	393.33	20.850	20.740	2.011	.402	1.475	.00057
BASELINE	63.000	3.7300	310.00	25.600	25.990	2.413	.402	1.877	.00047
BASELINE	64.000	2.4916	254.44	31.070	32.740	2.815	.402	2.413	.00035
BASELINE	65.000	4.9609	382.22	20.440	21.330	4.826	.536	1.609	.00050
BASELINE	66.000	3.7300	310.00	25.100	26.500	5.630	.402	.938	.00042
BASELINE	67.000	2.4916	248.89	30.960	32.810	6.032	.402	1.609	.00028
BASELINE	69.000	4.9609	390.56	20.560	20.920	4.424	.402	.804	.00031
BASELINE	70.000	3.7300	312.78	25.590	26.260	6.300	.670	.938	.00025
BASELINE	71.000	2.4916	257.22	31.540	32.070	5.496	.804	1.340	.00020
BASELINE	72.000	4.9609	393.33	20.900	20.600	4.155	.268	.938	.00033
BASELINE	73.000	3.7300	315.56	26.250	25.840	4.960	.268	.938	.00022
BASELINE	74.000	2.4916	257.22	32.210	32.130	5.228	.134	1.475	.00015

* -1.000 indicates missing data.

APPENDIX D
Heat Release Rate Diagrams

NOMENCLATURE

- 100-percent Load
- — — 75-percent Load
- — — — 50-percent Load

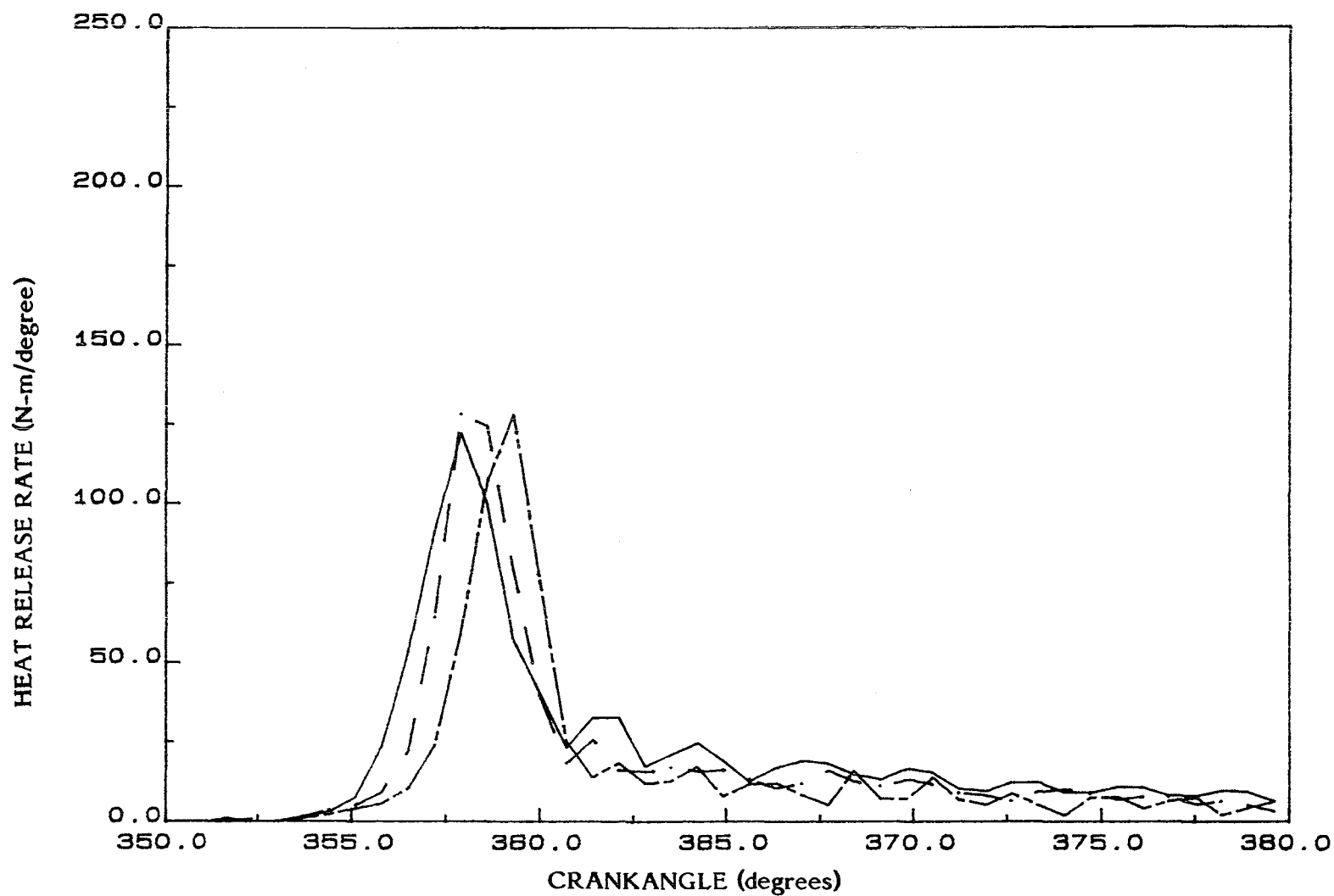


FIGURE D1. HEAT RELEASE RATE VERSUS CRANKANGLE FOR BASELINE, THREE LOADS AT 1500 RPM, IN THE DIRECT-INJECTION ENGINE, RUN NUMBERS (2), (3), (4)

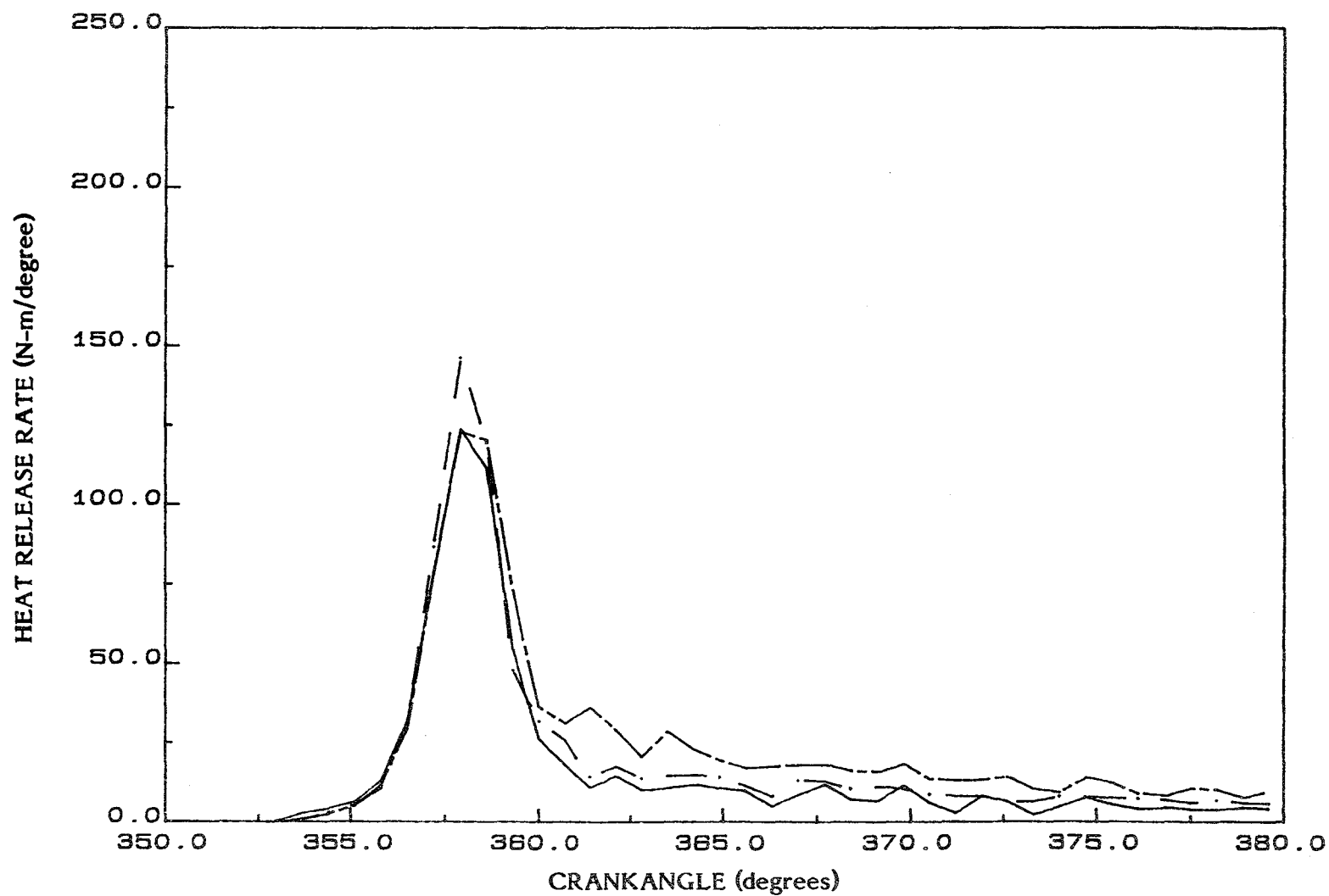


FIGURE D2. HEAT RELEASE RATE VERSUS CRANKANGLE FOR BASELINE,
THREE LOADS AT 1500 RPM, IN THE DIRECT-INJECTION ENGINE,
RUN NUMBERS (5), (6), (7)

D-5

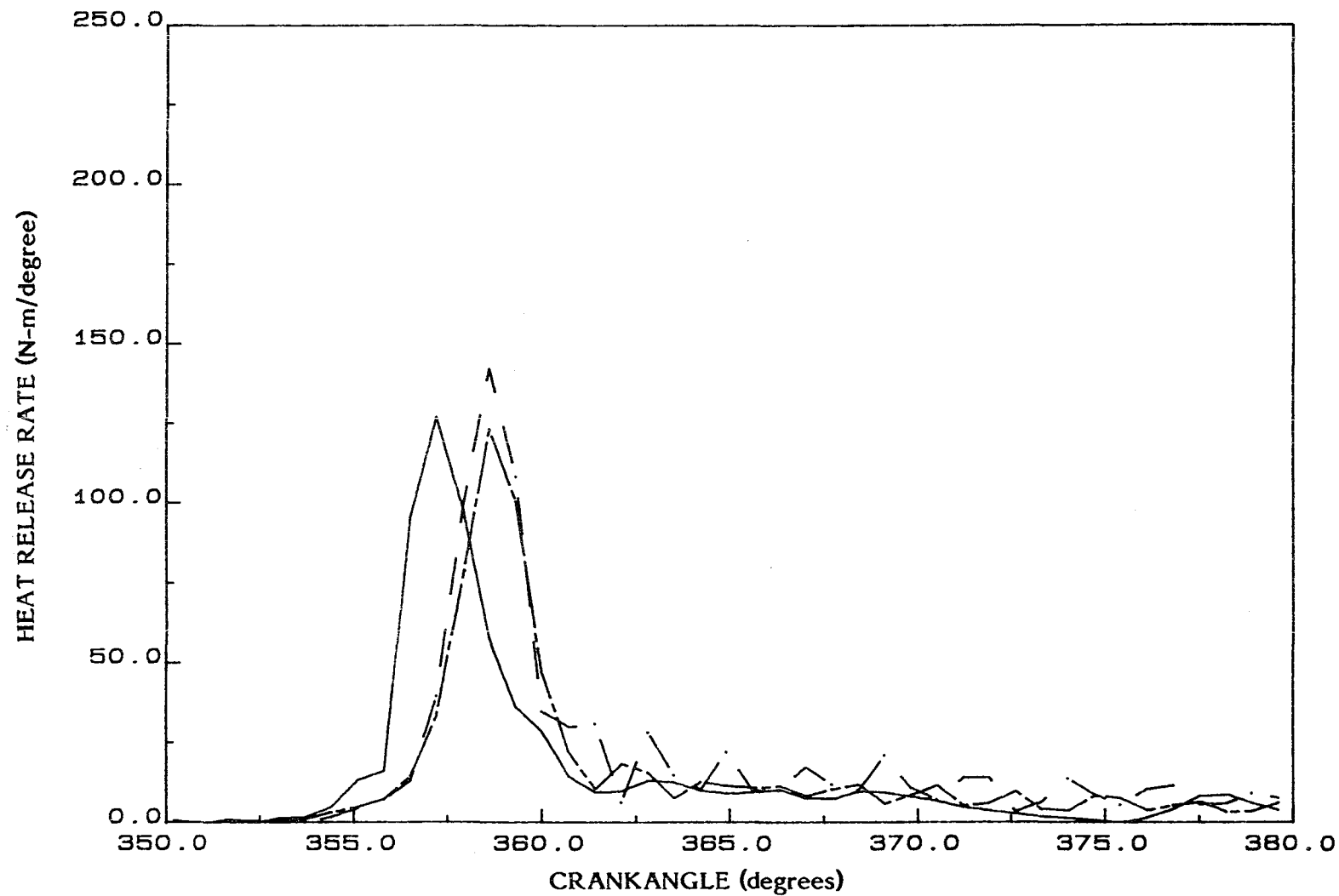


FIGURE D3. HEAT RELEASE RATE VERSUS CRANKANGLE FOR BASELINE, THREE LOADS AT 1500 RPM, IN THE DIRECT-INJECTION ENGINE, RUN NUMBERS (8), (9), (10)

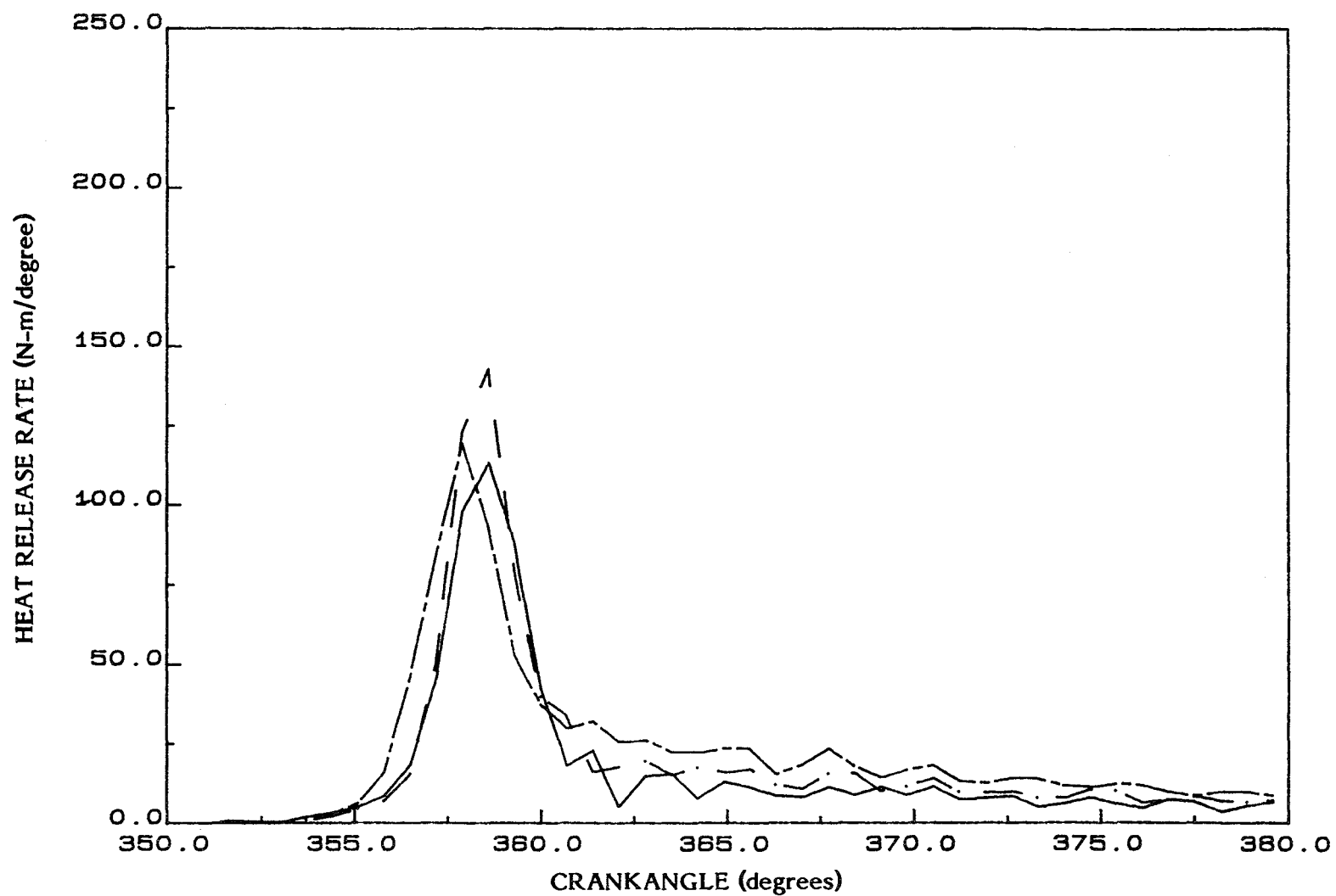


FIGURE D4. HEAT RELEASE RATE VERSUS CRANKANGLE FOR BASELINE,
THREE LOADS AT 1500 RPM, IN THE DIRECT-INJECTION ENGINE,
RUN NUMBERS (11), (12), (13)

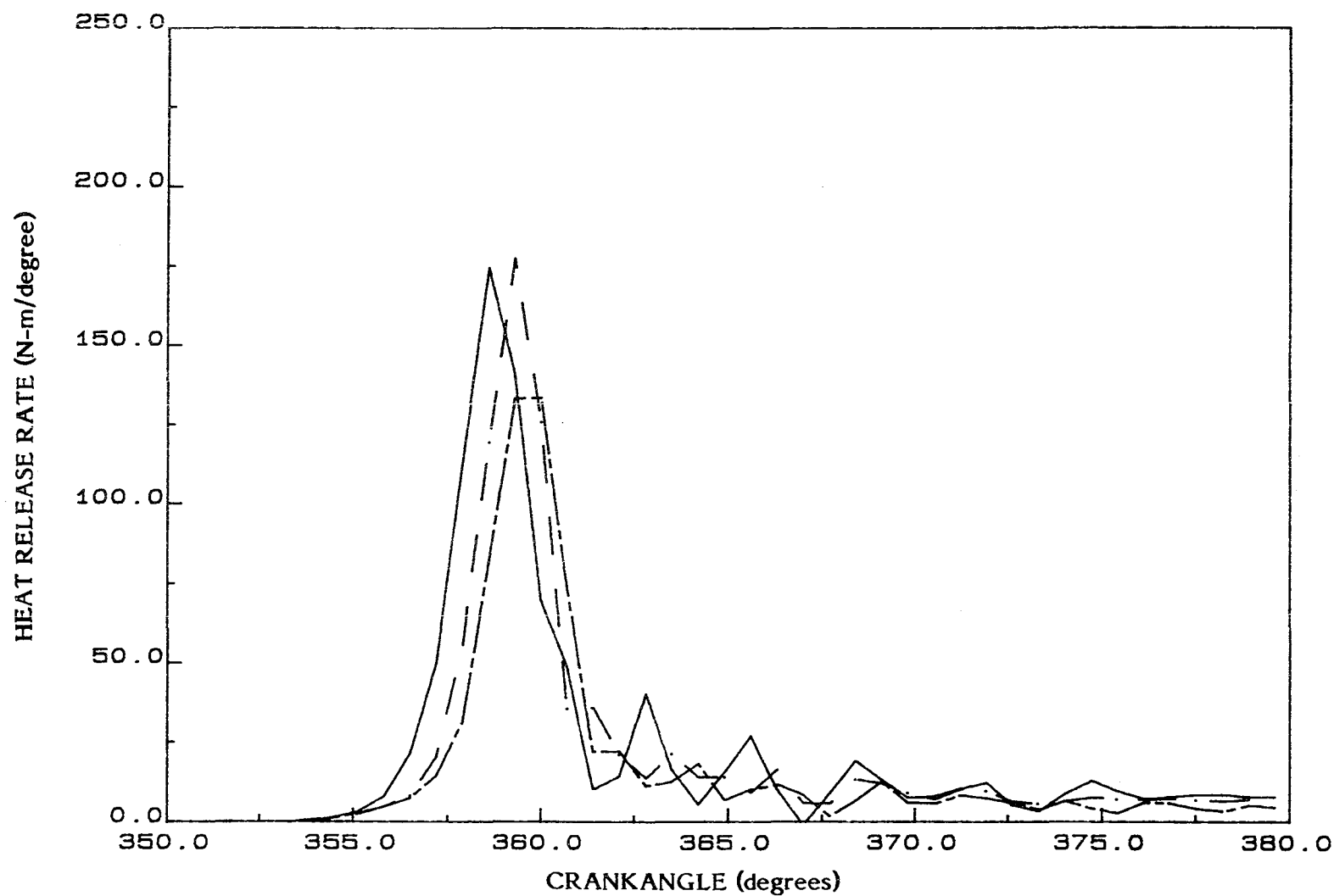


FIGURE D5. HEAT RELEASE RATE VERSUS CRANKANGLE FOR BASELINE, THREE LOADS AT 1500 RPM, IN THE DIRECT-INJECTION ENGINE, RUN NUMBERS (20), (21), (22)

D-8

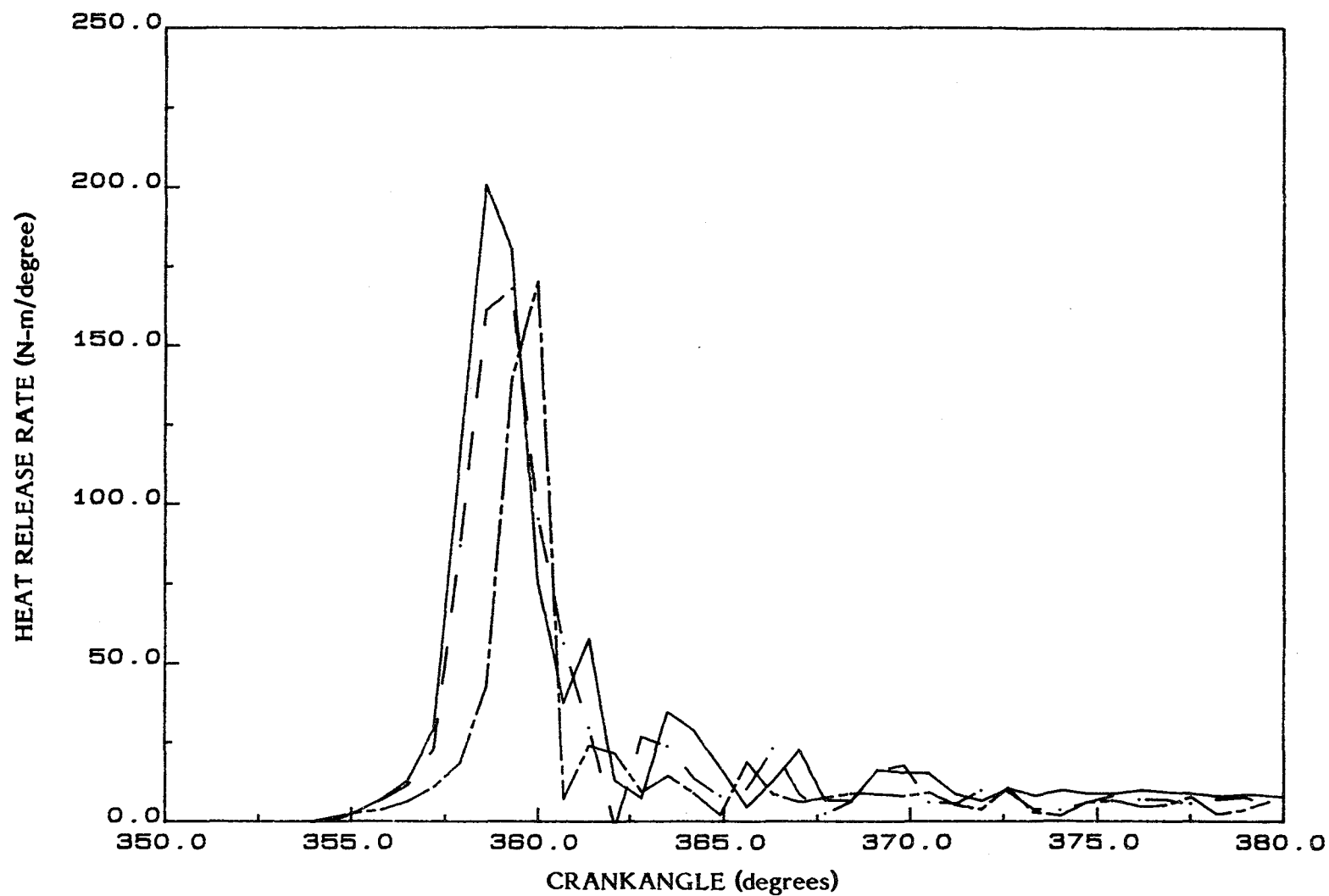


FIGURE D6. HEAT RELEASE RATE VERSUS CRANKANGLE FOR BASELINE,
THREE LOADS AT 1500 RPM, IN THE DIRECT-INJECTION ENGINE,
RUN NUMBERS (23), (24), (25)

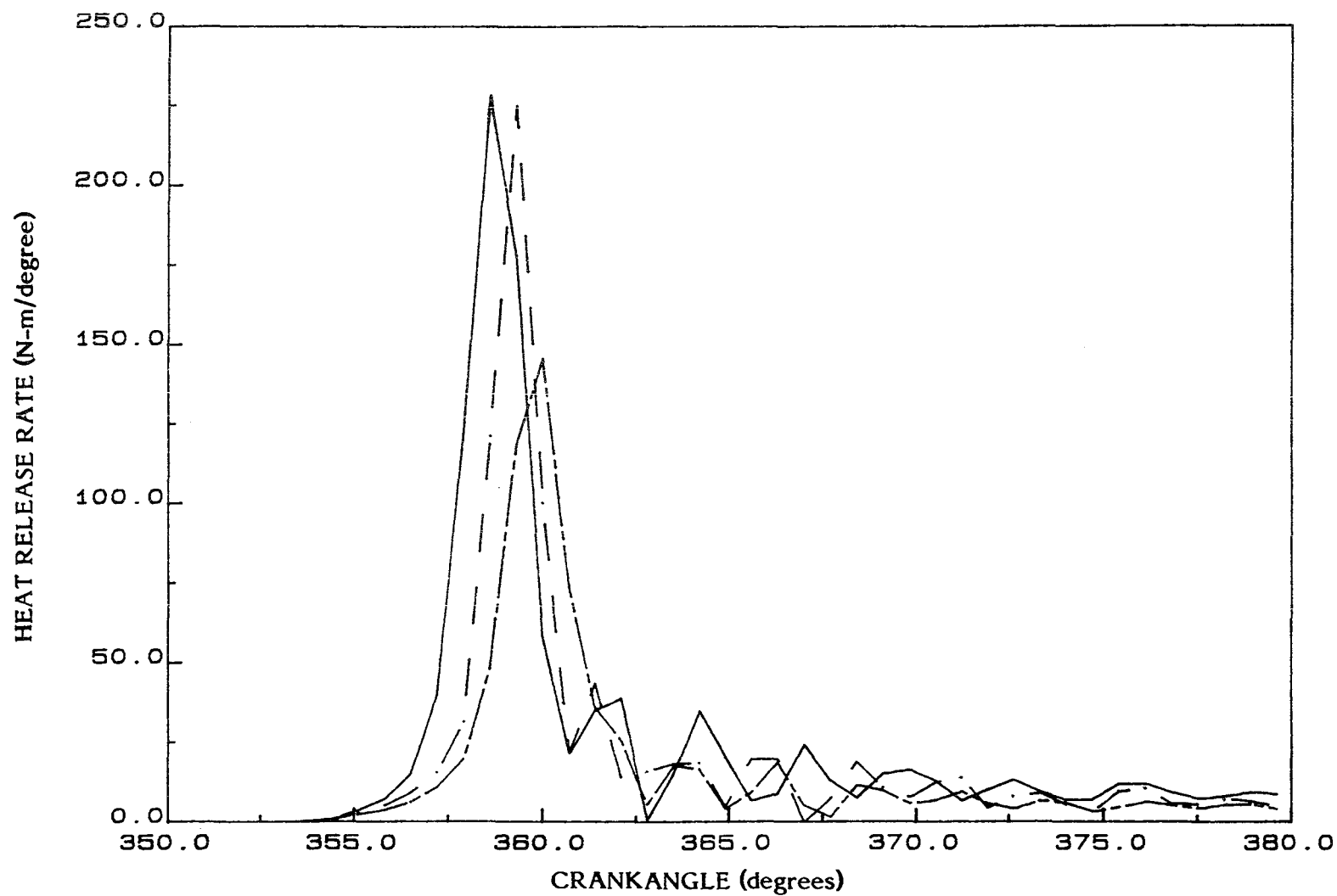


FIGURE D7. HEAT RELEASE RATE VERSUS CRANKANGLE FOR 10% MOGUL L,
THREE LOADS AT 1500 RPM, IN THE DIRECT-INJECTION ENGINE,
RUN NUMBERS (33), (34), (35)

D-10

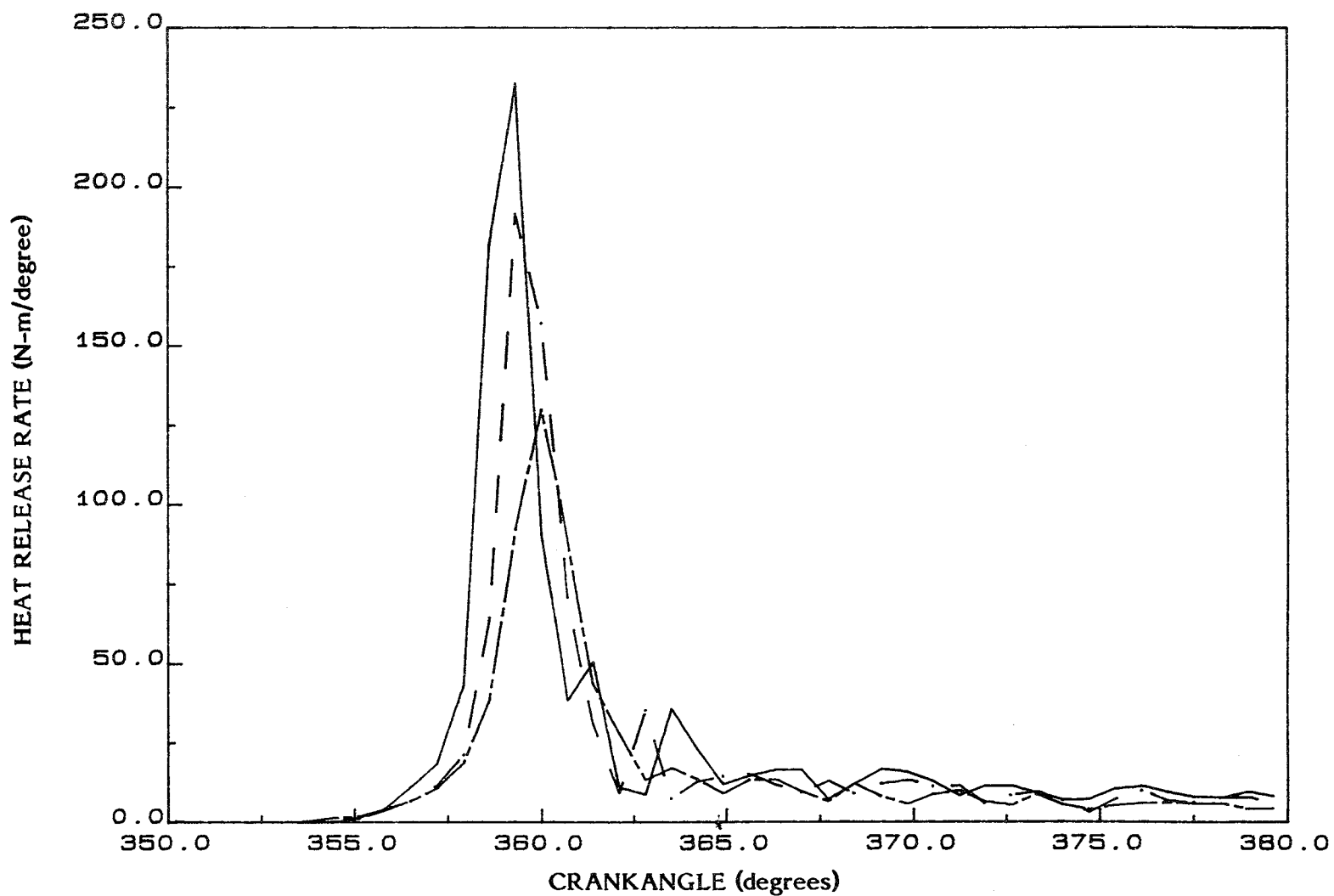


FIGURE D8. HEAT RELEASE RATE VERSUS CRANKANGLE FOR 10% MOGUL L,
THREE LOADS AT 1500 RPM, IN THE DIRECT-INJECTION ENGINE,
RUN NUMBERS (36), (37), (38)

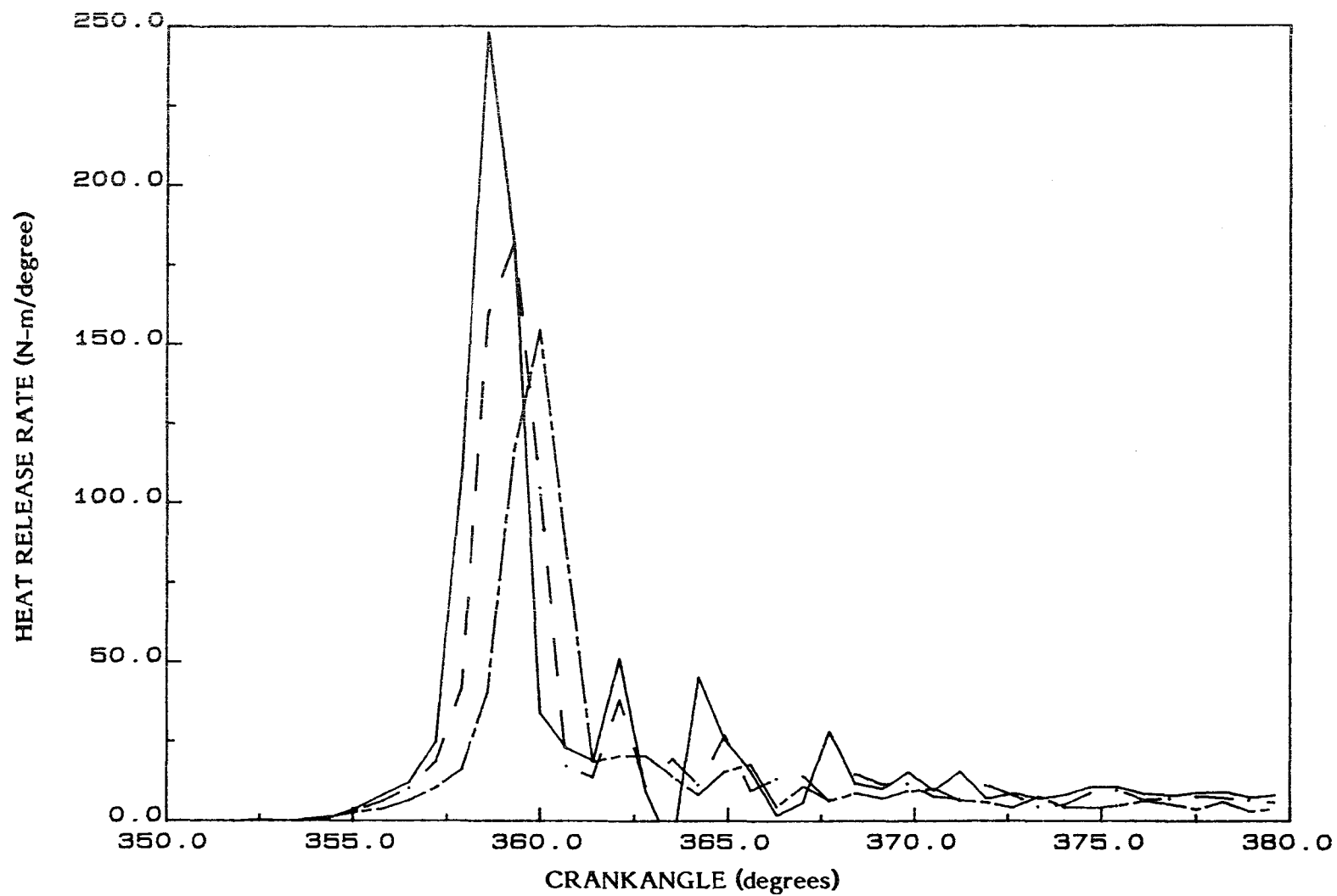


FIGURE D9. HEAT RELEASE RATE VERSUS CRANKANGLE FOR 20% MOGUL L,
THREE LOADS AT 1500 RPM, IN THE DIRECT-INJECTION ENGINE,
RUN NUMBERS (27), (28), (29)

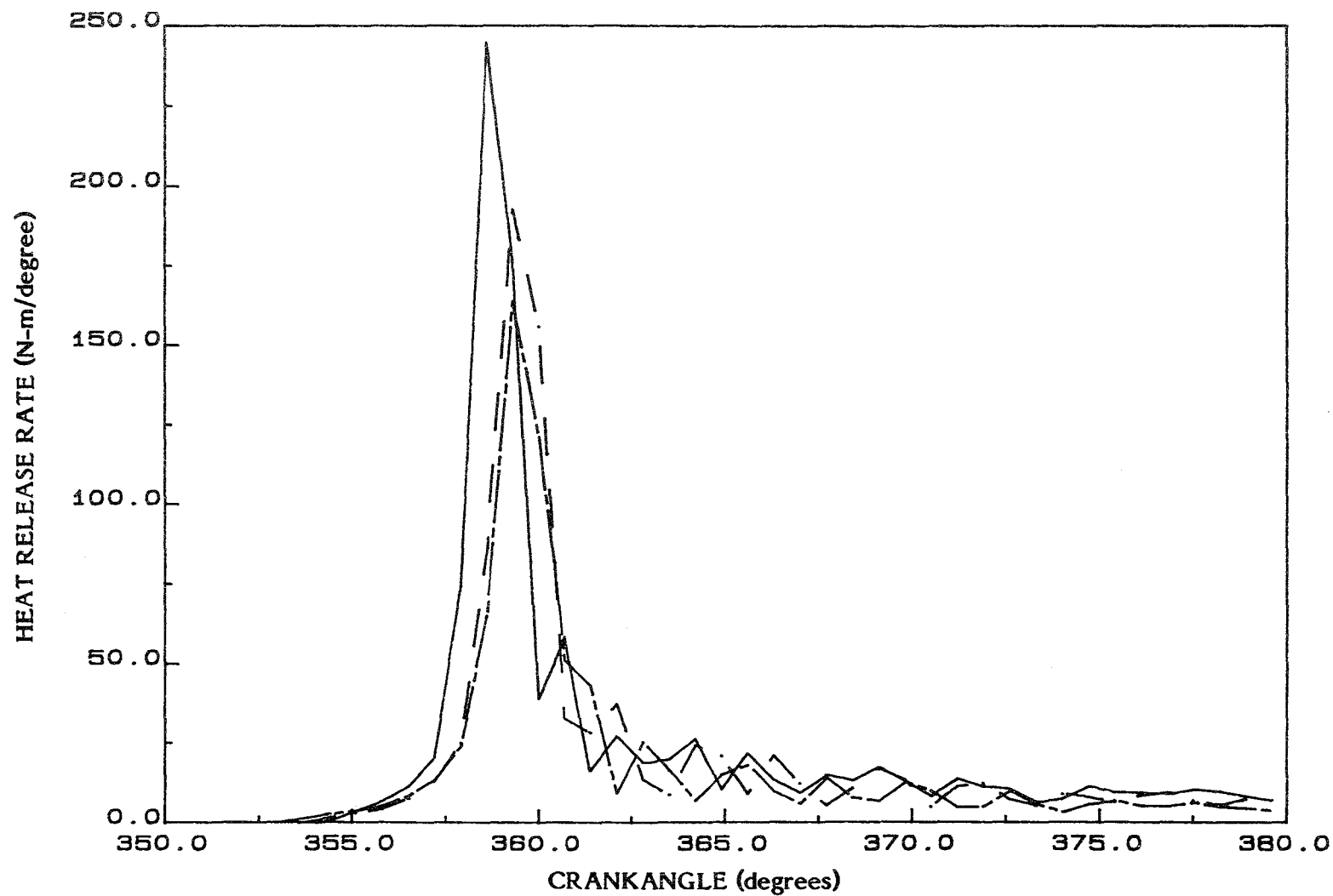


FIGURE D10. HEAT RELEASE RATE VERSUS CRANKANGLE FOR 20% MOGUL L,
THREE LOADS AT 1500 RPM, IN THE DIRECT-INJECTION ENGINE,
RUN NUMBERS (30), (31), (32)

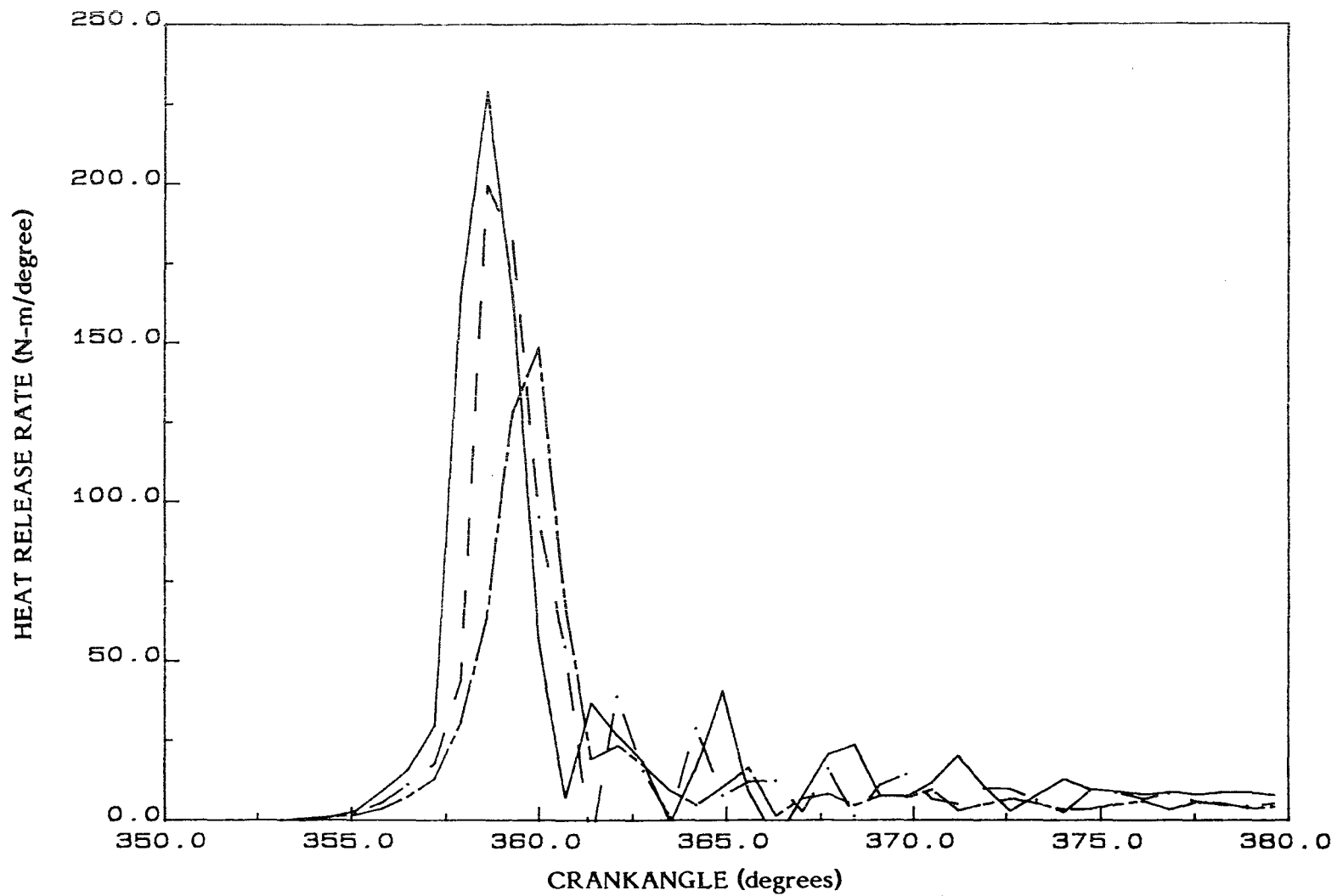


FIGURE D11. HEAT RELEASE RATE VERSUS CRANKANGLE FOR 10% SRC I,
THREE LOADS AT 1500 RPM, IN THE DIRECT-INJECTION ENGINE,
RUN NUMBERS (39), (40), (41)

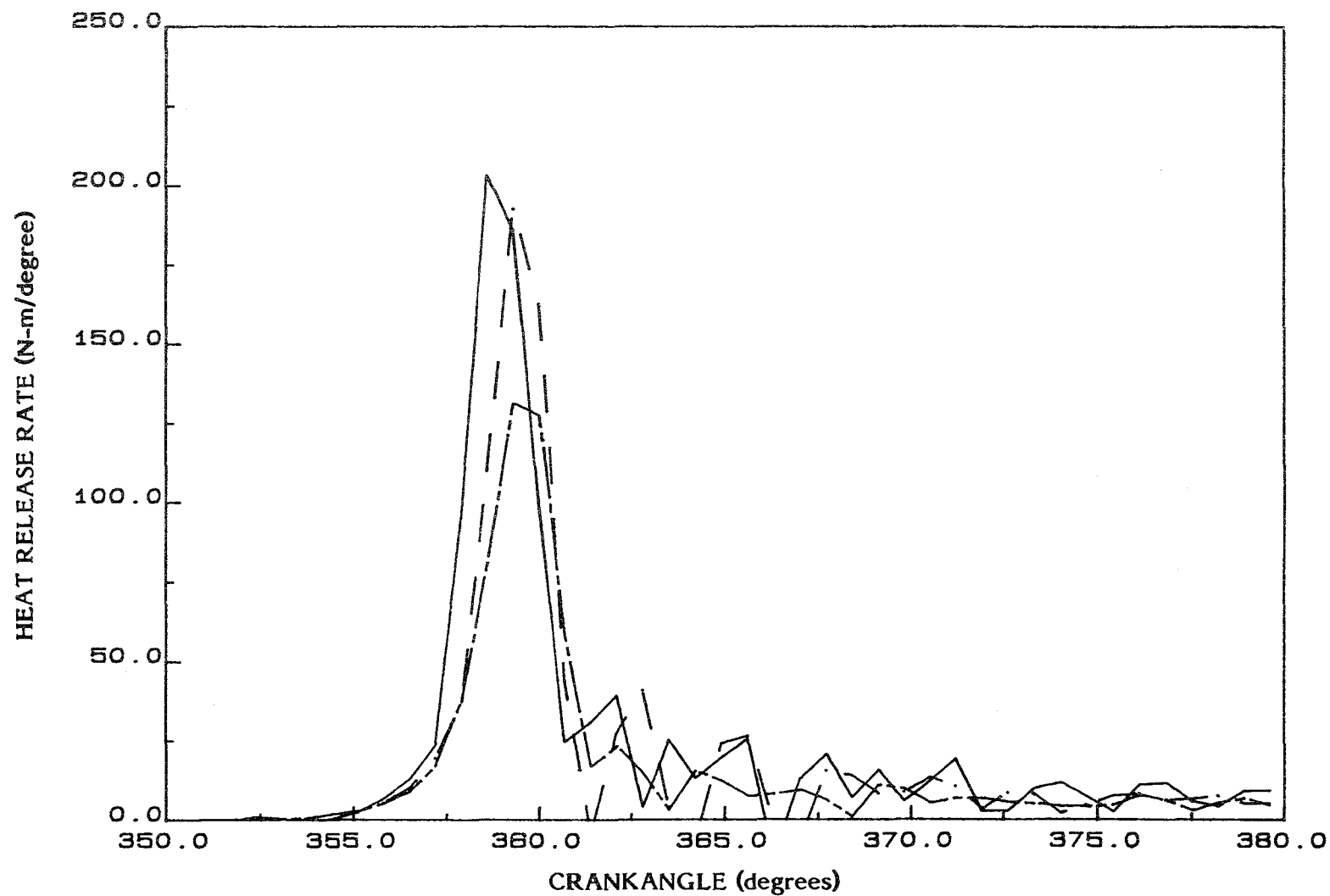


FIGURE D12. HEAT RELEASE RATE VERSUS CRANKANGLE FOR 10% SRC I,
THREE LOADS AT 1500 RPM, IN THE DIRECT-INJECTION ENGINE,
RUN NUMBERS (42), (43), (44)

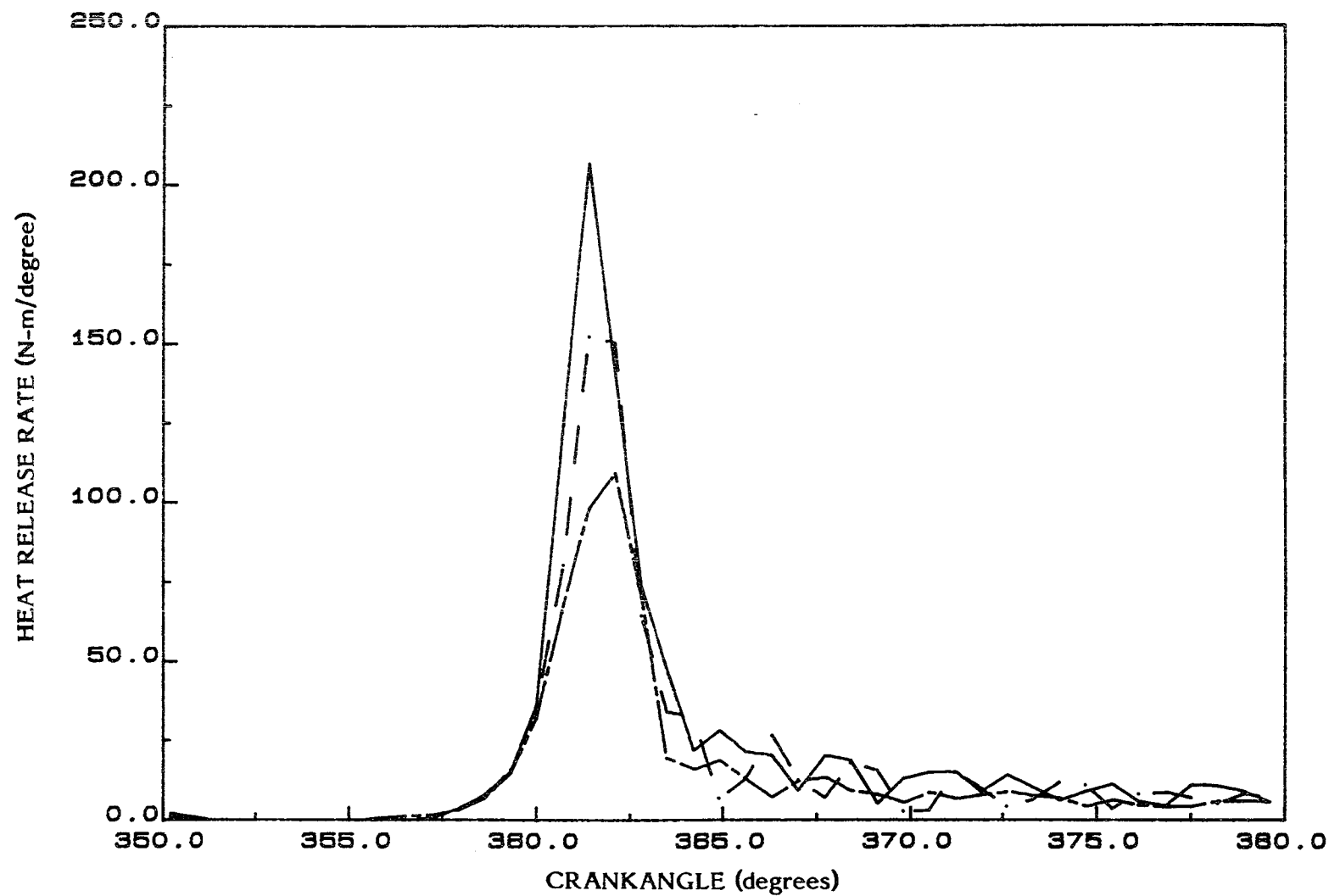


FIGURE D13. HEAT RELEASE RATE VERSUS CRANKANGLE FOR 20% SRC I,
THREE LOADS AT 1500 RPM, IN THE DIRECT-INJECTION ENGINE,
RUN NUMBERS (15), (16), (17)

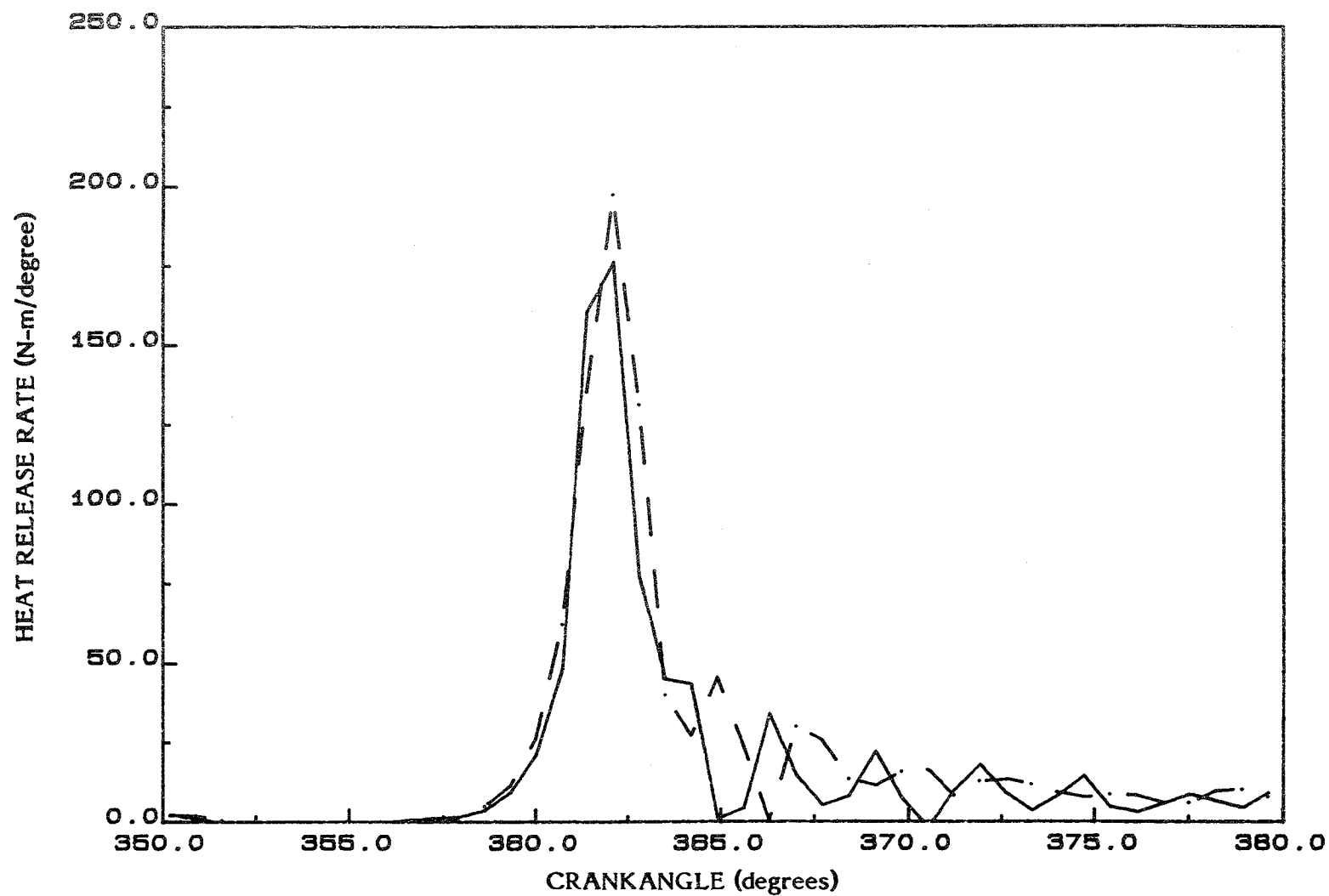


FIGURE D14. HEAT RELEASE RATE VERSUS CRANKANGLE FOR 20% SRC I, THREE LOADS AT 1500 RPM, IN THE DIRECT-INJECTION ENGINE, RUN NUMBERS (18), (19)

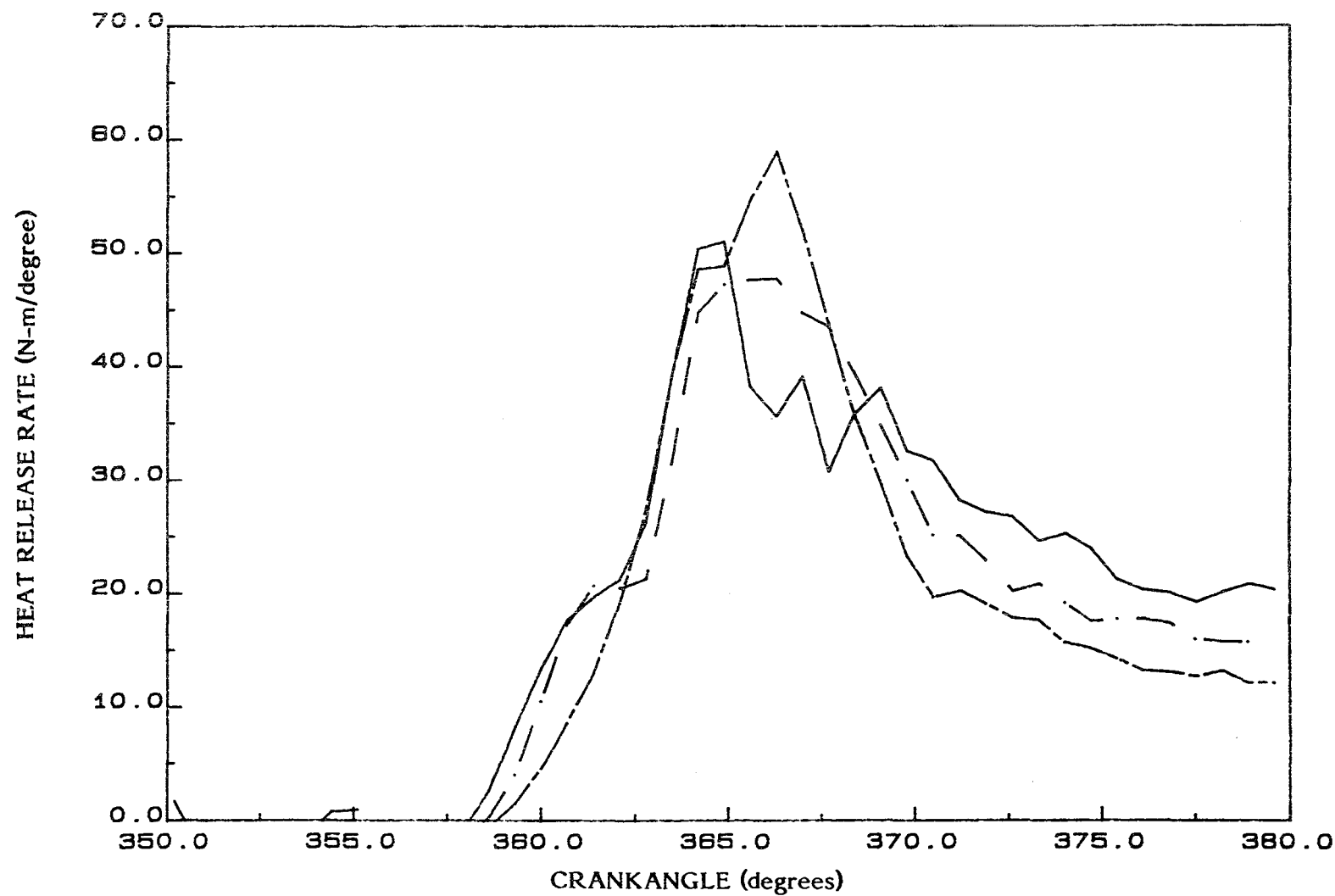


FIGURE D15. HEAT RELEASE RATE VERSUS CRANKANGLE FOR BASELINE, THREE LOADS AT 1500 RPM, IN THE INDIRECT-INJECTION ENGINE, RUN NUMBERS (65), (66), (67)

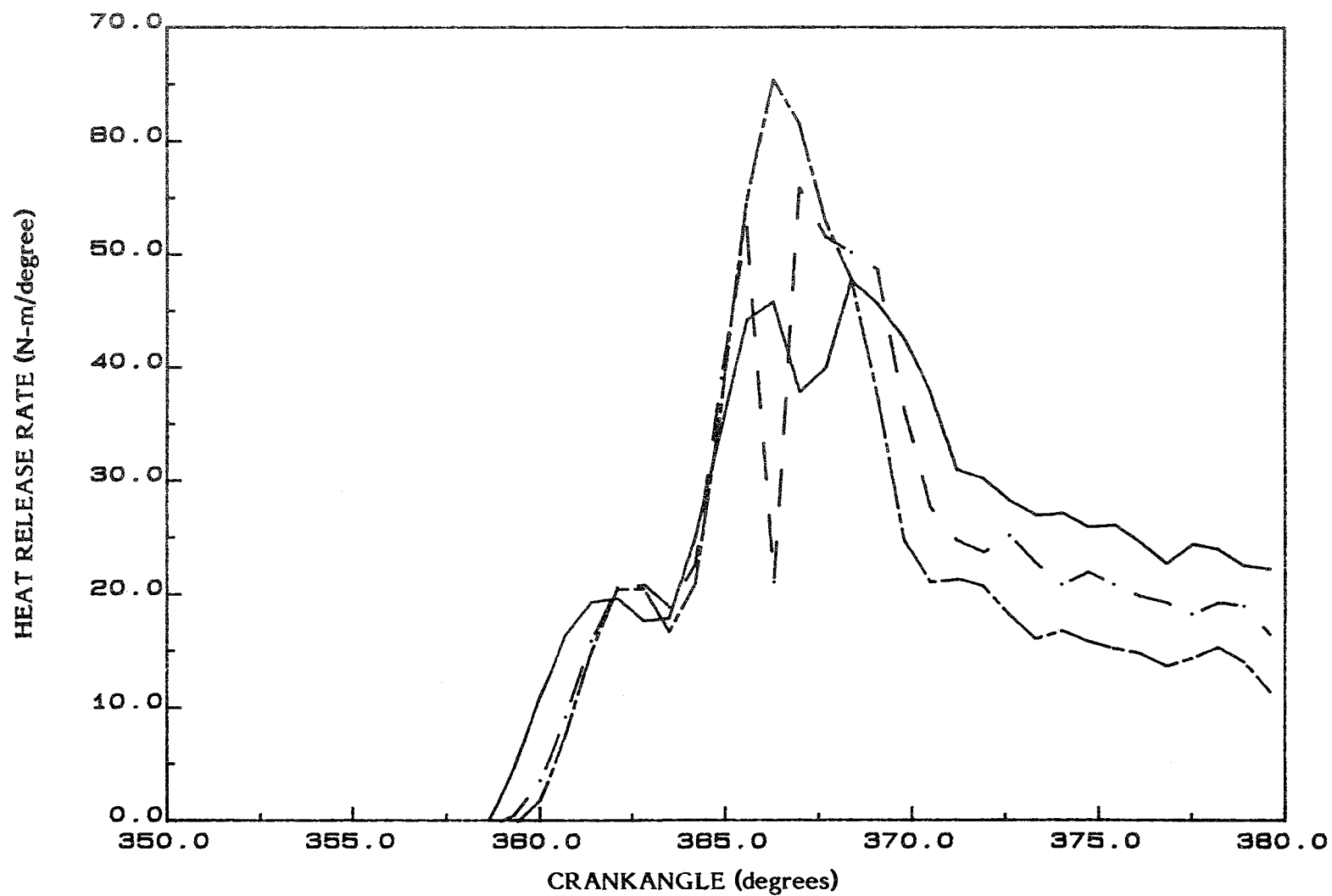


FIGURE D16. HEAT RELEASE RATE VERSUS CRANKANGLE FOR BASELINE, THREE LOADS AT 1500 RPM, IN THE INDIRECT-INJECTION ENGINE, RUN NUMBERS (69), (70), (71)

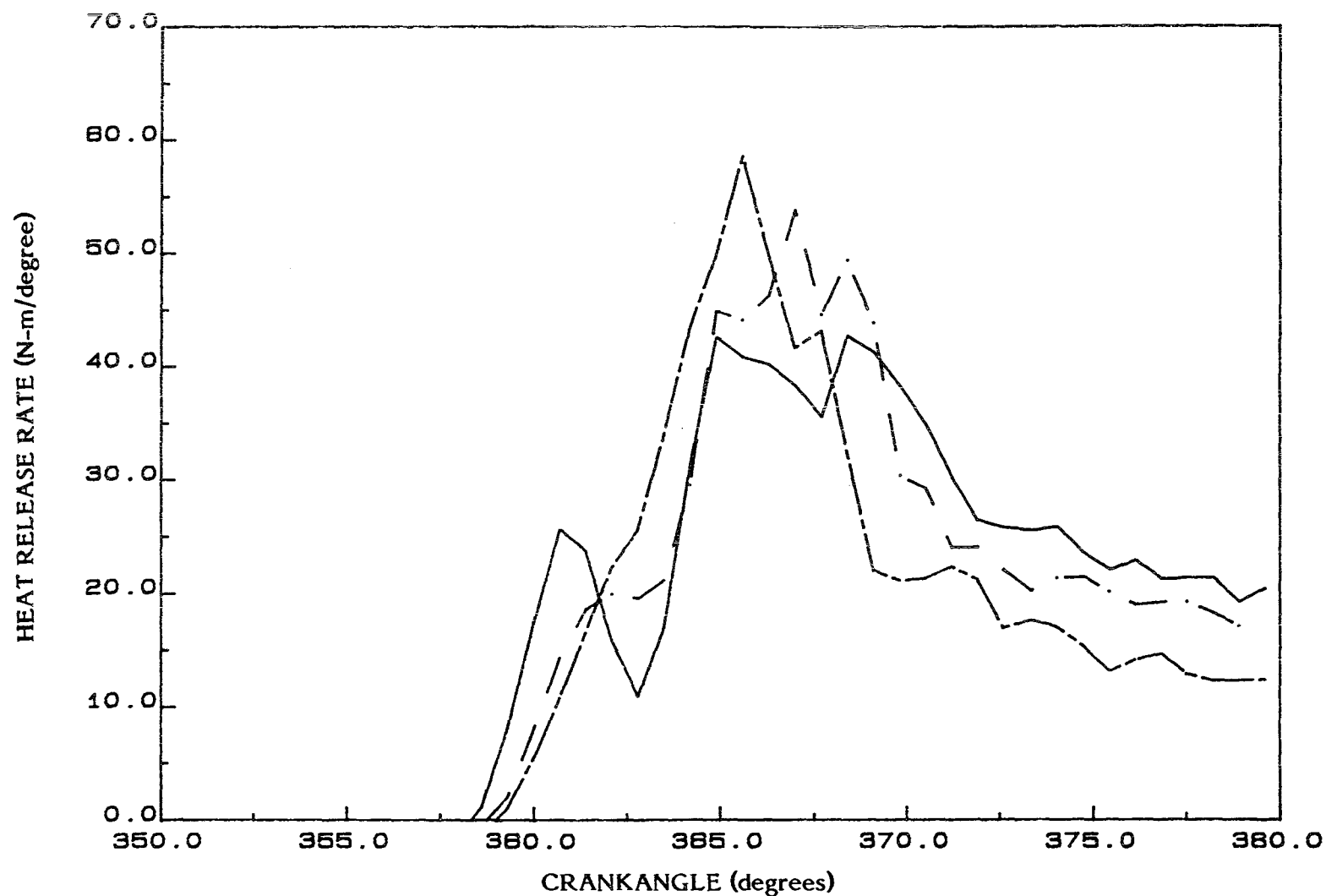


FIGURE D17. HEAT RELEASE RATE VERSUS CRANKANGLE FOR BASELINE, THREE LOADS AT 1500 RPM, IN THE INDIRECT-INJECTION ENGINE, RUN NUMBERS (72), (73), (74)

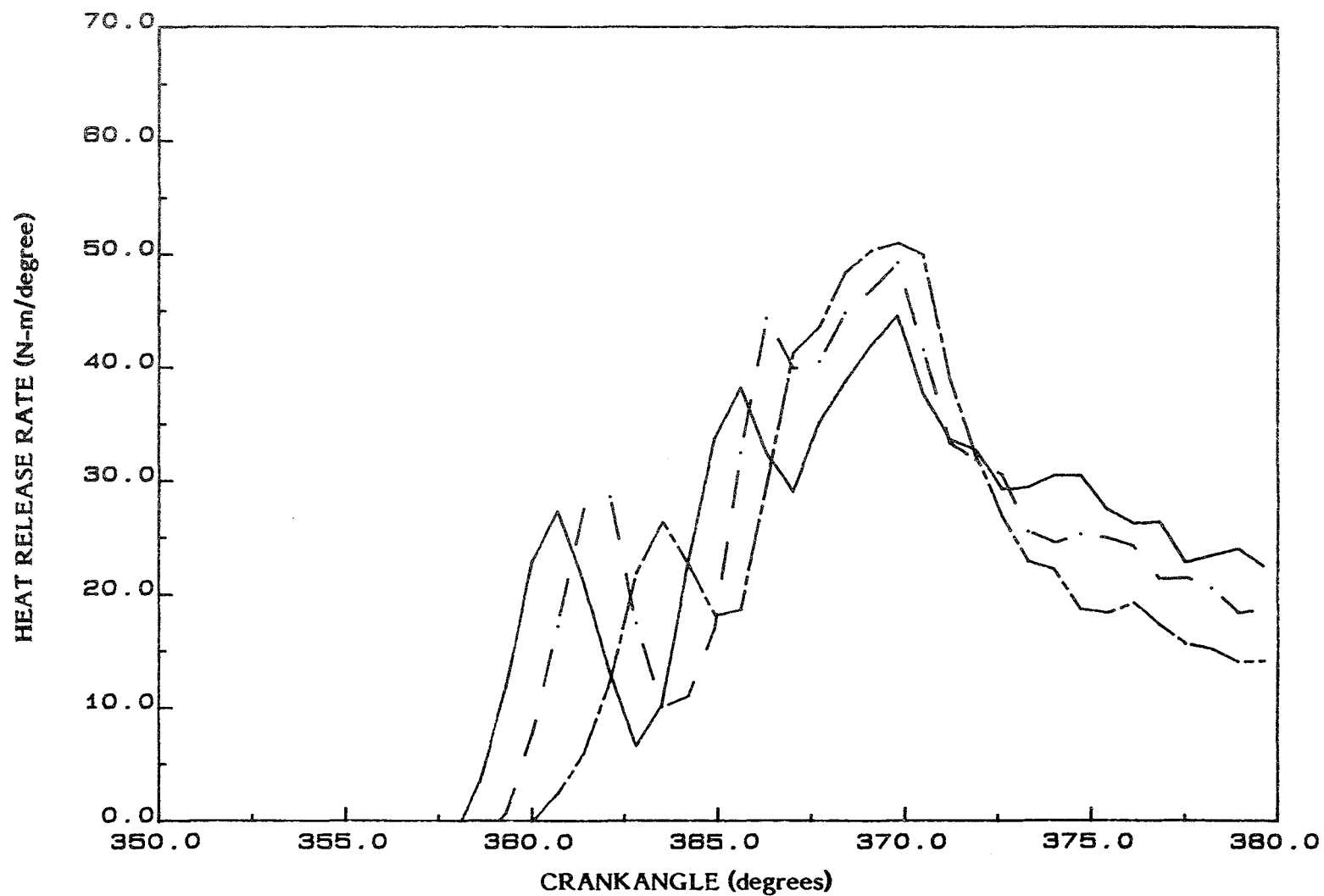


FIGURE D18. HEAT RELEASE RATE VERSUS CRANKANGLE FOR 20% MOGUL L, THREE LOADS AT 1500 RPM, IN THE INDIRECT-INJECTION ENGINE, RUN NUMBERS (81), (82), (83)

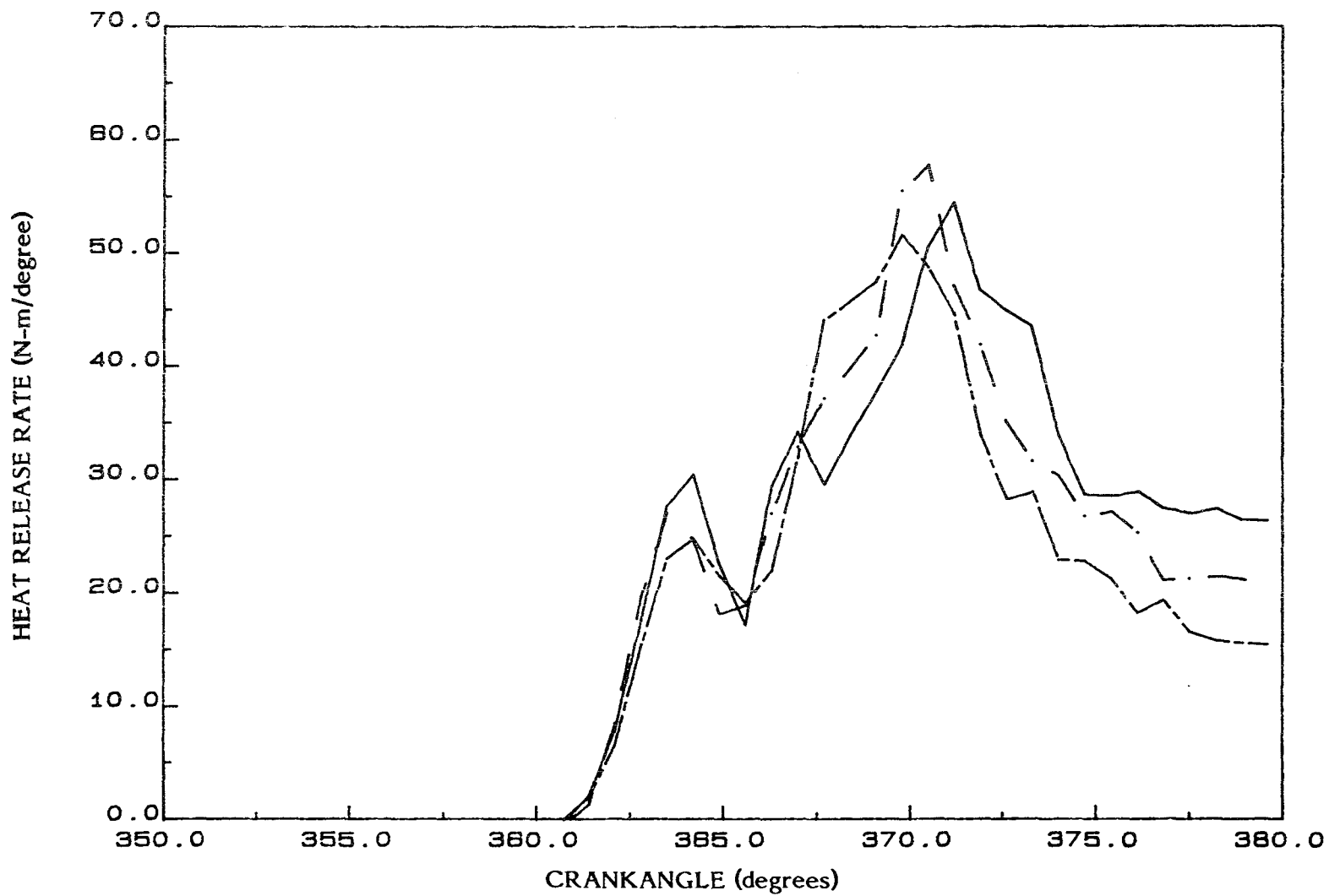


FIGURE D19. HEAT RELEASE RATE VERSUS CRANKANGLE FOR 30% MOGUL L,
THREE LOADS AT 1500 RPM, IN THE INDIRECT-INJECTION ENGINE,
RUN NUMBERS (75), (76), (77)

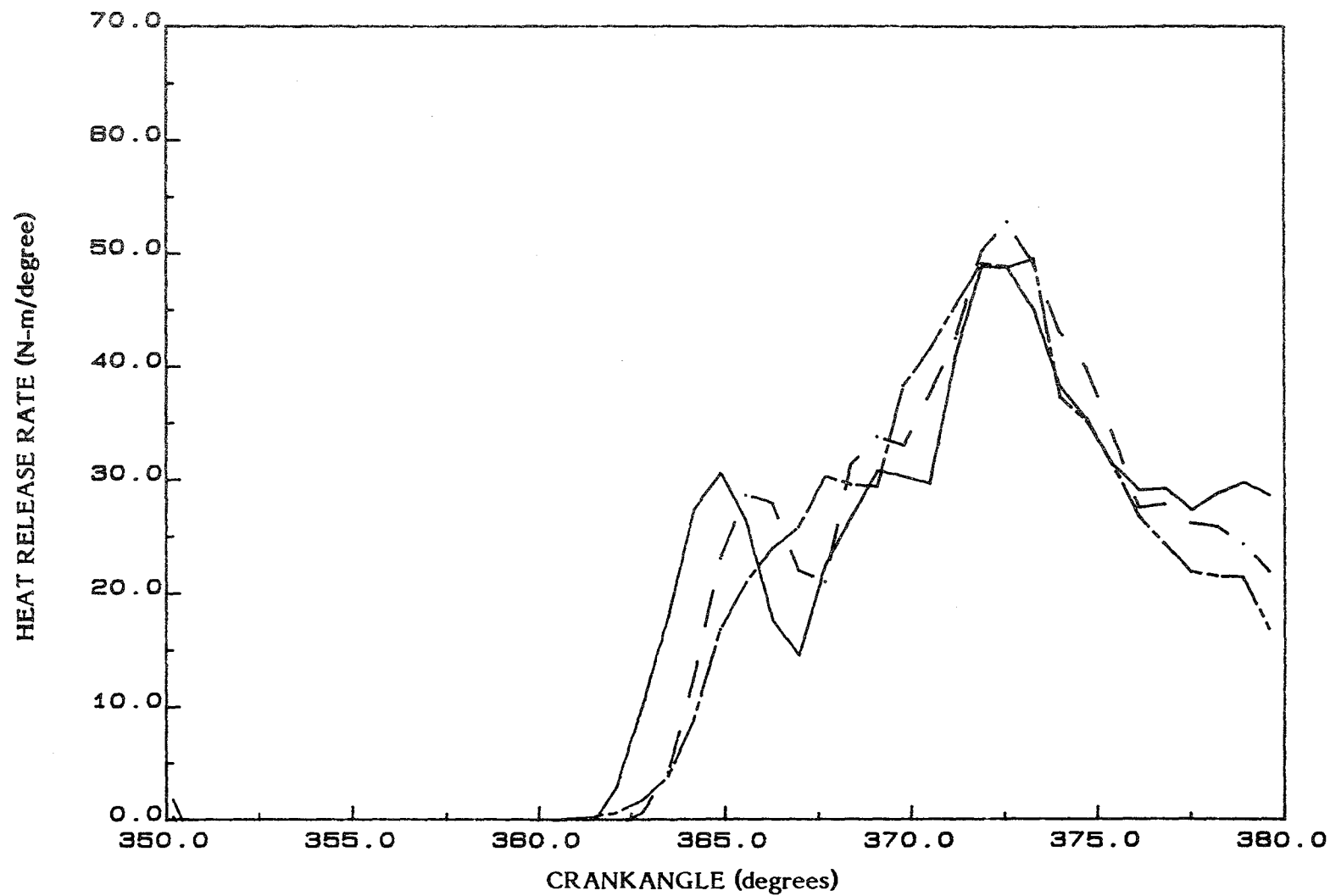


FIGURE D20. HEAT RELEASE RATE VERSUS CRANKANGLE FOR 30% MOGUL L, THREE LOADS AT 1500 RPM, IN THE INDIRECT-INJECTION ENGINE, RUN NUMBERS (78), (79), (80)

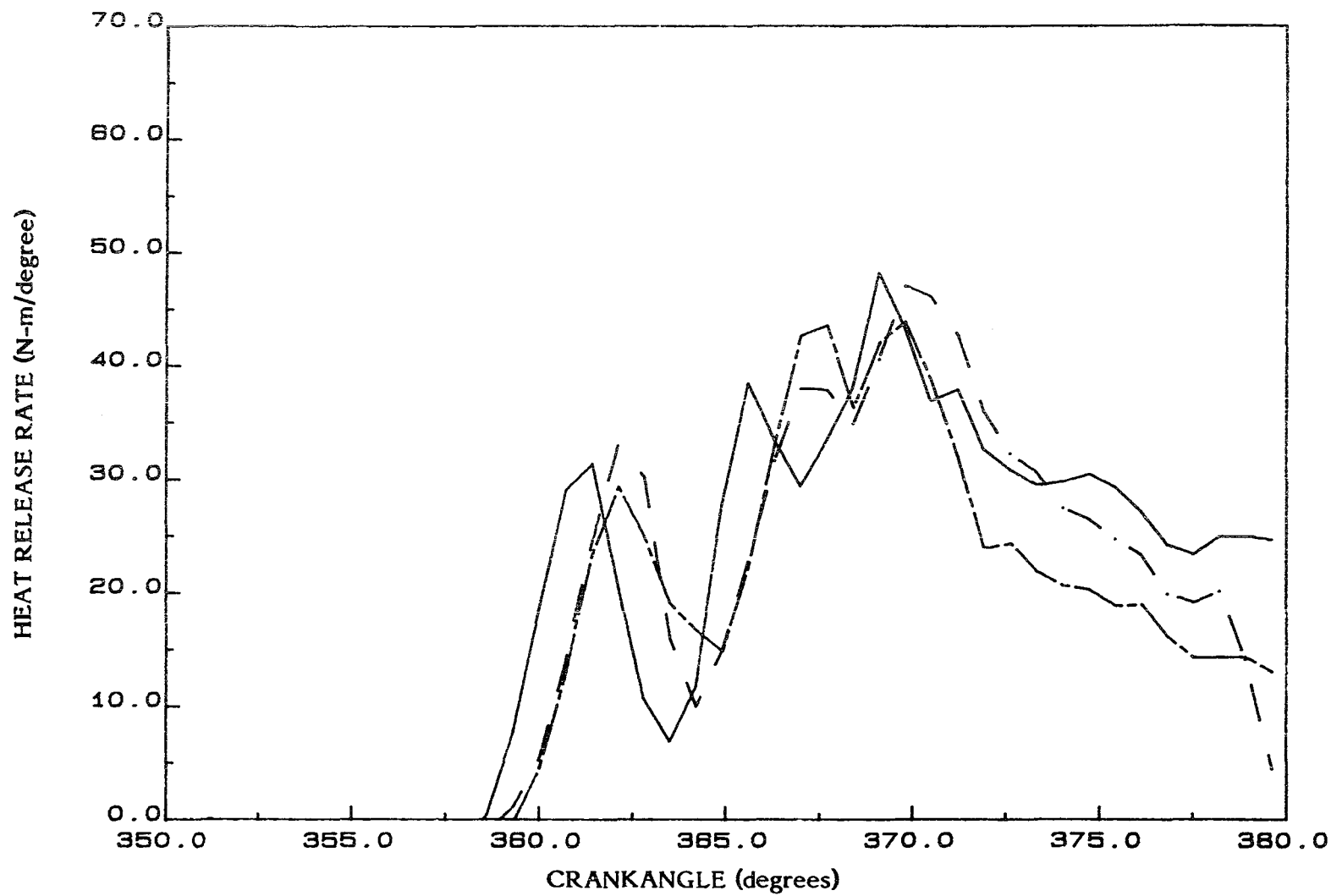


FIGURE D21. HEAT RELEASE RATE VERSUS CRANKANGLE FOR 30% FAIRLESS COKE, THREE LOADS AT 1500 RPM, IN THE INDIRECT-INJECTION ENGINE, RUN NUMBERS (84), (85), (86)

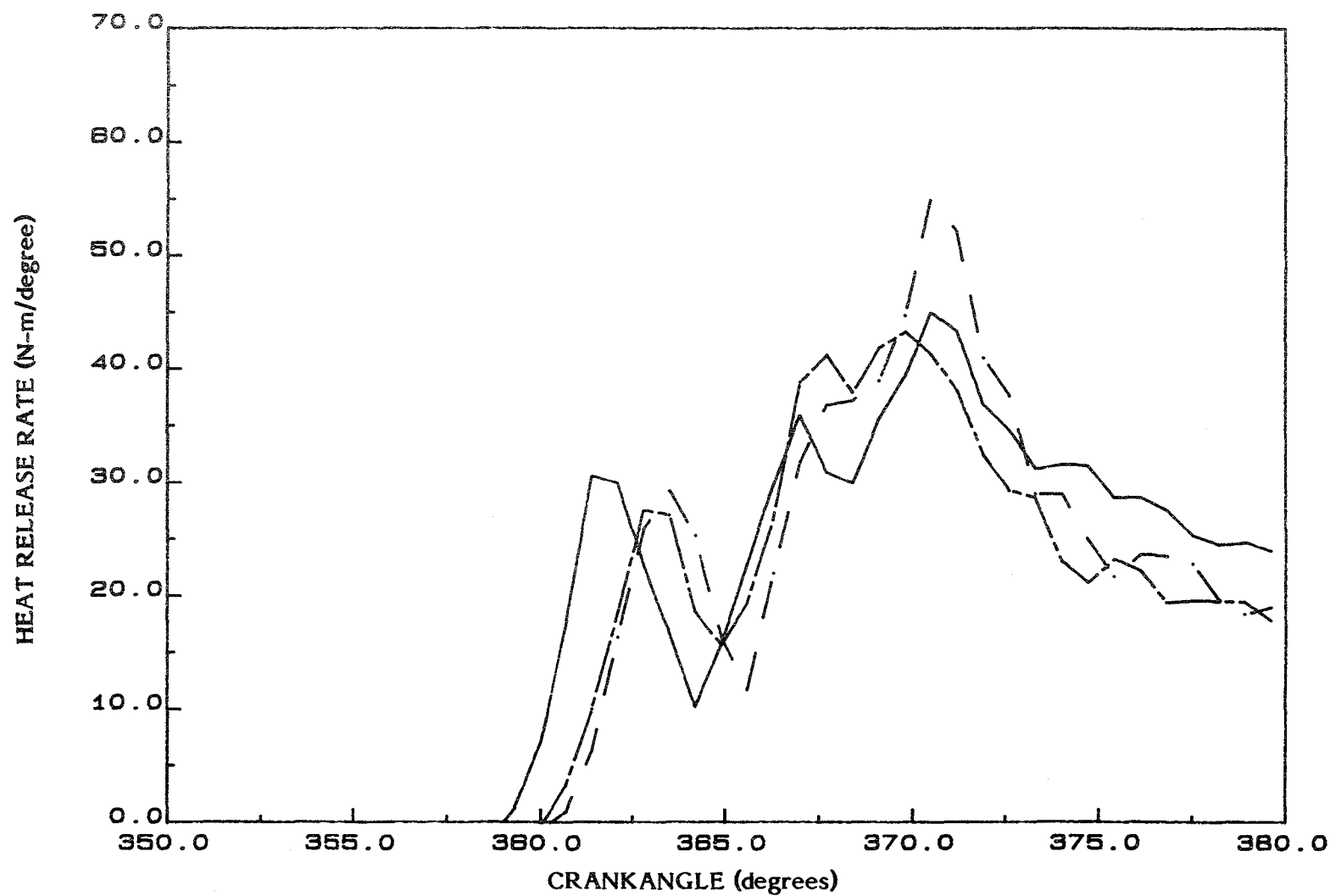


FIGURE D22. HEAT RELEASE RATE VERSUS CRANKANGLE FOR 30% FAIRLESS COKE, THREE LOADS AT 1500 RPM, IN THE INDIRECT-INJECTION ENGINE, RUN NUMBERS (87), (88), (90)

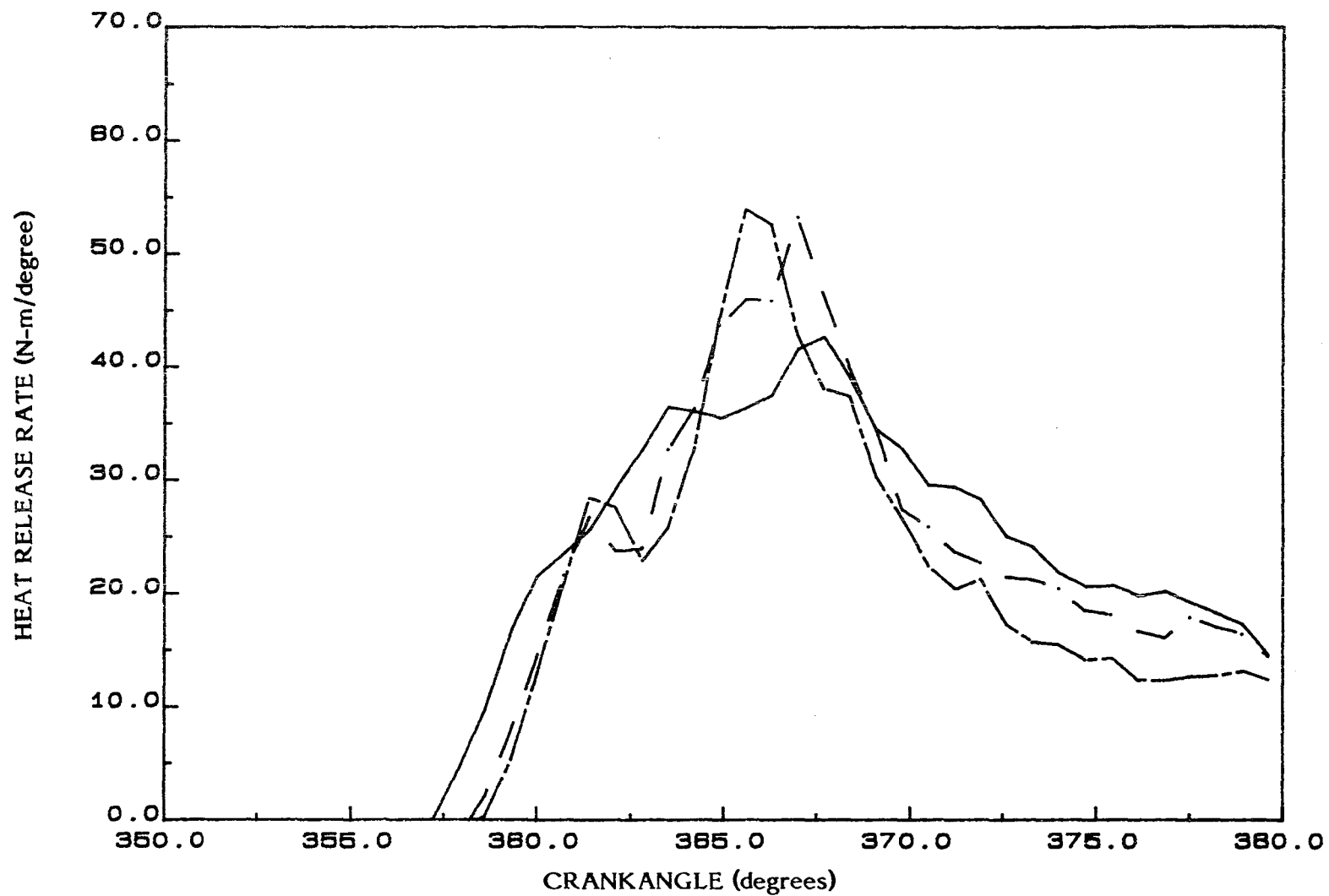


FIGURE D23. HEAT RELEASE RATE VERSUS CRANKANGLE FOR 30% EUREKA, THREE LOADS AT 1500 RPM, IN THE INDIRECT-INJECTION ENGINE, RUN NUMBERS (93), (94), (95)

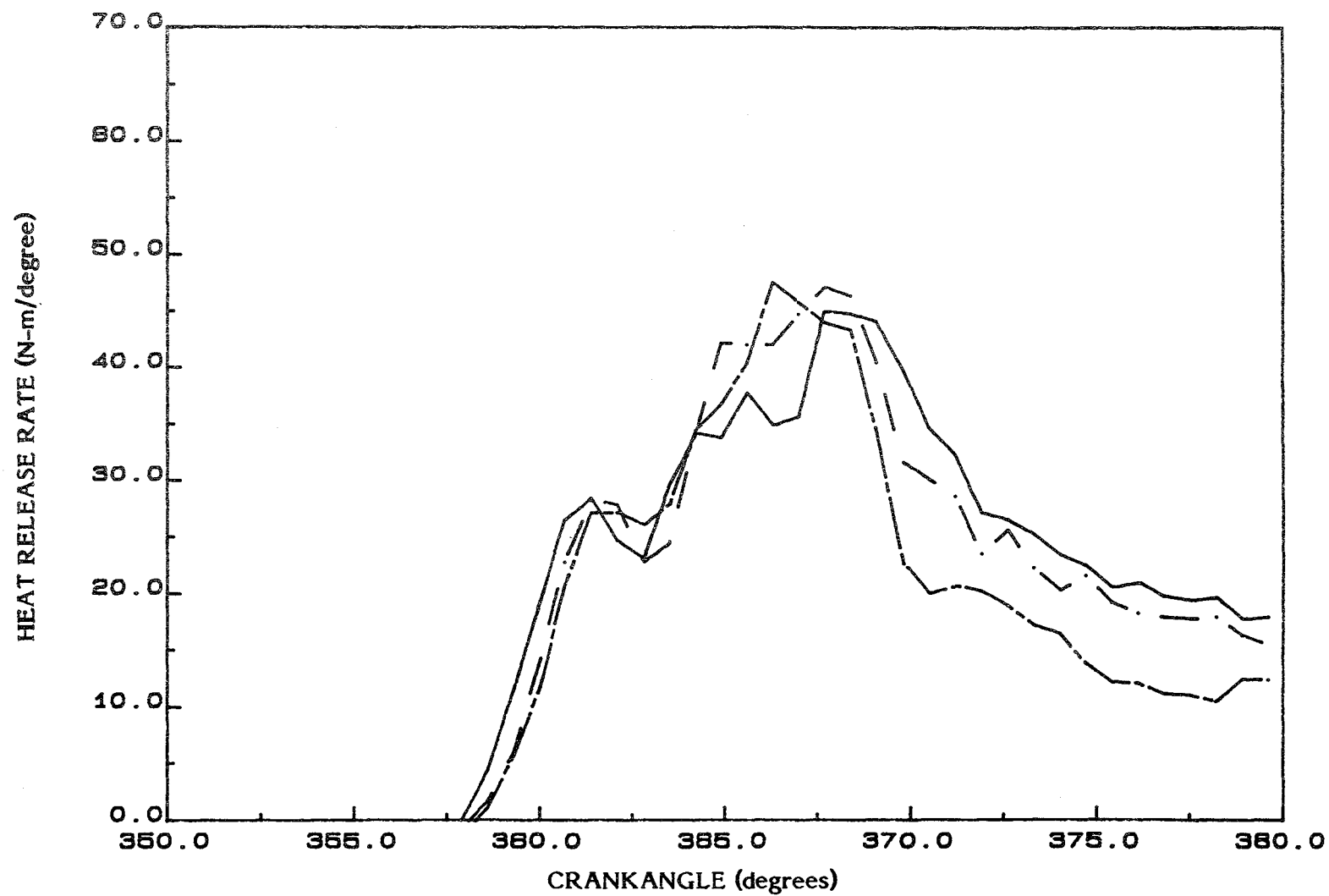


FIGURE D24. HEAT RELEASE RATE VERSUS CRANKANGLE FOR 30% EUREKA, THREE LOADS AT 1500 RPM, IN THE INDIRECT-INJECTION ENGINE, RUN NUMBERS (96), (97), (98)

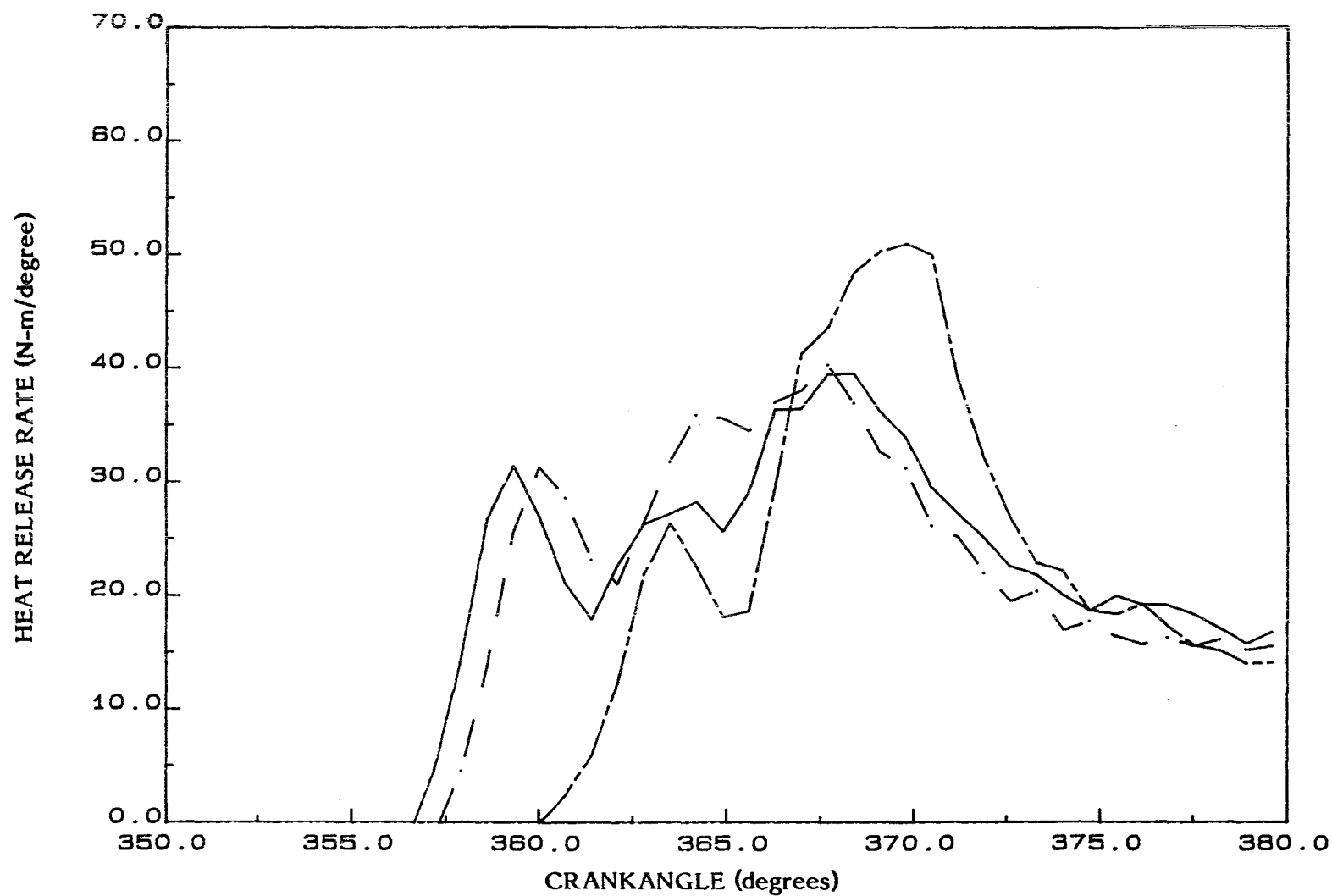


FIGURE D25. HEAT RELEASE RATE VERSUS CRANKANGLE FOR 30% CLEAN COAL, THREE LOADS AT 1500 RPM, IN THE INDIRECT-INJECTION ENGINE, RUN NUMBERS (101), (102), (103)

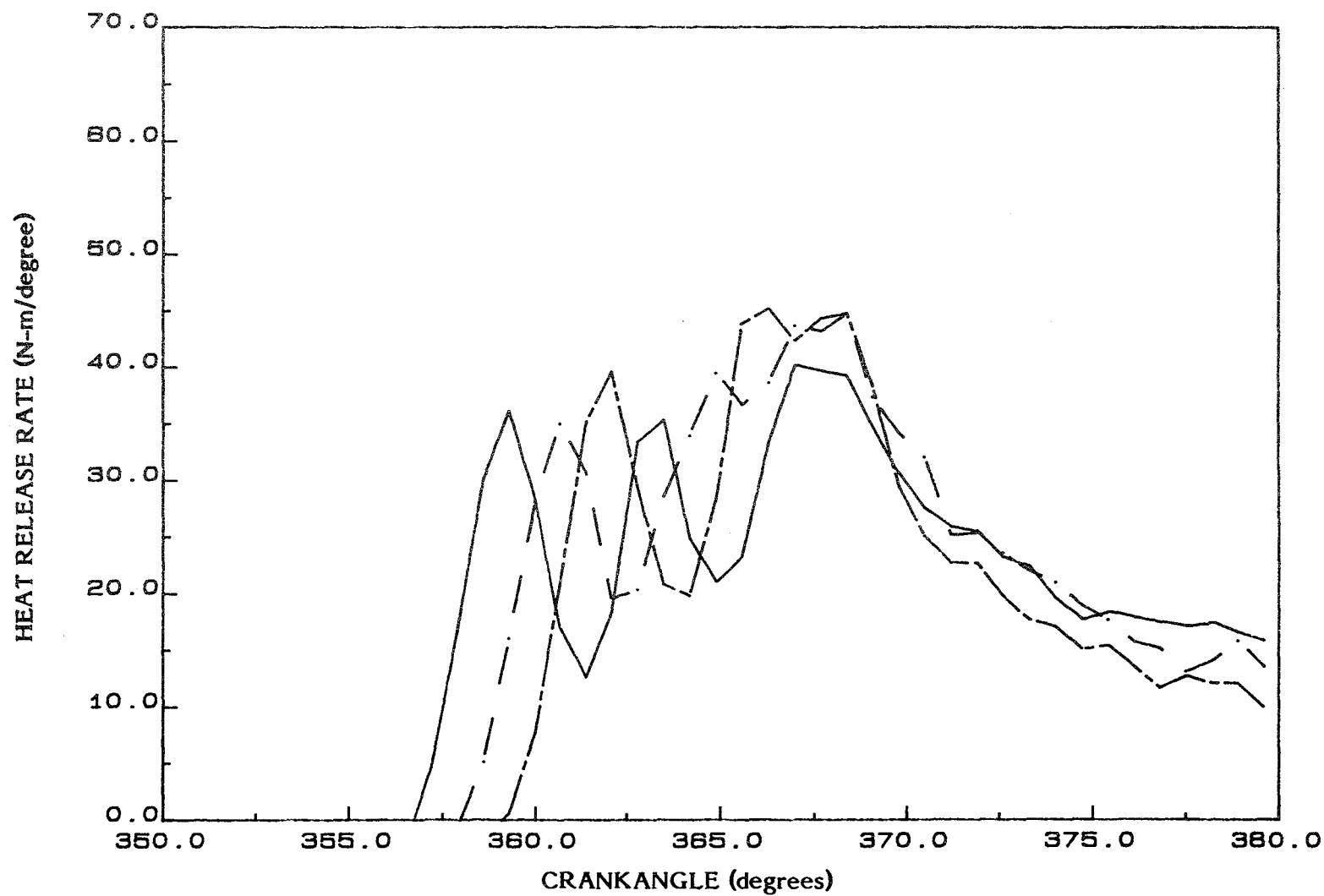


FIGURE D26. HEAT RELEASE RATE VERSUS CRANKANGLE FOR 30% CLEAN COAL, THREE LOADS AT 1500 RPM, IN THE INDIRECT-INJECTION ENGINE, RUN NUMBERS (104), (105), (106)

APPENDIX E
High Concentration Carbon Black Slurry
Test Results

As indicated in the text, preliminary experiments were performed involving the formulation and testing of a high-concentration slurry fuel. Carbon black (Mogul L) was selected for these tests because it was used as the basis for development of the low and moderately-loaded slurries, and because there was considerable experience with this material.

Initial attempts to formulate a 50-wt percent slurry were unsuccessful due to the extremely high viscosity and the dry appearance of the mixture. The use of dispersing agents did not alleviate the problem.

A fluid slurry was produced, however, when the carbon black concentration was reduced to 40-wt percent. These results would tend to indicate that the vast majority of the carbon black particles in the slurry are in the 0.5 micron size range and that the particles are very porous. Spherical particles in the 1.0 micron size range would not be expected to reach this volume-filled situation until the concentration is in excess of 60-wt percent.

Even though the 40-percent slurry was fluid, a special pressurized fuel supply system was required in order to force the slurry into the injection pump. The pressurized fuel system could not be installed on the electronic weigh base due to its excessive weight. Mass fuel flowrate measurements were therefore not possible with this fuel system. Heat-release rate data was obtained at three different load conditions. Figure E1 is a plot of the heat-release rate diagrams for the 100-, 75-, and 50-percent load test conditions. During these runs, the engine appeared to be performing fairly well in terms of injection nozzle performance. The heat-release rate diagrams showed, however, that the early stages of combustion were extremely slow, indicating degraded spray quality. The later stages of combustion appeared to be

normal except that the total heat release was below normal. Reliable fuel delivery to the injection pump was a problem resulting apparently from the high viscosity of this slurry. Possible solutions include the use of additives and/or development of, or adaptation of slurry pumping equipment.

1. Report No. NASA CR-174659		2. Government Accession No.		3. Recipient's Catalog No.	
4. Title and Subtitle Development of Carbon Slurry Fuels for Transportation (Hybrid Fuels Phase II)				5. Report Date May 1984	
				6. Performing Organization Code	
7. Author(s) Thomas W. Ryan, III, and L. G. Dodge				8. Performing Organization Report No. SwRI Report No. 6948	
				10. Work Unit No.	
9. Performing Organization Name and Address Southwest Research Institute 6220 Culebra Road P.O. Drawer 28510 San Antonio, Texas 78284				11. Contract or Grant No. DEN 3-263	
				13. Type of Report and Period Covered Contractor Report	
12. Sponsoring Agency Name and Address U.S. Department of Energy Office of Vehicle and Engine R&D Washington, D.C. 20585				14. Sponsoring Agency Code Report No. DOE/NASA/0263-1	
15. Supplementary Notes Final Report. Prepared under Interagency Agreement DE-AI01-81CS50006. Project Manager, George M. Prok, Aerothermodynamics Fuel Division, NASA Lewis Research Center, Cleveland, Ohio 44135.					
16. Abstract Slurry fuels of various forms of solids in diesel fuel were developed and evaluated for their relative potential as fuel for diesel engines. Thirteen test fuels with different solids concentrations were formulated using eight different materials. A variety of properties were examined including ash content, sulfur content, particle size distribution, and rheological properties. Attempts were made to determine the effects of these variations on these fuel properties on injection, atomization, and combustion processes. The injection and atomization characteristics (transient diesel sprays) of the test fuels were examined in a spray bomb in which a nitrogen atmosphere was maintained at high pressure and temperature, 4.2 MPa and 480°C, respectively. The diagnostics of the sprays included high-speed movies and high-resolution still photographs. The slurries were found to affect the global spray characteristics of penetration rate and cone angle and the particle-size distribution within the spray. In general, the drop size increased, the penetration rate increased and the cone angle decreased with the slurries as compared to a baseline diesel fuel. The slurries were also tested in a single-cylinder CLR engine in both direct-injection and prechamber configurations. The data included the normal performance parameters as well as heat release rates and emissions. In most cases, the slurries performed very much like the baseline fuel. The combustion data indicated that a large fraction (90 percent or more) of the solids were burning in the engine. It appears that the prechamber engine configuration is more tolerant of the slurries than the direct-injection configuration.					
17. Key Words (Suggested by Author(s)) Slurry fuel Diesel injection Diesel combustion				18. Distribution Statement Unclassified - unlimited STAR Category 26 DOE Category UC-96	
19. Security Classif. (of this report) Unclassified		20. Security Classif. (of this page) Unclassified		21. No. of pages 177	
				22. Price* A09	

End of Document